

3
C.2

MODELS FOR HIGH ENERGY PROCESSES

RECEIVED
LAWRENCE
RADIATION LABORATORY
AUG 25 1969
LIBRARY AND
DOCUMENTS SECTION

J. D. Jackson

May 19, 1969

AEC Contract No. W-7405-eng-48

• TWO-WEEK LOAN COPY

*This is a Library Circulating Copy
which may be borrowed for two weeks.
For a personal retention copy, call
Tech. Info. Division, Ext. 5545*

LAWRENCE RADIATION LABORATORY
UNIVERSITY of CALIFORNIA BERKELEY

DISCLAIMER

This document was prepared as an account of work sponsored by the United States Government. While this document is believed to contain correct information, neither the United States Government nor any agency thereof, nor the Regents of the University of California, nor any of their employees, makes any warranty, express or implied, or assumes any legal responsibility for the accuracy, completeness, or usefulness of any information, apparatus, product, or process disclosed, or represents that its use would not infringe privately owned rights. Reference herein to any specific commercial product, process, or service by its trade name, trademark, manufacturer, or otherwise, does not necessarily constitute or imply its endorsement, recommendation, or favoring by the United States Government or any agency thereof, or the Regents of the University of California. The views and opinions of authors expressed herein do not necessarily state or reflect those of the United States Government or any agency thereof or the Regents of the University of California.

MODELS FOR HIGH ENERGY PROCESSES

J. D. Jackson

Department of Physics and Lawrence Radiation Laboratory
University of California, Berkeley, California

May 19, 1969

A review paper prepared for the Lund International Conference
on Elementary Particles, June 25-July 1, 1969.

Table of Contents

	Page
I. <u>Introduction</u>	1
1. Preamble	1
2. Framework	3
II. <u>Sampling of Recent Data</u>	6
1. π^-p Elastic Scattering	6
2. Nucleon-nucleon Scattering	7
3. Inelastic Proton-proton Collisions	7
4. Polarization in π -N and K-N Scattering	8
5. Resonance Production	10
6. Tests of Quark Model Predictions on Decay Correlations	11
7. Backward K^+p and K^-p Scattering	12
8. Forbidden Exchanges	14
III. <u>Regge Pole Models</u>	15
1. Difficulties With Pure Pole Models	15
2. Recent Developments in Models With Poles Only	18
(a) Dips, front, and back	19
(b) Cyclic residues to give structure at large $ t $	21
(c) SU(3) tests and exchange degeneracy	23
(d) Higher symmetries	25
IV. <u>Multiple Scattering, Optical Models and Regge Cuts</u>	28
1. Impact Parameter Formalism for Multiple Scattering and Optical Models	29
(a) Scattering of a structureless particle by a Potential	31

(b) Scattering of a structureless particle by N fixed scatterers	31
(c) Scattering by a composite system, the optical model	32
(d) Scattering of one composite system by another . . .	34
(e) Multiple scattering series and its inverse	36
2. Chou-Yang Model, Hybrid Model, and Multiple Pomeranchon Exchanges	37
(a) Chou-Yang model	37
(b) Hybrid Model	40
(c) Multiple Pomeranchon exchanges	42
3. Cuts in the J-plane	44
4. Absorptive Model Recipe for Generating Regge Cuts . . .	49
5. Unitarity Corrections Versus Absorptive Corrections . .	54
V. <u>Finite Energy Sum Rules and Duality</u>	56
1. Equations and Basic Results	56
(a) Standard formulas for FESR and CMSR	57
(b) Classic results	60
(c) Further results	62
2. What do FESR actually prove?: A Case Study of Pion Photoproduction	65
3. Duality and its Evolution	69
(a) Simple duality and Schmid circles	69

	Page
(b) Exchange degeneracy and the presence or absence of resonances	70
(c) The special role of the Pomeron Regge Pole	76
4. Duality Diagrams	78
5. Duality, the Deck Effect, and Multiperipheralism	82
VI. <u>Veneziano Models</u>	85
1. Pion-pion Scattering	85
(a) Resonances and Regge behavior	86
(b) Detailed properties	90
(c) Soft pion results	93
2. Generalization to n Particles	94
3. Attempts at Unitarization	97
4. Applications	99
VII. <u>Some Aspects of Multiperipheralism</u>	103
1. Three-body and Quasi-three-body Final States	103
2. Four Bodies and More in the Final State	105
3. Particle Spectra in Inelastic Proton-proton Collisions	106
4. Self-consistent Regge Singularities and the Pomeron	109
VIII. <u>Miscellaneous Aspects of Production Processes</u>	115
1: Pion-pion Phase Shifts	115
2. K- π Phase Shifts	119
3. On the Connection of Production Mechanism and the Decay of Resonances at High Energies	120
Concluding Remarks	124

	Page
Bibliography.	125
Table I.	138
Table II.	139
Table III.	140
Figure Captions.	141

I. INTRODUCTION

1. Preamble

An invitation to present a review at a conference affords the reviewer the opportunity to survey afresh the subject matter, to collect his own thoughts about it, and hopefully to present a concise and clear picture, emphasizing the good and fruitful and omitting the spurious and bad. I have this opportunity. Whether the realization matches the potential, the reader must judge for himself. Six or more months ago, when I accepted the invitation to review high-energy phenomenology, I gave the task only passing thought. As the time grew close, the enormity of the enterprise slowly dawned on me. Then the preliminary program arrived to show that I was "clean-up man" on the team of reviewers with an assignment vague enough and all-encompassing enough to exclude, by general agreement, only Professor Steinberger's review of weak interactions. I therefore apologize for the overlap between my text and those of Professors Lohrmann and Lipkin (in my oral presentation, I shall mercifully keep the duplication to a minimum). Of course, the lack of clear boundaries between electromagnetic interactions of hadrons and purely hadronic processes on the one hand, and between the low energy domain of resonances and the high energy domain of peripheral processes on the other, is one of the more exciting aspects of our field today. Indeed, lack of clear boundaries is misleading in its understatement. Intimate connection and interplay is closer to the truth. Of this you have already heard today, and I will say more.

Before beginning my review proper I want to let you see what we, as experimenters and theorists, are doing to earn our keep. Tables I and II show the thrust of our activities, as evidenced by publication in two letter journals, Physical Review Letters and Physics Letters. The time period covered is roughly 1968 and the first half of 1969 (actually three volumes of each journal). The ten categories in experiment and eleven in theory are somewhat arbitrary. I leave detailed study and interpretation to the reader. Only three comments: (i) There is some evidence from a peaking in the second half of 1968 that those who publish in Physical Review Letters are somewhat meeting-conscious (the Vienna meeting in this instance), while those who publish in Physics Letters are steadier in their output. (ii) Theorists who publish in Physical Review Letters have hoed the row of current algebras and the like much harder than their Physics Letter counterparts. (iii) Current and field algebras seem on the decline, while Veneziano models are rising with meteoric speed.

The overall picture is displayed in Fig. 1 where the areas of the circles for experiment and theory are in proportion to the numbers of papers (304 and 360) in each field. In experiment the finding and studying of resonances accounts for 28% of all the publications. When production mechanisms is added in, the total resonance or resonance-related effort amounts to 40%. The great bulk of this research is done with bubble chambers. Counter experiments on elastic or quasi-elastic scattering account for roughly 16%, while photon and electron-initiated processes provide 24%, and experiments on weak interactions contribute 20% of the publications. How does this compare to the money spent? I do not know.

The theorists' activities appear to be slightly more uniformly distributed (is this just a reflection of a better choice of categories?), with no one subdivision over 13% of the total. It is noteworthy, however, that various aspects of S-matrix theory, with its ideas of analyticity crossing, and unitarity, account for 35% of the theoretical publications. Does the volume of publication indicate progress in our understanding? I am too close to it to judge.

2. Framework

Let us assume that high energy phenomenology has to do mainly with collisions of hadrons at incident momenta above, say 2 GeV/c. Then the framework of gross empirical facts and main theoretical concepts consists of the following:

(i) There exist $SU(3)$ singlets and octets of mesons and singlets, octets and decimets of baryons of a variety of different spins and parities.

(ii) The quantum numbers of the observed meson and baryon multiplets can be generated by the mnemonic of the quark model, with $(\bar{q}q)$ for the mesons and (qqq) for the baryons. [This particular empirical fact will need modification as soon as any "exotic" resonance is firmly established.]

(iii) Two-body and quasi-two-body processes are peripheral, showing peaking at forward directions (small t) and/or backward directions (small u).

(iv) Integrated cross sections, or differential cross sections at fixed momentum transfer, show approximate power law behavior in the energy. In particular, total cross sections seem to become constant asymptotically and obey Pomeranchuk's theorem.

(v) Virtually all occurrences or nonoccurrences of peripherality in a given process (iii) can be understood in terms of the exchanges of the internal quantum numbers of the known $SU(3)$ multiplets of mesons and baryons (i).

(vi) A modest amount of analyticity in the kinematic invariants, plus crossing symmetry, relates the phase of an amplitude at high energies to its power-law behavior, (iv). This connection is more general than, but the same as, that given by Regge pole theory.

(vii) The known mesonic and baryonic states, (i), can plausibly be placed on Regge trajectories and the trajectories are approximately linear in the square of the masses. This gives great impetus to the use of Regge exchanges to unify items (iv), (v), and (vi) into an aesthetically pleasing whole.

In the subsequent sections we explore some of the recent developments in various models and ideas in order to show the diversity of the attempts to cope with ever increasing amounts of data whose quality also improves, as well as to expose some of the limitations, difficulties, and unanswered questions. The existence of proceedings from the Berkeley, Heidelberg, and Vienna Conferences, along with some recent books (for

example, Collins and Squires, 1968; Kokkedee, 1969),* allows me to omit specific references to much of the earlier work, and to assume on your part a knowledge of the state of the art circa 1967.

Van Hove's report at Berkeley (Van Hove, 1966b), with an Appendix by Wetherell, surveys both theory and experiment. Subsequent developments on the experimental side are reviewed at Heidelberg by Di Lella (1967), at the CERN Topical Conference by Colley (1968), Derrick (1968), and van Rossum (1968), among others, and by Bellettini (1968) at Vienna. The theoretical side of high energy collisions is surveyed by Bertocchi (1967) at Heidelberg, by Barger (1968), Biazas (1968), and Salin (1968) at the CERN Topical Conference, and by Chan (1968) at Vienna.

* References are cited in "standard" British fashion, with papers and books listed at the end in a bibliography arranged alphabetically by first author. One abnormality occurs: Proceedings of Conferences are cited fully in a special list at the beginning of the bibliography. This permits an abbreviated entry by author, as, for example, Bellettini, G. (1968). Vienna, p. 329.

II. SAMPLING OF RECENT DATA

Although almost all of the data published since the Vienna Conference were presented there and extensively reported by Bellettini (1968) and others, it is worthwhile, I think, to remind ourselves of the quality and range of data presently available. Accordingly there follows a sampling of data, with only brief comments. Some of these data and others are elaborated on in the subsequent sections dealing with the various models. The data are only representative; they are not necessarily the best and certainly not the worse available.

1. π^-p Elastic Scattering

The data of the Cornell-BNL collaboration (Orear et al., 1968) on π^-p elastic scattering at 9.7 and 13.6 GeV/c are shown in Fig. 2, together with earlier results of experiments at Brookhaven. The noteworthy features are (i) the well-known diffraction peak for $|t| < 0.6$ (GeV/c)², (ii) a secondary convex shoulder leading to a pronounced local minimum at $t \simeq -3$ (GeV/c)², (iii) a relatively flat (e^{At} , $A \sim 0.5$) region from $t = -4$ to -10 , where there may be unresolved structure, and the cross section is of the order of 10^{-5} - 10^{-7} times its value at $t = 0$, and (iv) a steep, but small, backward peak (e^{Bu} , $B \sim 4$). Comparison with data at lower energies shows that the convex shoulder is the remnant of a broad secondary maximum that followed a dip at $t \simeq -0.6$. There is thus a pronounced energy dependence in the shape of the cross section, at least in the energy range up to 10 GeV/c.

Above that, one may be seeing the beginnings of a stabilization of $d\sigma/dt$ towards an energy-independent shape, as expected from some models (see Section IV, 2 below).

2. Nucleon-nucleon elastic scattering

Even more spectacular are the proton-proton scattering data taken at CERN by Allaby et al. (1968a) and shown, along with results at lower energies, in Fig. 3. These results have received widespread attention. Mention need be made only of the apparent tendency at fixed t for the cross section to approach an asymptotic energy-independent value, with the cross sections approaching the limit more slowly the larger the $|t|$ value. The break at $|t| \sim 1 \text{ (GeV/c)}^2$ is the outstanding feature of the data at the highest energy.

Corresponding data for antiproton-proton elastic scattering are shown in Fig. 4 (from Orear et al., 1968). There are three observations here. (i) The diffraction peak at very small $|t|$ is larger and narrower than for proton-proton scattering. (ii) There is structure, perhaps a dip and definitely a shoulder, at $t \simeq -0.6 \text{ (GeV/c)}^2$. This is considerably closer in than the structure seen in the p-p data. (iii) There seems to be a sudden increase in slope again beyond $t \simeq -3 \text{ (GeV/c)}^2$.

3. Inelastic Proton-proton Collisions

A number of experiments have been done on inelastic proton-proton interactions using a missing-mass spectrometer (Ankenbrandt et al., 1968, Allaby et al., 1968b). Figure 5 shows the results of

Allaby et al. (1968 b) on the differential cross section for $pp \rightarrow pN^{*+}$ at 19.2 GeV/c, where the N^* 's are defined by the indicated areas the 1520 MeV and 1688 MeV regions. Beyond $|t| = 1 \text{ (GeV/c)}^2$ the slopes of all the inelastic cross sections are similar to the elastic slope, while for $|t| < 1$, the inelastic cross sections seem flatter than the steep diffractive elastic peak. At lower energies the inelastic cross sections for $N^*(1520)$ and $N^*(1688)$ production tend to be flatter at all momentum transfers than the elastic, the effect being greatest at the lowest energy (Ankenbrandt et al. 1968). It should be recalled in contrast that the mass region around 1400 MeV has long been known to be produced very peripherally. It may be that the small $|t|$ behavior can be understood in terms of the details of the inelastic transition (spin and parity of the resonance, quark model wave function, etc.), and that the large $|t|$ behavior at high energies stems from some common cause for all processes (see Section IV, 2 below).

4. Polarization in π -N and K-N Scattering

Polarized targets continue to be used to provide additional information on the amplitudes that enter into high energy elastic scattering. Limitations on intensity have generally restricted the high energy polarization data to the region $|t| < 1 \text{ (GeV/c)}^2$, but some accurate data at larger momentum transfers are now available. One such set of measurements made at Argonne (Esterling et al., 1968) on π^+p scattering at 5.15 GeV/c is shown in Fig. 6. The range of momentum transfers is $0.2 < |t| < 2.0 \text{ (GeV/c)}^2$. The interesting features are

(i) the approximate reflection symmetry, $P(\pi^+p) \simeq -P(\pi^-p)$, (ii) the quadratic extremum near zero at $t \simeq -0.6 \text{ (GeV/c)}^2$, and (iii) the relatively large polarization for $|t| > 1 \text{ (GeV/c)}^2$. Other data at higher energies show that there is little change in the polarization for $|t| < 0.6 \text{ (GeV/c)}^2$ up to 14 GeV/c (see Fig. 37 of Bellettini, 1968), but that for larger $|t|$ values the polarization probably decreases in magnitude with energy. The rough relation, $P(\pi^+p) \simeq -P(\pi^-p)$, indicates that the polarization is caused mainly by interference between $C = +1$ and $C = -1$ exchange amplitudes with different phases. Since the obvious Regge exchanges are P , P' , and ρ , the near-vanishing of the polarization at $t \simeq -0.6 \text{ (GeV/c)}^2$ correlates nicely with $\alpha_\rho = 0$ and the known dominance of the t -channel spin-flip amplitude B_ρ in the process, $\pi^-p \rightarrow \pi^0n$. The double zero at $t \simeq -0.6 \text{ (GeV/c)}^2$ and the possible behavior of the polarization at larger $|t|$ values, even beyond $|t| = 2 \text{ (GeV/c)}^2$, are discussed in Section III, 2(b), below.

Polarization measurements on K^+p elastic scattering at 1.22 and 2.48 GeV/c by Andersson et al. (1969) throw light on the possible existence of $S = +1$ baryonic states at ~ 1900 MeV and also on aspects of exchange degeneracy and duality. These data are shown in Fig. 7. The positive polarization at 1.22 GeV/c agrees well with a calculation by Lea, Martin, and Oades (1968) without any resonant states (dashed curve) and disagrees with the prediction involving an $I = 1$, $J^P = \frac{1}{2}^+$ resonance at 2020 MeV (solid curve). The higher energy results show a relatively featureless positive polarization that remains remarkably

large at forward angles. The two curves are from a calculation involving a purely imaginary diffractive amplitude (P exchange) and exchange-degenerate spin-flip contributions from ρ and A_2 exchange. (Blackmon and Goldstein, 1969). The solid (dashed) curve has negative (positive) relative sign between the ρ and A_2 amplitudes. The data indicate somewhat better agreement with the negative relative sign, consistent with the duality picture which couples the absence of s-channel resonances in the K^+p channel and the flatness in energy of the total cross section to the cancellation of the imaginary parts of the contributions from exchange-degenerate partners. (See Section V,3 below for more on duality and exchange degeneracy.)

5. Resonance Production

Since bump hunting and related activities occupy a large fraction of the effort in experimental high energy physics (see Fig. 1), selection of a representative experiment is difficult and arbitrary. I have chosen the work of Crennell et al. (1968) on the properties of the $g(1650)$ meson. Their results on the two-pion mass distributions in $\pi^-p \rightarrow \pi^-\pi^+n$, $\pi^-p \rightarrow \pi^-\pi^0p$, and $\pi^+p \rightarrow \pi^+\pi^+n$ at 6 GeV/c are shown in Fig. 8. The upper histograms show the mass distributions, while the lower panels show the mass dependence of the coefficients A_L , $L = 2,4,6$, of the Legendre polynomial expansion of the $\pi-\pi$ "scattering" angular distribution in the two-pion rest frame. Note first one of the characteristics of bubble chamber experiments nowadays, large numbers of events (over 5,000 in $\pi^-\pi^+n$, 3000 in $\pi^-\pi^0p$, 1200 in the "blank" run of $\pi^+\pi^+n$).

The $Q = 2$ $\pi\text{-}\pi$ system is featureless with a smooth mass plot and A_2 coefficient. The $Q = 0$ configurations show strong ρ^0 and f^0 signals, as well as a small but clear bump at 1.6 GeV (the g meson). The $Q = 0$ Legendre polynomial coefficients behave in just the manner expected for the known spins (1^- and 2^+) of the ρ^0 and f^0 . In A_2 there is evidence for resonant behavior at 1.6 GeV, but nothing is seen in A_4 or A_6 for $Q = 0$. In view of the background under the small peak at 1.6 GeV, the absence of signals in A_4 and A_6 is not surprising.

The $Q = -1$ configurations reveal a strong ρ^- and a reasonable g^- peak. [In passing we note that there is no sign of a peak in the f^0 mass region. This means that there is no $I = 1$ $\pi\text{-}\pi$ state (ρ') degenerate with the f^0 , at least not with appreciable elastic width.] Again the behaviors of the A_L below 1 GeV are consistent with a ρ spin of 1^- . In the region of the g , all three coefficients seem to show resonant structure, although A_6 cannot be taken too seriously. The quantitative behavior is in agreement with $J^P = 3^-$ (or greater, e.g. 5^- , 7^-) for the g -meson.

6. Tests of Quark Model Predictions on Decay Correlations

One of the most peculiar phenomena in high energy physics is the continuing success of the "realistic" quark model. The use of quarks as a mnemonic has widespread acceptance, but the idea of dynamic or even kinematic considerations with "real" quarks leaves some segments of our community cold. Nonetheless, intrepid theorists push the model further

and, further. One area of prediction is that of joint decay correlations in double resonance production (Biazas and Zalewski, 1968). These predictions have been tested in several experiments (Alderholz et al., 1968 b; Bockmann et al., 1968; De Baere et al., 1969; Friedmann and Ross, 1969). Figure 9 shows a portion of the results of Friedmann and Ross (1969) on $K^-p \rightarrow \bar{K}^*\Delta$ at 2.6 GeV/c (3300 events). The predictions of the quark model are divided into classes (A, B, C) depending on how many assumptions are made about the individual quark-quark scattering amplitudes. The comparisons shown in Fig. 9 are for the five class A predictions concerning the correlations in the average values of various combinations of powers of the direction cosines of the decay directions of the two resonances. The agreement between model and experiment is very impressive for these predictions which depend only on the assumption of additivity of the quark-quark amplitudes. Class B predictions usually work out well, but the success of the more detailed Class C results is spotty.

The enemies of the quark model may eventually be able to find alternative explanations for these correlations, but in the meantime one must ponder the meaning of such detailed successes.

7. Backward K^+p and K^-p Scattering

One of the empirical facts cited in Section I,2, is that forward or backward peaks occur if, and only if, the quantum numbers allow the exchange of a member of an $SU(3)$ singlet, octet or decimet. K^+p and K^-p backward scatterings afford illustrations of this fact and recent data make it quantitative. For K^+p the u-channel exchange

require $B = 1$, $Y = Q = 0$, $I = 0, 1$. Thus Λ , Σ^0 , Y_1^{*0} exchanges are possible; there should be a modest amount of backward scattering. For K^-p the corresponding quantum numbers are those of the K^+p channel, $B = 1$, $Y = Q = 2$, $I = 1$. A state with such quantum numbers lies outside the known $SU(3)$ multiplets. No good evidence for such states exist (see Section (4) above, and Tripp, 1968, Section 3). Hence the K^-p backward scattering should be negligible at high energies, as should backward peaks in $K^-p \rightarrow \bar{K}^0 n$, $K^-p \rightarrow \bar{K}^* p$, etc.

Lundby and co-workers at Brookhaven (Carroll et al., 1968) and CERN (Baker et al., 1968; Baker et al., 1969; Banaigs et al., 1969) have studied $K^\pm p$ backward scattering at a number of incident momenta from ~ 1.4 GeV/c to 6.9 GeV/c. Some of their results are shown in Fig. 10. The solid points are the cross sections $(d\sigma/du)_{u=0}$ for K^+p , while the open circles (none above 2.5 GeV/c) are for K^-p . The straight lines indicate power-law behavior, as s^{-4} for K^+p and s^{-10} for K^-p . The dashed curves give the behavior of the backward cross sections for $\pi^\pm p$. Two comments here: (a) The s^{-4} dependence for K^+p , corresponding to an effective $\alpha(0) \simeq -1$, seems very reasonable for the exchange of a strange baryon (Λ , Σ^0 , Y_1^{*0}). (b) The very rapid fall-off for K^-p , if it can be shown to hold at higher energies, implying as it does $\alpha_{\text{eff}} \lesssim -4$, has direct bearing on the importance of Regge cuts. This point was made by Chew at the Vienna Conference (p. 364) and is discussed in Section IV,3 below.

report (Bertocchi, 1967). A year later, at Vienna, various ramifications of these questions were being pursued (see Chan, 1968), but at the same time certain difficulties with pure pole models were emerging. These troubles all follow from the hypothesis of factorization of Regge pole residues, a concept firmly rooted in the idea of a pole and in unitarity. If the residue of a Regge pole of definite quantum numbers, including parity, in the amplitude for a transition from state a to state b (the label a specifies the particles and their helicities in state a) is β_{ba} , then factorization of residues requires the residues of the pole for $a \rightarrow b$, $a \rightarrow a$, $b \rightarrow b$ be related according to

$$\beta_{ba}^2 = \beta_{bb} \beta_{aa} .$$

A well-known difficulty occurs with the residues of the ω -trajectory: The conventional analysis of high energy pp and $\bar{p}p$ elastic scattering involves the Regge pole combinations, $(P + P' \pm \omega)$, where the trajectory symbol stands for the corresponding amplitude. Since the differential cross section for $\bar{p}p$ is larger at $t = 0$, and falls more rapidly away from $t = 0$, than the pp cross section, there is a "cross-over" point which is attributed to the vanishing of the residues $\beta^{(\omega)}$ of the ω -trajectory there. Factorization then implies that the residues $\beta_{ba}^{(\omega)}(t) = 0$ at $t \simeq -0.15$ (GeV/c)² for all processes. Inelastic reactions like $\pi N \rightarrow \rho N$ (with an ω -contribution that is difficult to extract) and $K^+ p \rightarrow K^{*+} p$ (with what is believed to be a large ω -contribution) show no sign of a dip that could be

associated with this zero in $\beta^{(\omega)}$. Secondary trajectories (ω') can be invoked to avoid contradiction with factorization, but more likely are Regge cuts in the J-plane.

Another famous example that bears on conspiracies is discussed by LeBellac (1967). The use of a parity-doublet conspiracy for the pion ($M = 1$ pion) in interpreting the forward peaking in $pn \rightarrow np$ and $\gamma p \rightarrow \pi^+ n$ leads, via factorization, to the prediction of a zero at $t = 0$ in the pion's contribution to the amplitude for production of ρ^0 with zero helicity in the process, $\pi^+ p \rightarrow \rho^0 \Delta^{++}$. Data at 8 GeV/c (Alderholz et al., 1968a) show that (a) the great bulk of the ρ^0 's are produced with zero helicity near $t = 0$, and (b) the cross section shows a very strong forward peaking, rather than a dip. Again, the failure of factorization can be avoided by the use of additional unnatural parity trajectories, e.g., A_1 , to give a forward peaking, (Arbab and Brower, 1968) but this leads to further complications with factorization in other processes (unpublished analysis by G. C. Fox). The excellent fits obtained with the absorption model to the shape of the cross section at $|t| < 0.2$ (GeV/c)² and to the density matrix elements for this reaction argue for Regge cuts, as well as poles, as the most plausible explanation (see Section IV,4).

If still more documentation on the limitations of pure pole models is needed, I cite the somewhat more theoretical question of an $M = 1$ pion and PCAC. The $M = 1$ assignment for the pion, deduced from experiment assuming a minimum of poles, was used by Mandelstam (1968a) to derive Adler's self-consistency condition, PCAC, and soft-

pion results. This successful intrusion of S-matrix theory into the domain of current algebras was, however, short-lived. Mandelstam himself (unpublished) and Sawyer (1968) showed that factorization required a decoupling of the $M = 1$ pion, not only for soft-pion processes, but for all processes (see also Arbab and Jackson, 1968). At present there is no evidence which requires an $M = 1$ assignment for the pion (see Section V,2).

2. Recent Developments in Models with Pole Only

In spite of the limitations and difficulties discussed above, phenomenologists (there must be a better name for theorists interested in experiment!) continue to correlate data with models involving the exchange of a small number of Regge trajectories. There are several reasons for this:

(i) The gross features and even some details do seem to be described by trajectories $(P', \omega, \rho, A_2, \pi; N, \Delta)$ identified with more or less well-known sequences of particles, plus the Pomeranchuk trajectory (P) .

(ii) Secondary trajectories (ρ', ω', π') can be used to produce effects akin to more complicated J-plane behavior.

(iii) Pole models with exchanges of $SU(3)$ multiplets can be used to test $SU(3)$ and higher symmetries. Of course, failures of such tests are difficult to interpret if other J-plane singularities are important, similarly for successes. A good example of a relatively straightforward, but systematic and thorough, analysis of a large sample

of high energy data is that of Dass, Michael, and Phillips (1969). They concentrate on $K^{\pm}p$ scattering, but use high-energy data from all sources and FESR to constrain the possibilities.

We now discuss briefly some specific recent applications of Regge pole models.

(a) Dips, front and back

The classic dips seen in $\pi^{-}p \rightarrow \pi^{0}n$ and $\pi^{+}p \rightarrow \pi^{0}\Delta^{++}$ at $t \simeq -0.6$ (GeV/c)² need no discussion. The standard explanation involves the vanishing of a t-channel spin-flip amplitude at the point where $\alpha_{\rho}(t) = 0$. An even more dramatic dip occurs in the backward scattering, $\pi^{+}p \rightarrow p\pi^{+}$, as can be seen in Fig. 11 where the data of Baker et al., (1968) on $\pi^{+}p \rightarrow p\pi^{+}$ at 5.2 and 6.9 GeV/c and $\pi^{-}p \rightarrow p\pi^{-}$ at 6.9 GeV/c are displayed. The curves are the result of a Regge pole fit using the Δ -trajectory for $\pi^{-}p$ and the Δ (determined by isospin rotation from the $\pi^{-}p$ fit) and the N-trajectory for $\pi^{+}p$. The dip at $u \simeq -0.15$ (GeV/c)² is explained as a result of the vanishing of $(\alpha_{N} + \frac{1}{2})$ at that point.* Other Regge pole fits to these and other data have been made by Barger and Cline (1968) and Paschos (1968). One aspect worthy of comment is the empirical evidence from the spectrum of baryonic states that the trajectories

* Called a wrong-signature, nonsense point - see Chan (1968), Section 2, for explanation of these terms and a summary of the behavior of Regge residues at such values of α .

seem to be approximately even in $W = (u)^{\frac{1}{2}}$, even though a priori there is no reason to expect states of opposite parity (remember MacDowell symmetry) to be degenerate. Most of the evidence for $\alpha = \alpha(u)$, rather than $\alpha = \alpha[(u)^{\frac{1}{2}}]$, comes from fitting sequences of states with $W > 0$, but there is the approximate degeneracy of the $I = \frac{1}{2}$, $Y = B = 1$ states of spin-parity $\frac{5}{2}^+$ and $\frac{5}{2}^-$ at ~ 1685 MeV. Extension of the approximately linear Δ -trajectory towards negative u leads to the expectation of a dip (indeed, a zero) in the cross section for $\pi^-p \rightarrow p\pi^-$ at $u \simeq -1.9$ $(\text{GeV}/c)^2$, where $\alpha_{\Delta} + \frac{3}{2} = 0$.^{*} Although the data of Fig. 10 do not extend far enough to cover this region of u , other data (see Fig. 14 of Bellettini, 1968), show no evidence of significant structure all the way out to $|u| = 2.4$ $(\text{GeV}/c)^2$. This discrepancy can, of course, be remedied by modifying the Δ trajectory at negative u values, either by having it asymptotically level off to some negative constant larger than $-\frac{3}{2}$ (Barger and Cline, 1968), by assuming the form $\alpha_{\Delta} = a + b(u)^{\frac{1}{2}} + cu^2$ so that for negative u , $\text{Im } \alpha_{\Delta} \neq 0$ even in $\text{Re}(\alpha_{\Delta} + \frac{3}{2}) = 0$ (Paschos, 1968), or by other, easily conceived modifications.

Another example of structure in the backward direction and its interpretation in terms of Regge exchanges is the process, $\pi^-p \rightarrow K^0\Lambda$. The u -channel quantum numbers are $B = 1$, $Y = 0$, $Q = 1$, $I = 1$, corresponding to Σ -like trajectories, $\Sigma_{\alpha}(\frac{1}{2}^+, \frac{5}{2}^+, \dots)$,

* See footnote on p.19.

$\Sigma_Y\left(\frac{3^-}{2}, \frac{7^-}{2}, \dots\right)$, $\Sigma_P\left(\frac{1^-}{2}, \frac{5^-}{2}, \dots\right)$, and $\Sigma_\delta\left(\frac{3^+}{2}, \frac{7^+}{2}, \dots\right)$. Preliminary data of Michelini et al. (1969) on the backward differential cross section and polarization of the outgoing Λ , are shown in Fig. 12, together with the theoretical curves of Barger, Cline and Matos (1969). The cross section data, and, more dramatically, the polarization, show evidence of structure at $u \simeq -0.7$ (GeV/c)². The Regge pole model, using exchange-degenerate Σ_α and Σ_Y trajectories, gives more than adequate description of the cross section and the large and momentum-transfer-dependent polarization. The change in sign of the polarization at $u \simeq -0.7$ (GeV/c)² is associated in the model with a wrong-signature, nonsense zero at $\alpha_{\Sigma_Y} = -\frac{3}{2}$. Note that the residues are obviously not exchange-degenerate, even though the trajectories are.

(b) Cyclic residues to give structure at large $|t|$

The true believer in Regge poles leaves no application untried, no challenge unaccepted. If there is structure in a cross section at $t \simeq -3$ (GeV/c)², as in the π^-p cross section shown in Fig. 2, he will fit it. Never mind that the model is normally applied to small $|t|$ values, say $|t| < 1$ (GeV/c)². As Magellan rounded the Horn and opened uncharted seas, so Barger and Phillips (1969), two of the most dedicated apostles of the gospel according to Saint Tullio,* have thrust into the large $|t|$ region. The vehicle for generating dips at large $|t|$ is a cyclic residue. There is, on the one hand, evidence for zeros in

* I am unable to locate this saint's name on the recently revised list from the Vatican.

amplitudes at wrong-signature points (e.g., $\pi^- p \rightarrow \pi^0 n$, $\alpha_\rho(-0.6) = 0$; $\pi^+ p \rightarrow p\pi^+$, $\alpha_N(-0.15) = -\frac{1}{2}$). With a relatively flat Pomeranchuk pole, the structure in the average of the $\pi^+ p$ and $\pi^- p$ differential cross sections at $t \simeq -0.5$ and -2.8 (GeV/c)² can be explained by an oscillating residue for the P' trajectory, with zeros at $\alpha_{P'} = 0, -2$ (Booth, 1968; Beretvas and Booth, 1969). These are right-signature points for the P' trajectory. Barger and Phillips use only nonflip t-channel amplitudes for the P and P', both flip and nonflip for the ρ . They postulate linear trajectories and assume that the residues for the P' and ρ behave for negative t as

$$\beta(t) = \xi(t) \sin \frac{\pi}{2} \alpha(t) ,$$

where the $\xi(t)$ is a "smooth function" and the amplitudes are written as

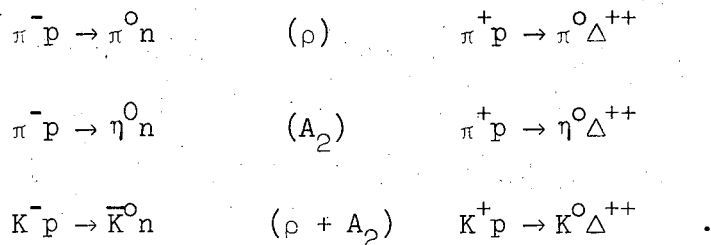
$$A = \beta i^m \exp\left(-i \frac{\pi}{2} \alpha\right) v^{\alpha-n} ,$$

with $m = 1$ for ρ , $m = 2$ for P, P', and $n = 0$ for the nonflip amplitude (A'), $n = 1$ for the flip amplitude (B). For the P trajectory, their slope is so small that $0 < \alpha_P < 1$ for $|t| < 4$ (GeV/c)² and the question of vanishings at $\alpha_P = -1, -3, \dots$ never arises. The curves shown in Fig. 13 illustrate the application of this model to $\pi^\pm p$ elastic scattering and polarization for $0 < |t| < 4$ (GeV/c)². The behavior of the cross section with incident momentum is well reproduced, as are the polarization data of Fig. 6. It should be remarked that the choice of almost the same trajectory for P' and ρ , together

with the cyclic residue assumption for both, causes the double zero in the polarization at $t \simeq -0.6 \text{ (GeV/c)}^2$, and the traversals back and forth across zero in the region, $t \simeq -(2.5 - 2.7) \text{ (GeV/c)}^2$. Polarization data beyond $|t| = 2 \text{ (GeV/c)}^2$ are devilish difficult to obtain, but given the challenge of such interesting predictions, who can refuse to try? Better polarized targets, please!

(c) SU(3) tests and exchange degeneracy

Over the years a number of tests of SU(3) in Regge exchanges have been made, most often on total cross sections. One recent analysis of a set of elastic and inelastic reactions has been made by Mathews (1969). He examined all the data on the six reactions,



The left-hand column contains the "elastic" processes, the right-hand the "inelastic" processes with the final nucleon replaced by a Δ (1236). At high energies the two reactions on each line are believed to proceed in a common manner via the exchange of the Regge trajectories indicated in parentheses between them. Several interesting conclusions emerge from an intercomparison of these processes:

- (i) The trajectory inferred from the "elastic" reaction compares reasonably with that from the less accurate "inelastic" process

for the ρ , but not very well for the A_2 . In particular, while the values of $\alpha(0)$ are in accord, the "inelastic" data imply a much steeper slope for the A_2 trajectory at negative t , steeper even than for the ρ .

(ii) Exchange degeneracy between the ρ and the A_2 trajectories is approximate at best. The $\alpha(0)$ values may differ by as much as 0.2.

(iii) The differential cross sections for the corresponding "elastic" and "inelastic" reactions have remarkably similar shapes.

(iv) The shapes of the cross sections for the three pairs are very different. The first (π^0 in the final state) has a relatively sharp forward peak and a dip at $|t| \simeq 0.6 \text{ (GeV/c)}^2$; the second (η^0) is rather broad and bell-shaped; the third (K^0) process is intermediate in shape.

(v) The assumptions of exchange degeneracy and exact SU(3) vertices allow the prediction of the cross sections for $K^- p \rightarrow \bar{K}^0 n$ and $K^+ p \rightarrow K^0 \Delta^{++}$ from the π^0 and η^0 reactions:

$$\frac{d\sigma}{dt} (K^0) = \frac{1}{2} \frac{d\sigma}{dt} (\pi^0) + \frac{3}{2} \frac{d\sigma}{dt} (\eta^0) .$$

As can be seen in Fig. 14, this test works quite well for the "elastic" reaction, and moderately for the "inelastic" process, when judged relative to the very different t -dependences of the component cross sections.

(vi) Evidence in support of exchange degeneracy in its strong form (for residues as well as trajectories) comes from the decay

correlations of the Δ^{++} in all three reactions. Admittedly with sizeable errors in some instances, all the decay correlations are the same, independent of energy, and in rough agreement with the Stodolsky-Sakurai model.

The anticipated use of neutral K-meson beams at SLAC for the study of collision processes has led Gilman (1969) to examine the connection between the various quasi-two-body processes initiated by K and \bar{K} . The inference from Mathews's work of significant amounts of ρ and A_2 exchange in $K^-p \rightarrow \bar{K}^0 n$ and $K^+p \rightarrow K^0 \Delta^{++}$ means that exchange degeneracy and crossing can be tested by comparison of cross sections and decay correlations for $K^-p \rightarrow \bar{K}^0 \Delta^0$ and $K^0 p \rightarrow K^+ \Delta^0$, for example.

Further remarks on exchange degeneracy are deferred until the idea of duality is described in Section V.

(d) Higher symmetries

In the category of higher symmetries I lump both internal symmetries and their union with external degrees of freedom like spin, and also the Lorentz symmetry of scattering amplitudes at vanishing 4-momentum. About the latter I will say virtually nothing. Both Chan (1968) and Frazer (1968) touched on Lorentz poles at Vienna, remarking that the powerful group theoretical considerations of Toller, Domokos, and others could be duplicated by more pedestrian means, using analyticity and factorization for UU, EU, and EE scattering processes. The question of assignment of the Lorentz pole quantum number M to

physical particles is only slightly clearer, and in a negative way, now than a year ago. As mentioned already in Section III,1, and also in Section V,2 below, there are serious difficulties with an $M = 1$ assignment for the pion and no compelling evidence from experiment favoring it. Explanations alternative to the parity-doublet conspiracy can be found for the forward peaking in $np \rightarrow pn$ and $\gamma p \rightarrow \pi^+ n$. The present status is thus that there is no experimental evidence from collision processes requiring anything except $M = 0$ for all mesonic trajectories.

On the higher internal symmetry front I comment on only one paper, concerned with the six "elastic" and "inelastic" reactions discussed in the last section (Delbourgo and Salam, 1969). These processes, which involve both octets and decimets of baryons, are unified by means of the symmetry scheme, $[U(6) \otimes U(6)] \times O(3)$. This symmetry, with its $U(6)_W$ vertices, is basically the quark model with orbital excitations. The assumption of exchange degeneracy for the ρ and A_2 trajectories and residues allows the description of all six processes with s_0 and an overall scale as the only parameters. How well this model works is shown in Fig. 15, where data on the three "elastic" reactions are compared with the model in the top row and for the "inelastic" processes at the bottom. The comparison is not perfect in all respects, but the authors suggest that their model is a good starting point from which to make improvements (symmetry breaking, absorptive Regge cut corrections, etc.).

A rather extreme extension of this model has been made by Delbourgo (1969) who points out that pion residues singular at $t = 0$ obviate the need for conspiracies, Regge cuts, etc. to explain forward peaks. He finds a basis for such behavior in the composite nature of the pion implied by the quark model, and not surprisingly, is able to fit various data. The violation of traditional ideas on analyticity will make this model difficult for many to swallow.

IV. MULTIPLE SCATTERING, OPTICAL MODELS, AND REGGE CUTS

We have seen in Section II that elastic scattering data (see Figs. 2, 3, 4) can be interpreted as approaching a regime at high energies where $d\sigma/dt$ becomes independent of s and only a function of t . This behavior is reminiscent of the classical scattering of waves by opaque obstacles. Furthermore, the structure seen in the cross sections (dips, changes in slope in different $|t|$ regions, etc.) has similarities to the scattering of fast nucleons by nuclei, where multiple scattering effects are known to be important (Glauber, 1967; Bassel and Wilkin, 1967; and many others). These considerations led Yang and collaborators to explore the use of the concepts of the optical model and multiple scattering in an attempt to understand $d\sigma/dt$ in terms of the extended structure of particles, as evidenced by their electromagnetic form factors.

In a parallel development, the successes of the absorptive model for pion exchange processes and inadequacies in the Regge pole model (described to some extent in Section III, 1) led a number of theorists to consider multiple t -channel exchanges, the most concrete schema being the Regge eikonal model of Arnold (1967).

The formalism of impact parameters and two-dimensional Fourier transforms can be used to discuss all models of high energy scattering at moderate angles. It is not surprising, then, that the model of Chou and Yang (1967, 1968a, 1968b) and of Arnold (1967) bear a formal resemblance to Glauber's theory of the multiple scattering of nucleons by nuclei (Glauber, 1959, 1967), even though the physical bases and

interpretations are quite different. We first present a sketch of the impact parameter formalism, the eikonal approximation, the nuclear optical model, etc., and try to show the differences among the various models. Then we turn to specific applications. We will use the term "multiple scattering" rather loosely, including circumstances where we are merely referring to successive terms in the expansion of $\exp(2i\delta)$ in powers of $(2i\delta)$, as well as real multiple scattering processes, as occur in nuclei. The reader should be aware that this usage is imprecise.

1. Impact Parameter Formalism for Multiple Scattering
and Optical Models

For simplicity we consider small angle elastic scattering and ignore spin. At high energies where many partial waves enter significantly, the discrete partial wave sum can be replaced by an integration over impact parameter $(b \simeq (l + \frac{1}{2})\lambda)$ in a well-known manner. It is convenient to deal with the amplitude,

$$a(\underline{k}', \underline{k}) = \frac{-i}{k} f(\underline{k}', \underline{k}) \quad , \quad (\text{IV.1})$$

where $f(\underline{k}', \underline{k})$ is the center of mass scattering amplitude and k is the magnitude of the momentum in the center of mass. In terms of a , the differential scattering cross section is

$$\frac{d\sigma}{dt} = \pi |a(\underline{k}', \underline{k})|^2 \quad (\text{IV.2})$$

and for diffractive scattering at high energies, a is predominantly real and positive at $t = 0$.

The scattering amplitude a can be represented by the two dimensional Fourier transform,*

$$a(\underline{k}', \underline{k}) = \frac{1}{2\pi} \int d^2b e^{i\underline{q} \cdot \underline{b}} (1 - S(\underline{b})) \quad (\text{IV.3})$$

where

$$S(\underline{b}) = e^{2i\delta(\underline{b})}$$

is the "partial wave" S-matrix and $\underline{q} = \underline{k} - \underline{k}'$ is the momentum transfer ($t = -(\underline{q})^2$). In this approximation, $a = a(\underline{q})$.

* The more familiar expansion

$$a = \int_0^\infty db b J_0(b(-t)^{\frac{1}{2}}) (1 - S(b)) \quad ,$$

comes from assuming $S(\underline{b})$ is independent of azimuthal angle ϕ and performing the angular integration in $d^2b = b db d\phi$. The representation involving $J_0(b(-t)^{\frac{1}{2}})$ is valid at small and moderate angles ($\theta \lesssim 1$). A rough criterion is $|t| < (s/4)$, or $|t|(\text{GeV}/c)^2 < 0.5 P_{\text{Lab}}(\text{GeV}/c)$ for a nucleon target. At larger angles a Bessel representation using $J_0(b k \sin \theta)$ is possible, but then the connection between impact parameter and partial waves is lost.

(a) Scattering of a structureless particle by a potential

If a structureless particle of velocity \underline{v} is scattered by a potential $V(\underline{r})$, the assumption of small-angle deflections (almost linear path) and high energies leads to the following expression for the eikonal $(2\delta(\underline{b}))$:

$$2\delta(\underline{b}) = -\frac{1}{\hbar v} \int_{-\infty}^{\infty} dz V(\underline{b} + \hat{k}z) \quad , \quad (\text{IV.4})$$

where \hat{k} is a unit vector parallel to \underline{k} (or $(\underline{k} + \underline{k}')$), defining the z-axis.

(b) Scattering of a structureless particle by N fixed scatterers

For N fixed scattering centers, located at $\underline{r}_j = \hat{k}z_j + \underline{s}_j$, where \underline{s}_j is the transverse coordinate vector, the wave function of the incident particle accumulates phase from each one of the scatterers according to (IV. 4). Thus

$$S(\underline{b}) = \prod_{j=1}^N e^{2i\delta_j(\underline{b} - \underline{s}_j)} \quad . \quad (\text{IV.5})$$

This expression for $S(\underline{b})$ can be written in a more suggestive and useful form by considering the individual scatterings. The amplitude for the scattering of the incident particle by the j th center of force is

$$a_j(\underline{q}) = \frac{1}{2\pi} \int d^2b e^{i\underline{q} \cdot \underline{b}} \left(1 - e^{2i\delta_j(\underline{b})} \right) \quad . \quad (\text{IV.6})$$

We define the two-dimensional inverse Fourier transform of $a_j(\underline{q})$ [called the profile function by Glauber] by

$$\tilde{a}_j(\underline{b}) = \frac{1}{2\pi} \int d^2q e^{-iq \cdot \underline{b}} a_j(\underline{q}) \quad (\text{IV.7})$$

Then the S-matrix for the j th scattering is

$$e^{2i\delta_j(\underline{b})} = 1 - \tilde{a}_j(\underline{b})$$

and the complete S-matrix for the N fixed scatterers is

$$S(\underline{b}) = \prod_{j=1}^N \left(1 - \tilde{a}_j(\underline{b} - \underline{s}_j) \right) \quad (\text{IV.8})$$

The expansion of this product of N factors leads to Glauber's multiple scattering expansion, with the lowest order terms yielding the impulse approximation and the highest containing N successive scatters, as befits a model with forward collimation.

(c) Scattering of a structureless particle by a composite system,
optical model

For scattering by a composite system the internal motion of the scatterers must be taken into account. The assumption of a short collision time, implied by the other assumptions of the model, allows mere averaging by taking an expectation value of $S(\underline{b})$ for the ground state of the target. If independent particle motion is a reasonable approximation, we obtain

$$\langle i | S(\underline{b}) | i \rangle = \prod_{j=1}^N \int d^3 r_j \rho_j(\underline{r}_j) [1 - \tilde{a}_j(\underline{b} - \underline{s}_j)]$$

where $\rho_j(\underline{r})$ is the probability density for the j th particle.

With the further approximations that all the scatterers are the same (or that we average the different contributions) and that the spatial extension of $\tilde{a}_j(\underline{b})$ is small compared to the distances over which $\rho_j(\underline{r})$ changes appreciably, we obtain

$$\langle i | S(\underline{b}) | i \rangle \simeq \left[1 - \frac{2\pi \bar{a}(0)}{N} D(\underline{b}) \right]^N, \quad (\text{IV.9})$$

where $\bar{a}(0)$ is the average forward ($q = 0$) amplitude for an individual scattering and the two-dimensional density,

$$D(\underline{b}) = \int dz \rho(\underline{b}, z), \quad (\text{IV.10})$$

is a measure of the interacting matter encountered by the incident particle passing through the system at impact parameter \underline{b} . In (IV.10), $\rho = N\rho_j$ is the total density of interacting matter. For a large nucleus the approximation of $N \rightarrow \infty$, but ρ independent of N , is legitimate. Then (IV.9) becomes the standard optical model result,

$$\langle i | S(\underline{b}) | i \rangle \simeq \exp \left(-2\pi \bar{a}(0) D(\underline{b}) \right). \quad (\text{IV.11})$$

This type of formula plays an important role in the interpretation of the data on coherent photoproduction of ρ^0 mesons in nuclei and the

extraction of interesting quantities like $\sigma(\rho N)$ and $\gamma_0^2/4\pi$ (see Lohrmann (1969); Drell and Trefil, 1966; and as one specific example, McClellan et al., 1969). Another interesting application is to the coherent production of A_1 mesons from nuclei (Goldhaber et al., 1969). The inferred magnitude of the total cross section $\sigma(A_1 N)$ is such as to argue against the Deck mechanism wherein the A_1 is merely a π and a ρ produced in close proximity, but with little interaction.

(d) Scattering of one composite system by another

If the incident particle itself is a composite system the formulas of the preceding sections have simple modifications. The S-matrix (IV.8) has the generalization,

$$S(\underline{b}) = \prod_{j=1}^N \prod_{j'=1}^M \left[1 - \tilde{a}_{jj'}(\underline{b} + \underline{s}_{j'} - \underline{s}_j) \right], \quad (\text{IV.12})$$

where $\tilde{a}_{jj'}(\underline{b})$ is the inverse Fourier transform of the amplitude for scattering of constituent j in one composite by constituent j' in the other. If we are considering the elastic scattering of He^3 on He^4 or a realistic quark model, we proceed by taking expectation values of (IV.12) with respect to the nuclear ground states (see Czyz and Maximon, 1969, for specific examples).

If we view hadrons as extended objects, made up of finely divided interacting "stuff", we proceed differently. Imagine that the numbers, N and M , of constituents in each hadron become very large.

Correspondingly, the strength of the constituent-constituent scattering becomes very small, with \tilde{a}_{jj} , proportional to $(N \times M)^{-1}$. Then the first nontrivial term in the expansion of $S(\underline{b}) = e^{2i\delta(\underline{b})}$ can be equated to the sum of single-scattering terms on the right-hand side of (IV.12). * With assumptions paralleling those made in going from (IV.8) to (IV.11), we obtain

$$2i\delta(\underline{b}) = -K_{AB} \int d^2b' D_A(\underline{b} - \underline{b}') D_B(\underline{b}') , \quad (\text{IV.13})$$

where K_{AB} is a complex interaction parameter for the propagation of composite A through composite B, and D_A and D_B are the two-dimensional densities of interacting matter defined by (IV.10). If one of the densities is taken to be very highly localized, we recover the optical model result (IV.11) for a structureless particle propagating through a medium.

* This corresponds to neglecting the scattering of one infinitesimal constituent in one composite by more than one constituent in the other composite. Examination of (IV.12) shows that for $N, M \rightarrow \infty$, $\tilde{a}_{jj} \propto (NM)^{-1}$, this procedure is legitimate. The k th term in the multiple scattering series, (IV.15), below, is then the sum over all possibilities of the simultaneous scattering of k pairs of uncorrelated constituents, one member of a pair from each composite.

(e) Multiple scattering series and its inverse

It is instructive within the continuum approximation (as represented by (IV.13), or in the original (IV.3)) to expand $S(\underline{b})$ in powers of $\delta(\underline{b})$ so that the "multiple scattering" series (infinite now) can be exhibited. With the definition,

$$\Delta(\underline{q}) = -\frac{1}{2\pi} \int d^2\underline{b} e^{i\underline{q}\cdot\underline{b}} [2i\delta(\underline{b})] , \quad (\text{IV.14})$$

one finds

$$a(\underline{q}) = \Delta(\underline{q}) - \frac{1}{2!} \Delta(\underline{q}) \otimes \Delta(\underline{q}) + \frac{1}{3!} \Delta(\underline{q}) \otimes \Delta(\underline{q}) \otimes \Delta(\underline{q}) - \dots , \quad (\text{IV.15})$$

where

$$F(\underline{q}) \otimes G(\underline{q}) \equiv \frac{1}{2\pi} \int d^2\underline{q}' F(\underline{q} - \underline{q}') G(\underline{q}') , \quad (\text{IV.16})$$

is a convolution in momentum space. The corresponding expansion for $\Delta(\underline{q})$ in terms of the scattering amplitude is

$$\Delta(\underline{q}) = a(\underline{q}) + \frac{1}{2} a(\underline{q}) \otimes a(\underline{q}) + \frac{1}{3} a(\underline{q}) \otimes a(\underline{q}) \otimes a(\underline{q}) + \dots . \quad (\text{IV.17})$$

We note that $\Delta(\underline{q})$ is analogous to the Born approximation for potential scattering, or to the impulse approximation in the scattering of nucleons by nuclei. For potential scattering with a real phase shift $\delta(\underline{b})$, the successive terms in (IV.15) have phases such that the odd terms are imaginary and alternate in sign, while the even terms are

real and also alternate in sign. For the more realistic limit of real $\Delta(q)$, successive terms are real and alternate in sign, giving the possibility of interference minima, as seen in the data. If $\Delta(q)$ is approximated by a Gaussian, $\Delta(q) \propto e^{-\lambda q^2}$, it is easy to show that the n th term in (IV.15) is proportional to $e^{-\lambda q^2/n}$. Successive terms in the "multiple scattering" series thus tend to give flatter and flatter contributions that dominate at larger and larger angles.

Detailed studies of the convergence of the multiple scattering series and other aspects of the Glauber approach have been made recently by Czyz and Maximon (1969) and by Kofoed-Hansen (1969). I refer you to these papers for information on how reliable it is to terminate the series (IV.15) after only a few terms.

2. Chou-Yang Model, Hybrid Model, and Multiple Pomeron Exchanges

(a) Chou-Yang model

The model of Chou and Yang (1967, 1968a, 1968b), and the earlier models of Wu and Yang (1965) and Byers and Yang (1966), are based on the idea of hadrons as extended objects whose ability to interact is given by a well-defined density $D(\underline{b})$. For definiteness, the electromagnetic form factors are used as the indicator of how the ability to interact is distributed in space. Thus, the hadronic density $D(\underline{b})$ to be employed in (IV.13) is given by

$$D(\underline{b}) = \frac{1}{2\pi} \int d^2q e^{-iq \cdot \underline{b}} F_{em}(t = q^2) , \quad (IV.18)$$

and the first term in the "multiple scattering" series (IV.15) is

$$\Delta(q) = (\text{constant}) \times [F_{em}(q^2)]^2, \quad (\text{IV.19})$$

as can be verified from (IV.13) and (IV.14).^{*} For particles with spin there is some ambiguity as to what electromagnetic form factor to use. Chou and Yang choose the Dirac form factor, $F_1(q^2)$, for proton-proton scattering.

A number of calculations have been made with the Chou-Yang model. The originators themselves made two empirical fits to the high energy p-p scattering data for $|t| < 1 \text{ (GeV/c)}^2$ and then used the expansion (IV.17) to deduce the momentum transfer dependence of the electromagnetic form factor of the proton. They showed that the higher terms in (IV.17) were important only for $|t| \gtrsim 1 \text{ (GeV/c)}^2$, and that the inferred electromagnetic form factor of the proton was in general agreement with experiment for $|t|$ values as large as 20 (GeV/c)^2 .

*

It should be noted here that the approximate relation,

$$\frac{d\sigma_{AB}}{dt} \simeq (\text{const}) |F_{em}^A(q^2) F_{em}^B(q^2)|^2,$$

holding at small $|t|$ values, was arrived at from the quark model by Van Hove (1966a), and earlier by Wu and Yang (1965) for large $|t|$ values.

Of more immediate interest to us are the calculations of Durand and Lipis (1968), comparing the asymptotic Chou-Yang differential cross section for p-p scattering with data of 11 to 30 GeV/c incident momenta and $0 < |t| < 16 \text{ (GeV/c)}^2$. These are shown in Fig. 16. The solid curves are those of the model, while the dashed curves give the trends of the experimental data, shown in more detail in Fig. 3. The curves are calculated with a "dipole" form factor, $F_{em}(q^2) \propto (\mu^2 + q^2)^{-2}$, with $\mu^2 = 1 \text{ (GeV/c)}^2$. Curve a has a real constant, K_{pp} , in (IV.13), chosen to give the correct asymptotic total cross section for p-p interactions ($\sim 36 \text{ mb}$). Curve b has a complex constant K_{pp} , with the ratio of real to imaginary part chosen to yield the experimental value of $\alpha = \text{Re } f(0^\circ) / \text{Im } f(0^\circ)$ at 26 GeV/c. The presence of the complex interaction parameter washes out the deep diffraction dips and gives structure at $|t| \sim 1.3 \text{ (GeV/c)}^2$ remarkably like that seen at 20 GeV/c in Fig. 3. It is worth noting that within the framework of this model the deep diffraction minima are expected to become more and more visible as the incident energy increases, but if α vanishes slowly (eg., $(\ln s)^{-1}$) the approach to "infinite energies" may be rather slow.

While discussing the connection between the electromagnetic form factors and hadron-hadron scattering, mention should be made of the specific model of Abarbanel, Drell, and Gilman (1968, 1969). These authors return to the idea of Wu and Yang (1965) that the large angle scattering of hadrons is related directly to the electromagnetic form

factors. They propose a model with an empirical diffractive contribution at small t , presumed to be generated by normal hadronic dynamics, plus an elementary local current-current interaction whose manifestation at large $|t|$ is via the vector and axial vector form factors measured in electromagnetic and weak processes. Care is taken to incorporate the requirements of unitarity, at least approximately. One result of this is the observation that the deep minima of curve a in Fig. 16 may be a consequence of the neglect of direct channel unitarity in the Chou-Yang model.

Inelastic processes, corresponding to excitation of the collision partners without change in internal symmetry quantum numbers (G, I_3^2, I_3, Y, B), are discussed by Chou and Yang (1968b). Selection rules for these diffractive excitation processes are inferred by imagining that the densities $\rho(r)$ in $D(b)$, (IV.10), are not c-numbers, as assumed so far, but rather are quantum mechanical operators. These operators can cause excitation of the incident particles, but not transfer of internal attributes like charge or hypercharge. The selection rules are those obtained by assuming that the diffractive mechanisms can transfer only orbital angular momentum and its associated parity.

(b) Hybrid model

The basic idea of the Regge eikonal model of Arnold (1967) is that the eikonal phase shift, (IV.4) or its generalizations, is given by the sum of the Fourier transforms of the relevant t -channel Regge pole exchange amplitudes which provide the "potential". This means that

the first term, $\Delta(q)$, in (IV.15) is given by the sum of the Regge pole amplitudes themselves. Successive terms in the multiple scattering series then provide corrections presumably important at larger angles, as already described.

Chiu and Finkelstein (1968a,b) proposed a hybrid model, containing the Chou-Yang model at infinite energy, but having corrections at finite energies from Regge poles whose $\alpha_i(0) < 1$. In Regge pole language, the hybrid model fits into Arnold's framework with a set of "normal" Regge poles (P', ρ, ω, A_2 , etc.), plus a fixed pole at $J = 1$ instead of the Pomeron. The "Born term" for the multiple scattering series is thus

$$\Delta(s, t) = \Delta_{\text{diff}}(t) + \sum_j \beta_j(t) e^{-\frac{i\pi\alpha_j(t)}{2}} \left(\frac{s}{s_0}\right)^{\alpha_j(t)-1}, \quad (\text{IV.20})$$

where $\Delta_{\text{diff}}(t)$ is the diffractive Chou-Yang amplitude and the sum is over the remaining Regge poles.*

The presence of the Regge contributions in (IV.20), with their s dependences and their t -dependent phases, means that at finite energies the multiple scattering series (IV.15) will yield cross sections quite different in detail from the asymptotic behavior exemplified by curve a in Fig. 16. Calculated cross sections for p-p scattering,

* Note that $\beta_j(t)$ is real for odd-signatured amplitudes and purely imaginary for even-signatured amplitudes.

where the P' and ω trajectories dominate, are shown at several energies in Fig. 17. At 25 GeV/c there is no sign of a dip at $t = -5.8 (\text{GeV}/c)^2$ and only a shoulder, rather than a deep minimum, at $t \simeq -1.3 (\text{GeV}/c)^2$, in agreement with the data shown in Fig. 3. By 200 GeV/c incident momentum the calculated curves show clearly discernable minima at $t \simeq -1.3$ and $-5.8 (\text{GeV}/c)^2$, as well as some shrinkage towards the asymptotic shape. Another feature is the explanation of the "cross-over" effect (see Section III, 1) for p - p and \bar{p} - p scattering without requiring the residue of the ω Regge pole to vanish at $t \simeq - (0.15-0.20)(\text{GeV}/c)^2$.

Essentially the same hybrid model was used by Arnold and Blackmon (1968) to discuss πN scattering and polarization. They used a dipole for the electromagnetic form factor entering (IV.19) and included the P' and ρ Regge poles. The spins of the nucleons were handled in the impact parameter formalism in the way described by Arnold (1967). Generally good agreement with all available data on differential cross sections and polarization is found for incident momenta above roughly 5 GeV/c and $|t| < 0.5 (\text{GeV}/c)^2$. The cross over effect at small $|t|$ is obtained provided all the ρ -exchange amplitudes vanish at $\alpha_\rho = 0$ (ρ chooses nonsense).

(c) Multiple Pomeron exchanges

The Pomeron or vacuum trajectory has occupied a special position in the hierarchy of Regge poles because (i) it is the highest lying trajectory, (ii) its slope seems abnormally small

($\alpha'_p \simeq 0-0.3 \text{ (GeV)}^{-2}$), and (iii) there are serious doubts that it is a simple Regge pole. Some of the doubts concern the apparent slope and the lack of particles to associate with this trajectory; other stem from a belief that diffractive scattering is a complicated shadowing effect, far more involved than the exchange of a single Regge pole. The Chou-Yang and hybrid models make a clear distinction between diffraction and the exchange of other quantum numbers—they contain a degenerate Pomeron trajectory of zero slope. The other extreme is to assume that the Pomeron is a normal Regge pole with an ordinary slope, but that multiple scattering corrections are important. The observed flat trajectory is then a consequence of approximating the multiple scattering series (IV.15) by a single Regge pole amplitude. Frautschi and Margolis (1968a,b) consider this approach, simplifying their model to include only the Pomeron trajectory in (IV.20), and of course omitting $\Delta_{\text{diff}}(t)$. They obtain an elastic cross section which, at any one energy, resembles those of the Chou-Yang or hybrid models. But because of the finite slope [$\alpha'_p(0) \simeq 0.8 \text{ (GeV/c)}^{-2}$] the whole diffraction structure exhibits shrinkage. Present data are probably consistent with either behavior. Presumably, 70 GeV/c data from Serpukhov will begin to determine whether there is appreciable s dependence to $d\sigma/dt$ above 30 GeV/c.

Two perhaps bothersome points should be mentioned here concerning the picture of multiple P exchanges. With $\alpha_p(0) = 1$ and $\alpha'_p(0) > 0$ the "Born term", $\Delta(t)$, in (IV.15) is real and positive at

$t = 0$, but has a small positive imaginary for moderate physical $|t|$. The double scattering term, with its convolution over physical t values, will subtract off a term that has its phase in the first quadrant. This means that at $t = 0$, the first correction to $\Delta(0)$ diminishes it in magnitude and gives it a negative imaginary part. The total cross section will thus approach its asymptotic value, $4\pi \Delta(0)$, from below, and $\alpha = \text{Re } f(0^\circ) / \text{Im } f(0^\circ)$ will be positive. Neither of these predictions agree with data at $\sim 20-30$ GeV/c. Perhaps the incorporation of lower Regge poles, as in the hybrid model, will remove these difficulties. If so, the predicted behavior of $\sigma_t(s)$ and $\alpha(s)$ should set in at higher energies (another reason for still more powerful accelerators!).

While on the subject of multiple Regge exchanges, mention should be made of the Reggeon graph techniques of Gribov (1967b). The methods encompass the multiple scattering models discussed above and generate alternating signs for the successive terms in the multiple Reggeon exchange series, just as in (IV.15), as well as the behavior of $\sigma_t(s)$ and $\alpha(s)$ just described. Another application of multiple P exchange is that of Ansel'm and Dyatlov (1967) who show that at large $|t|$ there are oscillations produced in $d\sigma/dt$.

3. Cuts in the J-plane

The fact that Regge poles are not the only singularities in the complex angular momentum plane has been known for a long time. I refer you to Chapter V and VII of Collins and Squires (1968) for some of the details and references to the literature. Mandelstam (1963)

showed that there was every reason to expect that, in addition to Regge poles, there would be Regge cuts in the J-plane. Such a cut will give a contribution to a transition amplitude of the general form,

$$A(s, t) = \int_{-\infty}^{\alpha_c(t)} dJ \left(\frac{s}{s_0} \right)^J \text{disc } A(J, t) , \quad (\text{IV.21})$$

where $\text{disc } A(J, t)$ is proportional to the discontinuity of the partial wave amplitude across the cut and $\alpha_c(t)$ is the end point of the cut. If the discontinuity behaves as $[\alpha_c(t) - J]^n$ at the end point it is easy to show that the large s behavior of the amplitude is

$$\lim_{s \rightarrow \infty} A(s, t) \propto \frac{s^{\alpha_c(t)}}{\left[\ln \left(\frac{s}{s_0} \right) - \frac{i\pi}{2} \right]^{n+1}} , \quad (\text{IV.22})$$

where the phase in the denominator comes from keeping track of the phase of the signature factor.

The most popular way to generate Regge cuts is to allow multiple Regge pole exchanges. The location of the end point $\alpha_c(t)$ depends on the details of the trajectories of the poles exchanged. For the simple case of two linear trajectories, $\alpha_1(t) = \alpha_1(0) + \alpha_1'(0)t$, $\alpha_2(t) = \alpha_2(0) + \alpha_2'(0)t$, the expression for $\alpha_c(t)$ is

$$\alpha_c(t) = \alpha_1(0) + \alpha_2(0) - 1 + \frac{\alpha_1'(0) \alpha_2'(0)}{\alpha_1'(0) + \alpha_2'(0)} t . \quad (\text{IV.23})$$

We note that the slope of the cut is smaller than either slope (if $\alpha'_i > 0$). The intercept at $t = 0$ is generally below the lower of the two intercepts, but for one of the trajectories having $\alpha(0) = 1$, the intercept of the cut and the other pole coincide.

At first glance it would seem easy to establish empirically the presence of a Regge cut. All one needs to do is examine the high energy behavior and identify the presence of the logarithm in (IV.22). In order to disabuse you of that idea I display in Fig. 18 the absolute square of one power of the logarithm from (IV.22). Over presently accessible energies the standard methods of extracting a Regge trajectory from a cross section would be unable to see the logarithmic dependence and would infer instead an effective α value roughly $\Delta\alpha = -0.25$ below whatever s^α was present. The actual situation will undoubtedly be more involved. On the theoretical side, the logarithmic dependence shown in (IV.22) may not set in until quite high energies. And in any given process there may be a combination of effects, with a pole perhaps dominating at small $|t|$ and the cut or cuts only contributing (by virtue of their smaller slopes) at moderate or large $|t|$. Then the equivalence of the logarithm to an additional factor of $s^{-\frac{1}{2}}$ in the amplitude will only mask the flatter slope of the cut and simulate a

continuation of the trajectory of the pole.* Multiple Regge pole exchanges give higher powers of logarithms in (IV.22), but also flatter slopes to the end point of the cut.

If the logarithmic manifestations of the cuts are not identifiable in the energy dependence, how can one expect to verify their presence? One place to look is in a process where the exchange of a single Regge pole of normal quantum numbers is forbidden (Phillips, 1967a). A good example of such a reaction is backward K^-p scattering, discussed in Section II, 7. The u-channel exchange must have $B = 1$, $Y = Q = 2$, $I = 1$. This is provided by the exchange of a proton or Δ and a K^+ or K^{*+} . The effective $\alpha(0)$ for $Y = \pm 1$ meson exchanges is

* An apparent counter-example to my pessimism about extracting evidence for the existence of Regge cuts is given by Huang and Pinsky (1968). Their Fig. 1 displays an effective $\alpha(t)$ for p-p elastic scattering that is qualitatively similar to model calculations made by Rivers (1968) and can be taken as showing shrinkage according to single P exchange for $|t| < 5 \text{ (GeV/c)}^2$, double P exchange for $5 < |t| < 12 \text{ (GeV/c)}^2$, etc. While this is suggestive, it does not correspond quantitatively to the multiple scattering calculations (Section 2(b), (c)), for which the successive P exchanges begin at much smaller values of $|t|$.

$\alpha_{K^*}(0) = -0.25 \pm 0.25$, while the corresponding intercept for the Δ is $\alpha_{\Delta}(0) \simeq +0.15$. The end point of the Δ -K or Δ -K^{*} cut should therefore have an intercept, $\alpha_c(0) \simeq -1.1 \pm 0.3$, leading to a power law behavior of $s^{-4.7}$ in the cross section if allowance is made for the logarithm in (IV.22). This can be contrasted with the empirical s^{-10} dependence seen in Fig. 10 for incident momenta from 1.8 to 3.5 GeV/c. If the cross section continues its precipitous fall with increasing s ,^{*} the only conclusion open to us is that, for this reaction at least, multiple Regge pole exchanges and their associated cuts in the J-plane are unimportant.

While the unambiguous verification of the presence of cuts in the J-plane is difficult, their importance is indicated in a number of ways. In Section III, 1, we described some of the problems with models employing only poles - the need for conspiracies, the breakdown of factorization of pole residues, etc. Regge cuts were suggested, first on a purely empirical basis, as an alternative. The literature here is extensive. We cite only two representative examples:

(i) Polarization in π -p \rightarrow π^0 n (de Lany et al., 1967; Chiu and Finkelstein, 1967): The ρ pole amplitude interferes with a cut amplitude of different phase to produce polarization.

(ii) Forward peaking in $np \rightarrow pn$ and $\bar{p}p \rightarrow \bar{n}n$ (Kaidalov and Karnakov, 1968): The π and ρ pole amplitudes vanish at $t = 0$; interference with the cut amplitude, assumed to come from the exchange of π and P trajectories, gives a sharp forward peak just like the fits using two conspiring poles (Phillips, 1967b).

* Michael (1969) estimates ~ 5 GeV/c as the momentum at which the double exchange contribution should begin to dominate.

The evidence for important contributions from Regge cuts in the J-plane, while circumstantial, is quite convincing to me. Theory expects and needs them; experiment is more comfortable with them. There is, however, the suggestion of a peculiar absence of a cut contribution in K^-p backward scattering. Is it possible that the only important Regge cut amplitudes come from Pomeron exchange in addition to an ordinary Regge pole?

4. Absorptive Model Recipe for Generating Regge Cuts

One of the difficulties with Regge cuts is the lack of knowledge of the discontinuity function in (IV.21). At present there is no really satisfactory way to estimate the cut discontinuities, although some progress is being made via the multiperipheral bootstrap. The standard approach is to use the ideas of the absorption model (Jackson, 1965), or equivalently the Regge eikonal model with a sum of Regge poles as the Born approximation. The generalization of (IV.3) for inelastic processes in which the transition interaction is treated in lowest order, but full account is taken of the elastic scattering in the entrance and exit channels (the analog of the DWBA of nuclear physics) is

$$a_{ij}(s, t) = \frac{1}{2\pi} \int d^2b e^{iq \cdot b} e^{i\delta_i(b)} \tilde{\Delta}_{ij}(b) e^{i\delta_j(b)}, \quad (\text{IV.24})$$

where $\delta_i(b)$ and $\delta_j(b)$ are the elastic scattering phase shifts (complex at high energies) for the channels i and j , and $\tilde{\Delta}_{ij}(b)$ is

the inverse transform (IV.7) of the lowest order transition amplitude (to be approximated by a few Regge poles). Use of the equation above (IV.8) for the elastic phase shifts leads to the approximate expression*

$$a_{ij} \simeq \Delta_{ij} - \frac{1}{2}(a_{ii} \otimes \Delta_{ij} + \Delta_{ij} \otimes a_{jj}) \quad , \quad (\text{IV.25})$$

with the convolutions defined by (IV.16). This result can also be obtained from the "multiple scattering" series (IV.15) by assuming that $\Delta(q)$ is a matrix with a large diagonal part and small off-diagonal elements. Equations (IV.24) or (IV.25) are the basic formulas of the absorption model and have been used with considerable success for processes dominated by pion exchange. They also serve as the starting point for the generation of Regge cut amplitudes. Clearly the absorption model, the multiple scattering models described in Section 2, and models with Regge poles and cuts are all closely related, differing in their input for the elastic and inelastic amplitudes. Equation (IV.25) is essentially the first two terms in the "multiple scattering" series (IV.15); this is expected to be a good approximation in the small $|t|$ region.

Amati, Stanghellini, and Fubini (1962) showed that the convolution implied in (IV.25) generated an amplitude possessing cuts in the J-plane. Indeed, consider (IV.16) in the spirit of (IV.25) where

* If $\delta_i = \delta_j$, (IV.25) follows exactly from (IV.24).

one of the amplitudes is elastic scattering, and approximate $F(q)$ by an exponential in $q^2 = -t$,

$$F = AC \exp\left(-\frac{A}{2} q^2\right) . \quad (\text{IV.26})$$

Here A and C may be energy dependent (if F represents P exchange, for example, $A = 2\alpha'_P(0)[\ln(s/s_0) - i\pi/2]$ and $C \propto s^{\alpha_P(0)-1}$). With $G = G(s, q^2)$ it is straightforward to show that (IV.16) can be written as

$$F \otimes G = \frac{AC}{2} \int_{-\infty}^0 dt' e^{\frac{A}{2}(t+t')} I_0[A(tt')^{\frac{1}{2}}] G(s, t') . \quad (\text{IV.27})$$

If $G(s, t')$ is a Regge amplitude with a factor $(s/s_0)^{\alpha(t')}$, a change of variable will cast (IV.27) into the form (IV.21) with a definite expression for disc $A(J, t)$. Spins can be incorporated as in the impact parameter version of the absorption model by replacing $I_0(z)$ by $I_n(z)$, where $n = |\lambda - \mu|$ is the net s -channel helicity flip in the transition.

Equations (IV.25) and (IV.27), or closely related expressions, form the basis for numerous calculations of peripheral processes with "absorbed" Regge poles (Cohen-Tannoudji, Morel, and Navelet, 1967; Schrempp, 1968; White, 1968; Michael, 1968; Rivers and Saunders, 1968; Henyey et al., 1968; Henyey, Kajantie, and Kane, 1968; Jackson and Quigg, 1969; Kajantie and Ruuskanen, 1969). A number of these papers address themselves to the polarization seen in πN charge exchange to

which we referred above (see also Arnold and Blackmon, 1968), as well as the shape of the differential cross section. These are two viewpoints here. One is that the basic Regge pole amplitude Δ_{ij} in (IV.25) should be a traditional amplitude with appropriate factors to cause it to vanish at "nonsense" J values ($J < |J_z|$). The presence of one such factor, $\alpha(t)$, in the $B^{(-)}$ amplitude is, of course, the customary explanation of the dip in the πN charge exchange cross section at $t \simeq -0.6 \text{ (GeV/c)}^2$. If $G(s, t')$ in the convolution (IV.27) changes sign in the region of integration, there will be cancellation in the integral and the resulting cut amplitude will tend to be small. Thus the absorptive correction will cause only modest changes from the pure pole term. Dips will still be mainly a consequence of the structure of the pole amplitude itself. An alternative view, espoused by Henyey et al. (1968), is that in the presence of absorptive corrections all prior notions about sense-nonsense factors should be discarded. This idea draws support from the work of Jones and Teplitz (1967) and Mandelstam and Wang (1967) who showed that the standard arguments for the presence of sense-nonsense factors fail because the residues become singular at wrong-signature nonsense points when the third double spectral function is present.* In any event, if $G(s, t')$ has no α factors and so does

* We will see below, in Section V, 3, that exchange degeneracy may bring back the factors of α in spite of this argument. There is also some question as to the necessity of singular residues (i.e., multiplicative poles) (Oehme, 1968).

not change sign, the cut integral (IV.27) will be much larger. Then the mechanism for a dip in the cross section is the destructive interference between the pole and cut amplitudes, as shown schematically in Fig. 19. This kind of behavior is closely connected to the effects seen in Figs. 16 and 17 for the Chou-Yang and hybrid models.

The choice between structureless pole amplitudes, plus sizeable absorptive corrections, leading to structure in cross sections, and pole amplitudes with the standard α factors, plus more modest absorptive corrections, will not be clear for some time, if ever. I personally favor the more conservative idea that the pole amplitudes possess the sense-nonsense factors, partly from prejudice and partly because of the successes of exchange degeneracy in correlating the presence or absence of direct channel resonances with the Regge poles in the crossed channels (see Section V,3).

One important point should be made about $t = 0$. There are a number of processes ($pn \rightarrow np$, $\gamma p \rightarrow \pi^+ n$, $\pi^+ p \rightarrow \rho^0 \Delta^{++}$) that appear to be dominated by the exchange of a single Regge pole (in the examples listed, the pion). In some of these processes, the amplitude of the single Regge pole must vanish at $t = 0$ for kinematic reasons (see Bertocchi, 1967). The differential cross section is then expected to vanish in the forward direction. The observations show, on the contrary, sharp forward peaks. Such peaks find a natural explanation in terms of absorptive corrections. The cut amplitude (IV.27), being a convolution over t' , is smoothly varying and nonzero at $t = 0$. The

pole amplitude increases away from $t = 0$, causing destructive interference and a sharply falling cross section. This mechanism explains all the sharp forward peaks and avoids the difficulties of conspiracies (Section III, 1).

5. ASF Unitarity Corrections versus Absorptive Corrections

The generation of Regge cuts in the ASF multiperipheral model occurs through the application of unitarity in the s -channel. If the many particle intermediate states are assumed to give rise to the Regge pole, it is perhaps plausible to consider only the quasi-two-body channels as intermediate states in the unitarity equation where the individual amplitudes are given by Regge pole exchanges. If this is done, then in the usual high-energy, small angle approximation the unitarity equation reads

$$\operatorname{Re} a_{ij} \simeq \operatorname{Re} \Delta_{ij} + \frac{1}{2}(a_{ii} \otimes \Delta_{ij}^* + \Delta_{ij} \otimes a_{jj}^*), \quad (\text{IV.28})$$

where there are real parts instead of imaginary parts because of our definition (IV.1). In the approximation that $a_{ii} = a_{jj}$ we have unitarity and absorptive corrections giving the following different expressions for the modification of the real part of the amplitude,

$$\operatorname{Re} a_{ij} - \operatorname{Re} \Delta_{ij} \simeq \begin{cases} \operatorname{Re}(a_{ii}^* \otimes \Delta_{ij}) & (\text{two-body unitarity}) \\ -\operatorname{Re}(a_{ii} \otimes \Delta_{ij}) & (\text{absorption}) \end{cases} \quad (\text{IV.29})$$

Finkelstein and Jacob (1968) observed that, to the extent that the elastic amplitude a_{ii} is real, these two corrections are equal in magnitude, but opposite in sign. Various comparisons with experiment—the sign of the polarization in πN charge exchange, the forward peakings in $np \rightarrow pn$ and $\gamma p \rightarrow \pi^+ n$, the general success of the absorption model for pion exchange—favor the second sign in (IV.29) (Finkelstein and Jacob, 1968; Rivers and Saunders, 1968).

The fact that the two-body unitarity correction of ASF gives the wrong sign empirically is no cause for alarm. It has been appreciated for some time that the use of two-body unitarity at high energies means that the cut in the J-plane implied by the ASF correction is on an unphysical sheet of the energy variable. Mandelstam (1963) showed, in fact, that on the physical sheet the ASF cut is cancelled by contributions from many-particle intermediate states in the unitarity equation (see Collins and Squires, 1968, p. 128 ff and p. 183 ff). There are more complicated diagrams, suggested by Mandelstam, that do give rise to Regge cuts. These diagrams involve four or more particles in the intermediate state and resemble multiple scatterings of the constituents of composite systems via Regge exchanges. The sign of the correction term from these diagrams is the same as the absorption model sign in (IV.29), and in agreement with Gribov (1967b). It is interesting to note that a multiperipheral bootstrap using unitarity may generate self-consistent Regge singularities with the absorptive sign for the cut, provided the production amplitudes have absorptive corrections to begin with (Caneschi, 1969).

Another method of applying the constraints demanded by unitarity is used by Jacob and Pokorski (1969) to study elastic scattering. The first order corrections are similar to those of the absorption model or the Glauber multiple scattering series, but higher order terms are different. This analysis shows that the absorption recipe, (IV.25), or the double scattering term in (IV.15), are useful first order unitarity corrections, but cannot be expected to form the basis of a rigorous treatment of unitarity.

V. FINITE ENERGY SUM RULES AND DUALITY

The subject of finite energy sum rules (FESR) or generalized superconvergence relations is a large one with several aspects. Fortunately it has been covered by both Chan (1968) and Frazer (1968) at Vienna and by Horn (1969) and Dietz (1969) at Schladming. The early developments of the concept of duality were discussed at Vienna by Harari (1968) and the more recent aspects at Schladming by Jacob (1969). Lipkin (1969) has, of course, described the use of FESR, exchange degeneracy, and duality in his discussion of resonances. The existence of these reviews allows me to concentrate on those aspects that bear directly on models for high energy processes, omitting much interesting material on bootstraps and resonances.

1. Equations and Basic Results

The use of fixed momentum transfer dispersion relations and asymptotic behavior in order to correlate low and high energy properties dates back to Igi (1962). Two historical observations can be made here. The first is that Igi was concerned with using his sum rule as a test of whether Regge cuts existed in the J-plane. The second, more personal, observation concerns a conversation with Professor Chew in Urbana in late 1961 or early 1962 in which he described Igi's work, then just beginning, whereby Igi was subtracting out the Pomeranchon contribution from the forward dispersion relation for

$$C^{(+)}(\nu) = A^{(+)}(\nu) + \nu B^{(+)}(\nu).$$

The dispersion relation for $C^{(+)}(\nu)$ is divergent without subtractions and the hope was that, once the P

contribution was removed, the then convergent integral would yield the threshold scattering length. I said, "Geoff, if that works, I'll really begin believing in Regge poles." Professor Chew went home and nothing was heard for six months. Then Igi's letter appeared; the trick had not worked; Igi had discovered the P' trajectory instead! Much has happened in the intervening seven years. I now believe in Regge poles, and also Regge cuts. The interesting question of whether FESR can distinguish poles from cuts is touched on in Section 2 below.

(a) Standard formulas for FESR and CMSR

For two particle processes it is convenient to use the variables, $\nu = (s - u)/4m$ and t , where m is the mass of the target. The amplitudes $A^{(\pm)}(\nu, t)$, even and odd under $(s - u)$ crossing ($\nu \rightarrow -\nu$), are assumed to satisfy fixed t dispersion relations in ν :

$$A^{(\pm)}(\nu, t) = \frac{1}{\pi} \int_0^{\infty} d\nu' \operatorname{Im} A^{(\pm)}(\nu', t) \left[\frac{1}{\nu' - \nu} \pm \frac{1}{\nu' + \nu} \right], \quad (\text{V.1})$$

where the ν' integral has discrete (pole) contributions for $0 < \nu' < \nu_{\text{th}}$ and continuum contributions for $\nu > \nu_{\text{th}}$. Equation (V.1) is equivalent to Cauchy's theorem applied to a function that is analytic in the cut ν plane, apart from isolated poles on the real axis. There are several ways of getting from (V.1) to a FESR. One is to observe that an amplitude with power law behavior in ν and definite crossing properties satisfies the dispersion relation, (V.1). Now suppose that

for $|v| > v_1$ $A^{(\pm)}(v, t)$ can be written as an expansion in Regge poles (or power law terms):

$$A^{(\pm)}(v, t) = R^{(\pm)}(v, t) \quad (|v| > v_1) \quad , \quad (V.2)$$

where *

$$R^{(\pm)}(v, t) = \sum_j \beta_j(t) v^{\alpha_j(t)} \left\{ \begin{array}{l} i - \cot \frac{\pi}{2} \alpha_j \\ i + \tan \frac{\pi}{2} \alpha_j \end{array} \right\} . \quad (V.3)$$

Then the difference, $\Delta(v, t) = A(v, t) - R(v, t)$, satisfies (V.1) and vanishes for $|v| > v_1$. Furthermore, the integrand on the right-hand side of (V.1) vanishes for $v' > v_1$. By considering $v > v_1$ and expanding the denominators in (v'/v) , this dispersion relation for $\Delta(v, t)$ yields the set of integer-moment, finite-energy sum rules (FESR):

$$\int_0^{v_1} dv v^n \text{Im} A^{(\pm)}(v, t) = \int_0^{v_1} dv v^n \text{Im} R^{(\pm)}(v, t) , \quad (V.4)$$

where $n = 0, 2, 4, \dots$ for $A^{(-)}$ and $n = 1, 3, 5, \dots$ for $A^{(+)}$.

* Note that $R^{(+)}$ and $R^{(-)}$ have different Regge poles contributing. When spins are present, α_j may be replaced by $(\alpha_j - m)$, where m is a positive integer depending on the t-channel helicities

$[m = \max(|\lambda|, |\mu|), \lambda = \lambda_1 - \lambda_3, \mu = \lambda_2 - \lambda_4]$.

Since the right-hand side of (V.4) involves only powers of ν , the integral can be done explicitly and one finds

$$\int_0^{\nu_1} d\nu \nu^n \text{Im} A^{(\pm)}(\nu, t) = \sum_j \frac{\beta_j(t) \nu_1^{\alpha_j(t)+n+1}}{\alpha_j(t) + n + 1} \quad (\text{V.5})$$

Another way to obtain (V.5), or its equivalent, is to assume that $A^{(\pm)}(\nu, t)$ is given by an asymptotic form, $A_{\text{asym}}^{(\pm)}(\nu, t)$ for $|\nu| > \nu_1$. Then Cauchy's theorem for $\nu^n A^{(\pm)}$ can be applied around the contour shown in Fig. 20. This yields

$$\int_0^{\nu_1} d\nu \nu^n \text{Im} A^{(\pm)}(\nu, t) = -\frac{1}{2} \text{Re} \int_0^\pi d\theta (\nu_1 e^{i\theta})^{n+1} \times A_{\text{asym}}^{(\pm)}(\nu_1 e^{i\theta}, t) \quad (\text{V.6})$$

If $A_{\text{asym}}(\nu, t)$ is given by the Regge pole expansion (V.3), we recover the right-hand side of (V.5), but (V.6) has the virtue that more complicated asymptotic forms, including Regge cuts, can be evaluated in terms of an integral over a semicircle of radius ν_1 in the complex ν -plane (Michael, 1968). Nothing need be explicitly assumed about the behavior of $A_{\text{asym}}^{(\pm)}$ at small ν .

Continuous moment sum rules are generated by considering dispersion relations for $\nu A^{(+)}$ or $A^{(-)}$, multiplied by a factor, $(\nu_{\text{th}}^2 - \nu^2)^{\gamma/2}$, which is even in ν , real and positive for real

$|v| < v_{th}$, and has the phase $\exp(-i\pi\gamma/2)$ just above the cut for $v > v_{th}$. The finite energy sum rule for $A^{(-)}(v, t)$ is then

$$\int_0^{v_1} dv (v^2 - v_{th}^2)^{\gamma/2} \left[\cos\left(\frac{\gamma\pi}{2}\right) \text{Im } A^{(-)}(v, t) - \sin\left(\frac{\gamma\pi}{2}\right) \text{Re } A^{(-)}(v, t) \right]$$

$$= \sum_j \frac{\beta_j(t) v_1^{\alpha_j + \gamma + 1}}{\alpha_j + \gamma + 1} \left[\frac{\cos(\alpha_j + \gamma) \frac{\pi}{2}}{\cos \frac{\alpha_j \pi}{2}} \right].$$

(V.7)

Here we have assumed that the high energy behavior of given by a sum of Regge poles. For $v A^{(+)}$ the sum rule has the same form, but with $\alpha_j \rightarrow \alpha_j + 1$ (and Regge poles of opposite signature contributing, of course). When γ is equal to an even integer we recover the integer-moment FESR, (V.5). If γ is an odd integer, the left-hand side involves the real part of A - this is a "Gilbert" sum rule.*

(b) Classic results

Equations (V.5) or (V.7) relate the low energy properties of a scattering amplitude, expressed as an integral up to $v = v_1$, to the high energy properties in terms of Regge poles (or perhaps something more complicated). Since the low energy region is often dominated by direct

* Named after Walter Gilbert, a well-known molecular biologist.

channel resonances, while the high energy behavior is given by a few exchanges in the crossed channel. FESR give fruitful constraints on the possible parameters used to describe high energy processes. The classic work of Logunov, Soloviev, and Tavkhelidze (1967), Igi and Matsuda (1967a, b), and Dolen, Horn, and Schmid (1967, 1968) does not need to be described again here. It is sufficient to display in Fig. 21 the famous and elegant figure of Igi and Matsuda, showing the integrands on the two sides of (V.4) for the non-spin-flip, crossing-odd amplitude in πN scattering at $t = 0$. The resonant, low-energy contribution can be expressed in terms of the difference of total cross sections for π^+p and π^-p , while the high-energy side is given by the exchange of a ρ Regge pole. Figure 21 shows that high energy Regge parameters can be determined (in favorable instances like this one), or at least constrained, by low energy experimental data. It further illustrates an important aspect of our present thinking about asymptotic (Regge) behavior, the idea of semi-local averages. The Regge amplitude, extended all the way down to $\nu = 0$, far below the energy where we think of asymptotic behavior as setting in, provides a good average description of the resonance region. The implication here, as we will discuss in Section 3, is that t-channel and s-channel descriptions are complementary in some average sense. This is the essence of duality.

The original applications to πN scattering demonstrated how FESR provide a beautiful insight into the interplay of low energy and high energy behaviors. The main results are

(i) The ρ trajectory is consistent (although not determined well) with the form deduced by fitting high-energy data.

(ii) The sum rule for $\nu B^{(-)}(\nu, t)$ as a function of t demonstrates convincingly that the residue $\beta_{\rho}^{(B)}(t)$ has a linear zero at $t \simeq -0.5$ (GeV/c)², as required by the Regge pole fits to $\pi^{-}p \rightarrow \pi^{0}n$ at high energies.

(iii) The sum rule for $A'^{(-)}(\nu, t)$ as a function of t implies a zero in the residue $\beta_{\rho}^{(A)}(t)$ at small physical t values, consistent with the interpretation of the cross-over phenomenon in $\pi^{-}p$ and $\pi^{+}p$ elastic scattering as being the result of a zero in the ρ residue of A' at $t \simeq -0.2$ (GeV/c)².

(iv) The magnitudes of the residues deduced from FESR are in reasonably good agreement with the range of values used in various parameterizations at high energies, with a large residue for $\nu B^{(-)}$ compared to that for $A'^{(-)}$.

(c) Further results

With the realization that FESR provided powerful constraints on high energy Regge parameters, theorists struck out in all directions hoping to determine trajectories and residues for all important Regge poles. Low energy data on $\pi^{+}N$, $K^{+}n$, and pion photoproduction were used with integer-moment FESR and CMSR to learn about the P , P' , ω , A_2 , N_{α} , N_{γ} , and Δ Regge poles in addition to the ρ . We can only list a representative sample:

(i) Properties of the A_2 deduced from K^+N elastic scattering (Matsuda and Igi, 1967) - The residue* of the A_2 in the nonflip amplitude $A'^{(+)}$ shows a parabolic behavior in t with two zeros in the interval, $0.2 < |t| < 0.5$ (GeV/c)², while the A_2 residue in $B^{(+)}$ has one "ghost killing" zero at $\alpha_{A_2} = 0$ and may or may not have an additional zero near $t = -0.5$ (GeV/c)², depending on the choice of pole term contributions to the low-energy integral.

(ii) Properties of the A_2 deduced from pion photoproduction (Chu and Roy, 1968; Vasavada and Raman, 1968) - The residue of the A_2 in the combination $(A_1^{(-)} - 2m A_4^{(-)})$ is found by the first authors to have a quadratic zero at $t \simeq -0.5$ (GeV/c)², implying an additional factor of $\alpha(t)$ beyond the single power needed for "ghost-killing." The second authors disagree, finding two distinct zeros in the interval, $0.2 < |t| < 0.6$ (GeV/c)².

(iii) Properties of the P' deduced from πN elastic scattering (Barger and Phillips, 1968) - The ratio $\nu B^{(+)} / A'^{(+)}$ is found to be positive and of the order of unity, at least for moderate $|t|$ values, and the P' residue in $A'^{(+)}$ seems to vanish as $\alpha_{P'}^2$ near $\alpha_{P'} = 0$.

(iv) Properties of ω , P' , and A_2 from K^+N elastic scattering (Dass and Michael, 1968a, b) - Integer-moment FESR yield

* When we refer to residues we mean the β 's defined in (V.3), unless otherwise stated.

$(\nu B/A') \sim 1-3(\omega)$, ~ 1 (P'), ~ 10 (A_2), disagreeing with some published Regge pole fits, but yielding the correct sign for K^-p polarization.

The detailed t -dependences of the various sum rules indicate

$$\beta_{P'}^{(A)} \sim \alpha^2, \quad \beta_{P'}^{(B)} \sim \alpha^2; \quad \beta_{A_2}^{(B)} \sim \alpha; \quad \beta_{\omega}^{(A)}$$

has a zero at $t \simeq -0.15$ (GeV/c)², and so does $\beta_{\omega}^{(B)}$, but $\beta_{\omega}^{(B)}$ does not seem to vanish at $\alpha_{\omega} = 0$ (or else the ω trajectory is very flat).

(v) Properties of the P' from πN and KN elastic scattering (Gilman, Harari, and Zarmi, 1968)-With an ansatz concerning the P contribution to the FESR (see Section 3 below), these authors deduce the t -dependence of the P' residues of $A'^{(+)}$ and $B'^{(+)}$ in πN and KN scattering. Their results are shown in Fig. 22. Note that their residues for the $B'^{(+)}$ amplitude differ from those defined in (V.3) by a factor of $\alpha(t)$. For the $A'^{(+)}$ amplitude it is not clear whether the residue is proportional to α^2 or to α times another factor which vanishes at $t \simeq -0.25$ (GeV/c)². For the $B'^{(+)}$ amplitude the πN data, at least, make a clear statement that, in our notation, $\beta_{P'}^{(B)} \sim \alpha$, not α^2 .

(vi) Properties of N_{α} , N_{γ} , and Δ trajectories from fixed- u FESR (Chiu and DerSarkissian, 1968) - The s -channel contributions of πN resonances, plus a t -channel contribution from the ρ , imply residues for the N_{α} and Δ trajectories consistent with the presence of a dip in π^+p backward scattering at high energies and no dip in π^-p (See Fig. 11). The coupling of the N_{γ} trajectory in π^+p scattering is found to be small.

The reader who has paid attention to the details summarized in items (i) - (vi) will have noted certain disagreements among the different analyses. For example, the conclusion of Barger and Phillips (1968) that the P' trajectory chooses the "no-compensation" mechanism* at $\alpha = 0$ is contradicted by the results of Gilman, Harari, and Zarmi (1968). Similarly, the behavior of the residues of the A_2 near $\alpha = 0$ is unclear. These disagreements and uncertainties should not be allowed to obscure the fact that much is learned from FESR. The signs and magnitudes of $(\nu B/A')$, for example, are of great interest. The conclusion that $(\nu B/A') \sim +10$ for the A_2 supports the concept of exchange degeneracy of the A_2 and the ρ (see item (b), (iv) above).

2. What do FESR Actually Prove?: A Case Study of

Pion Photoproduction

One of the most striking applications of finite energy sum rules was the apparent elucidation of the mechanism for the sharp forward peaking in charged pion photoproduction. The data are summarized by Richter (1968) at Vienna and by Lohrmann (1969) here at Lund. Since the exchange of a Regge pion alone leads to a zero in the cross section at $t = 0$, Ball, Frazer, and Jacob (1968) and Henyey (1968) introduced a conspiring trajectory, corresponding to a parity-doublet partner of the pion, in order to fit the data. Such a conspiracy was well received in

* See Table 3 of Bertocchi (1967) for an explanation of these terms.

some quarters because of the implication of a Lorentz pole assignment of $M = 1$ for the pion. We have already discussed some of the difficulties with this assignment in Section III, 1. But at the time these difficulties were unforeseen. Strong independent support for this pion conspiracy came from the application of FESR (Bietti et al., 1968; Roy and Chu, 1968) and then CMSR (DiVecchia et al., 1968a, b; Raman and Vasavada, 1968) to determine the residues and trajectories of the pion and its conspirator from the low-energy data. With the assumption that the small t region is dominated at high energies by the pion (for unnatural parity exchanges) and the conspirator (for natural parity exchanges), the sum rules can be used to deduce $\alpha_{\pi}(t)$, $\beta_{\pi}(t)$, $\alpha_c(t)$, $\beta_c(t)$. The results showed that $\beta_{\pi}(0) \neq 0$ and that $\beta_{\pi}(0)/\beta_c(0)$ had the value required by the conspiracy relation. All this was a happy conjunction of concepts from different parts of high energy theory.

As the difficulties discussed in Section III, 1 became known, the FESR and CMSR results began to be quoted as the only convincing proof of the $M = 1$ assignment for the pion. Indeed, everywhere in peripheral processes where pion exchange appears to dominate, the absorptive model gives a good fit to cross sections and density matrix elements at small $|t|$. This implies that an evasive (ordinary) pion, with accompanying π -P generated cuts, is a more reasonable and plausible model than a pion conspiracy.

Then what about the FESR results on the conspiracy? It is perhaps obvious to the reader that FESR cannot really distinguish among

different models. Equations (V.4) and (V.6) contain the analyticity of fixed- t dispersion relations and the assumption of asymptotic behavior, but they become (V.5) or (V.7) only when it is assumed that the asymptotic behavior is given by a sum of Regge poles. For charged pion photoproduction an explicit demonstration has been given of the lack of discriminatory power of FESR or CMSR (Jackson and Quigg, 1969). It has been known to some for a long time (see Harari, 1967, p. 359) that at $t = 0$, at least, the Born term so dominates the forward dispersion relation that little can be learned about the mechanism responsible for the high energy cross section. Nevertheless, it is a useful exercise to construct explicitly a model which simultaneously fits the high-energy data at small $|t|$ and also satisfies the finite energy sum rules, but does not involve a parity-doublet pion conspiracy. The model involves evasive pion and A_2 poles, modified by absorptive corrections according to Eq. (IV.27). The forward peak results from destructive interference between a Regge cut amplitude and the pion pole contribution which is proportional to t for small t . Once the high-energy fit has been accomplished, the right-hand sides of the FESR or CMSR can be compared with the integrals over the low-energy region. The comparison is shown in Fig. 23, where the solid curves are the low-energy integrals (for $n = 0$ in (V.5) or $\gamma = 0$ in (V.7)) and the dashed curves are from the model with poles plus absorptive cuts. For $|t| < 0.1 \text{ (GeV/c)}^2$ the agreement is satisfactory. In particular, at $t = 0$ the proper conspiracy relationship occurs, but this time because of "conspiring" cuts, not poles.

The dots and open circles in Fig. 23 are indicative of an interesting result of the construction of the model. One can show that, for a large class of models of pion photoproduction involving poles and cuts, the right-hand side of (V.4) or (V.6) with $n = 0$ is approximately equal to $(-\pi v_1/2)\text{Re } A(v_1, t)$ where $A(v_1, t)$ is the appropriate high-energy amplitude, evaluated at $v = v_1$. The agreement of the dots with the dashed curves in Fig. 23 demonstrates this for the particular model in question. The empirical observation that $(d\sigma/dt)$ is closely proportional to s^{-2} implies that all the amplitudes are essentially real at high energies (Phragmén-Lindeloff theorem). Consequently the high-energy cross section is given almost entirely by the squares of the real parts of the amplitudes, and, because of the connection just discussed, these are given by the low-energy sum rule integrals. This allows the construction of a "pseudomodel" in which the cross sections for both unpolarized and linearly polarized photons can be expressed directly in terms of the sum rule integrals over the low-energy region, without the necessity of any explicit model for the high energy behavior. The good agreement of this "pseudomodel" with existing data for $|t| < 0.4 \text{ (GeV/c)}^2$ is a very satisfactory example of the power of analyticity. At the same time it demonstrates clearly the limitations of FESR. Basically it reduces to this: One must know or assume what the model is at high energies. Then FESR can help determine parameters inside the framework of that model, but they are unlikely to be able to discriminate between different models.

3. Duality and its Evolution

(a) Simple duality and Schmid circles

It has already been observed, in connection with Fig. 21, that a Regge amplitude, when extrapolated into the low energy region, provides an average description of the true amplitude. This implies that, at least in some average sense, the s-channel resonances are the t-channel Regge exchanges, and vice versa. This is duality in its simplest and vaguest form. Support for the idea comes from the detailed behavior in t of the ρ Regge residues and the properties of the dominant s-channel resonances in πN charge exchange (Dolen, Horn, and Schmid, 1968). The contributions of the major resonances have zeros at $t \simeq -0.2$ (GeV/c)² in $A'^{(-)}$ and at $t \simeq -0.5$ (GeV/c)² in $B^{(-)}$. These zeros at low and medium energies can be viewed as the cause of the "cross-over" zero in the ρ residue of $A'^{(-)}$ and the "sense-nonsense" zero in the ρ residue of $B^{(-)}$ at high energies.

Further impetus to the idea of duality was given by Schmid's calculation of the s-channel partial wave projections of the $B^{(-)}$ amplitude given by ρ -exchange (Schmid, 1968). These calculations gave resonance-like circles on the Argand diagram, with the energies at the tops of the circles correlating remarkably well with the positions of known πN resonances. Somehow the smooth Regge amplitude contains the s-channel resonances! Much has been published on the interpretation of the Schmid circles. Harari (1968b) discusses most of the work in his Vienna report. Schmid himself gives a rebuttal to his critics (Schmid, 1969b). I mention only two further papers (Chiu and Kotanski, 1969;

Sertorio and Wang, 1969) that illustrate the limitations of the idea. The circles on the Argand diagrams are caused mainly by the changing phase $e^{-i\pi\alpha(t)}$ in the signature factor, but their detailed properties (positions of the "resonances", etc.) depend crucially on what is assumed about the t -dependence of the residues, relative signs of different Regge terms, etc. The general conclusion is that Schmid was lucky and that the best that can be hoped for at present is semi-quantitative agreement, both for the location of resonances and for the behavior of the full amplitude at low energies.

The idea of duality runs counter to the assumptions of the interference model (Barger and Cline, 1967) in which the amplitude is built up from direct channel resonances, plus t - or u -channel Regge pole contributions. A controversy can be traced in the literature on whether or not the interference model involves serious "double counting" (Durand, 1968; Dolen, Horn, Schmid, 1968; Chiu and Stirling, 1968; Barger and Durand, 1968; Donnachie and Kirsopp, 1969). It is not profitable for us to go into the details here. Most, if not all, of the controversy stems from the latitude available in dividing an amplitude into "resonances" and "background." This is particularly relevant for the special treatment of Pomeron exchange, discussed in paragraph (c) below.

(b) Exchange degeneracy and the presence or absence of resonances

It is well known in potential scattering that the presence of Majorana exchange forces causes the force to be different in even ℓ and odd ℓ states, giving rise to two distinct families of bound states

or resonances. Conversely, the absence of exchange forces implies that states with even and odd l values can be treated together. In the language of Regge poles this means that trajectories will be exchange degenerate, with even and odd signature poles (e.g., A_2 and ρ) really being one Regge pole. In particle physics the mechanism is essentially the same. Consider a two-particle-to-two-particle process like $K^-p \rightarrow K^-p$. This reaction can be viewed alternatively in other channels. The three possibilities are called s-channel, t-channel, and u-channel, and for our example are

$$s : K^-p \rightarrow K^-p$$

$$t : K^+K^- \rightarrow p\bar{p}$$

$$u : K^+p \rightarrow K^+p$$

For physical values of the energy in each channel, the other channels can be viewed as providing the ordinary and exchange forces via resonant intermediate states. It is assumed that if there are no resonances in a given channel the corresponding force is weak. The absence of resonances in the u-channel above means that the forces governing the scattering in the t-channel are predominantly ordinary forces. Any resonances formed in the $\bar{K}K$ or $\bar{N}N$ system will therefore be exchange degenerate. Of course, our argument is incomplete because the $B = 0$ system involves many coupled channels, but consideration of nucleon-nucleon scattering leads to the same conclusion since there are no resonances in the NN system. The above argument for exchange degeneracy of mesonic Regge trajectories was first given by Arnold

(1965). It leads, when coupled with the idea of duality, to a remarkably coherent qualitative understanding of the implications of the presence or absence of resonances for high energy amplitudes.

In Fig. 24 are shown the total cross sections for K^-p and K^+p interactions as a function of ν . The presence of numerous resonances in the s-channel and the remarkable absence of structure in the u-channel are clearly visible. How does exchange degeneracy bear on this behavior? At high energies the elastic amplitude for K^-p is customarily described in terms of five Regge poles,

$$A(K^-p) = P + P' + \omega + A_2 + \rho ,$$

where the trajectory symbol stands for the complex amplitude of that Regge pole. For the crossed reaction, K^+p elastic scattering, the odd-signatured amplitudes change sign,

$$A(K^+p) = P + P' - \omega + A_2 - \rho .$$

The concept of exchange degeneracy groups the P' (not the P) with the ω and the A_2 with the ρ . Duality implies that an imaginary part, as evidenced by resonances at low and medium energies, goes along with an imaginary part at high energies. Hence in K^-p and K^-n the imaginary parts of the P' and ω (and also those of A_2 and ρ) must add, while in K^+p they cancel. The K^+p amplitude at high

energies is thus expected to be predominantly real,* apart from the Pomeron contribution. The amplitudes for the charge exchange process, $K^+n \rightarrow K^0p$, will be mainly real. For K^-p processes, on the other hand, one expects at high energies complex amplitudes with t -dependent phases.

Similar arguments on $\pi\pi$ and $\pi\rho$ scattering, and the absence of resonances in the $\pi^+\pi^+$ or $\pi^+\rho^+$ channel, lead to exchange degeneracy between the P' and ρ and the ω and A_2 . We therefore have approximate exchange degeneracy among all four trajectories, P' , ω , A_2 , ρ . The dashed curve on the right side of Fig. 24 is a rough representation, $17 + 16(\nu - m_K)^{-\frac{1}{2}} \text{mb}$, of the average K^-p cross section and is consistent with the idea of a common intercept of $\alpha(0) \simeq \frac{1}{2}$ for all four trajectories. Better evidence comes from $K^-p \rightarrow \bar{K}^0n$ at high energies - exchange degeneracy and $\alpha(0) = \frac{1}{2}$ imply that $d\sigma/dt(0^\circ)$ is given by the optical theorem value, a result in agreement with experiment from 5 to 16 GeV/c (see Fig. 12-A13 of Van Hove, 1966b). For K^+p elastic scattering at $t = 0$ we expect a largely imaginary contribution from the Pomeron and a real contribution from the other trajectories. This is consistent with the data from 4 to 16 GeV/c, summarized by Chien et al. (1969), where the observed $d\sigma/dt(0^\circ)$ is 25-30% larger than the optical theorem value.

* The imaginary part is zero because of the absence of resonances, but the real part is not zero because in a dispersion relation sense the K^+p amplitude (on the left in Fig. 24) receives contributions from the distant K^-p resonances (on the right in Fig. 24).

The assumption of exchange degeneracy for the mesons correlates well with the presence or absence of resonances in the direct channel, and via factorization arguments predicts the decoupling of $f'(1515)$ from pions and of ϕ from $\pi\rho$, in agreement with experiment (and $SU(3)$ magic mixing angles) (Chiu and Finkelstein, 1968c). It should also be noted that the absence of resonances in K^+p implies exchange degeneracy, not only of the mesons, but also of the Y^* baryons in the u-channel. Such degeneracy has potential for the determination of d/f ratios, partial widths, etc., but the complexity of the Y^* spectrum makes conclusions difficult (Schmid, 1969a; Capps, 1969). But all this is Lipkin's territory.

Of more relevance to models for high-energy processes is the discussion of exchange degeneracy and dips in cross sections at wrong-signature, nonsense points by Finkelstein (1969). We remarked in Section IV, 4(c) that the traditional explanation of the dip in the cross section for $\pi^-p \rightarrow \pi^0n$ at $t \simeq -0.5 (\text{GeV}/c)^2$ is put in jeopardy by the presence of fixed poles at wrong-signature, nonsense values of J and the consequent singular residues (Jones and Teplitz, 1967; Mandelstam and Wang, 1967). Finkelstein points out that, independently

of these considerations,* exchange degeneracy assures the presence of the dips. Briefly the argument is as follows. Consider $\pi^+ \pi^+$ elastic scattering with exchange-degenerate P' and ρ trajectories in the t -channel. The absence of direct channel resonances means that the amplitude of $P' + \rho$ is real. At a nonsense point such as $\alpha = -2$, the P' amplitude is real because $\alpha = -2$ is a right-signature point, but the ρ amplitude is purely imaginary. Since the sum is real, the ρ contribution must vanish at $\alpha = -2$. Now consider $\pi^+ \pi^- \rightarrow \pi^0 \pi^0$ where only the ρ enters. The ρ coupling is the same as before, apart from isospin factors, and consequently leads to a vanishing of the amplitude for charge exchange at $\alpha = -2$. The same kind of arguments, along with factorization, establish that the ρ contributions to both $A^{(-)}$ and $B^{(-)}$ in $\pi^- p \rightarrow \pi^0 n$ vanish at $\alpha_\rho = 0$. The empirical fact that the cross section does not vanish at $t \simeq -0.5 (\text{GeV}/c)^2$, but only shows a dip, argues for other contributions, e.g., Regge cuts, as does the existence of polarization. Nevertheless, the successes of duality and exchange degeneracy lead me to conclude that, no matter how important

* The independence of Finkelstein's argument is not completely clear. Matsuda (1969), in his discussion of FESR and bootstraps, claims to show that exchange degeneracy implies the absence of the third double spectral function (which led to the fixed poles at wrong-signature nonsense points), and vice versa. In any event, approximate exchange degeneracy seems to permit restoration of the simple-minded dip mechanism.

cuts are in the detailed interpretation of experiment, the basic Regge pole amplitudes possess, at least approximately, the sense-nonsense and other factors traditionally expected of them. I thus believe that the dip in $\pi^-p \rightarrow \pi^0n$ is probably caused by the presence of a factor of $\alpha_\rho(t)$ in the $B^{(-)}$ amplitude, not by the cancellation between a pole contribution and a cut contribution, as advocated by Henyey et al. (1968), and shown schematically in Fig. 19.

(c) The special role of the Pomeranchon Regge pole

At the beginning of Section IV, 2(c), we commented on the peculiarities of the Pomeranchon trajectory in high energy scattering. In finite energy sum rules it also occupies a special position. It was first observed by Freund (1968), in discussing the FESR bootstrap for $\pi\pi$ scattering, that the narrow resonance approximation works for the $I_t = 1$ amplitude, but fails for the $I_t = 0$ amplitude, because of the presence of the P in addition to the $P'(f^0)$. He suggested associating the P contribution with the background, and identifying the s-channel resonant contributions to the sum rule for the $I_t = 0$ amplitude with the P' trajectory. Soon after, Harari (1968a) made the conjecture that for all processes the normal Regge trajectories (P' , ρ , ω , A_2) are associated in the sense of FESR and duality with the direct channel resonances alone, and that the Pomeranchon is associated with only the background. The two sides of Fig. 24 graphically illustrate this idea. It appears strikingly obvious that the Pomeranchon contribution is present for both K^+p and K^-p , but that K^-p has resonant

contributions superimposed. The almost exact constancy with energy of the total cross sections for K^+p , K^+n , pp , and np follow directly from Harari's hypothesis, as does the approach from above towards constancy at $s \rightarrow \infty$ of the total cross sections for K^-p and other channels possessing resonances at low energy. Exchange degeneracy also emerges, as is obvious from our previous arguments in Section (b).

Gilman, Harari, and Zarmi (1968), and more recently Harari and Zarmi (1969), have analyzed the P and P' Regge poles in πN and KN elastic scattering. The FESR for the background do not serve to determine the P trajectory accurately. But if $\alpha_p(0) = 1$ is assumed, the calculated residue $\beta_p(0)$ agrees quite well with the values from high-energy fits. The results of Gilman, Harari, and Zarmi for the P' residues are shown in Fig. 22 and have already been discussed.

Just as with duality and the interference model, questions have been raised about the division of the low energy amplitude into resonances and background and whether the s -channel background does generate the Pomeron pole in the t -channel (Dance and Shaw, 1968; Donnachie and Kirsopp, 1969). The argument revolves around how one parameterizes the resonances, especially how large one allows the high-energy tails of the resonances to be. Evidence in support of the Harari idea comes from the phase shift analyses of πN scattering. By means of the isospin crossing matrix we can construct linear combinations of s -channel partial wave amplitudes that correspond to $I = 0$ and $I = 1$ in the t -channel. These combinations are

$$f_{l\pm}^0 = \frac{1}{3} \left(f_{l\pm}^{1/2} + 2f_{l\pm}^{3/2} \right) \quad (V.8)$$

$$f_{l\pm}^1 = \frac{1}{3} \left(f_{l\pm}^{1/2} - f_{l\pm}^{3/2} \right)$$

The $I_t = 1$ amplitude should be accounted for entirely by s-channel resonances in every partial wave. The $I_t = 0$ amplitude, on the other hand, should have a smooth, largely imaginary, background in addition to the s-channel resonances. This means that $I_t = 1$ partial waves should execute approximate circles centered more or less around the origin in the Argand diagram, while the $I_t = 0$ partial waves should show the "circles" displaced by a largely imaginary term which changes slowly from partial wave to partial wave. Figure 25 shows the Argand diagrams for the first seven partial waves from the phase shift analysis of Donnachie, Kirsopp, and Lovelace (1968), combined according to (V.8) into $I_t = 0$ and $I_t = 1$ (Harari and Zarmi, 1969). These diagrams show very clearly the presence of something other than resonances in the $I_t = 0$ combinations.

4. Duality Diagrams

The ramifications of duality and the absence of "exotic" resonances can be codified neatly by means of duality diagrams (Harari, 1969; Rosner, 1969). One assumes that all known particles and resonances which appear as internal as well as well as external lines have internal quantum numbers (Q, I, I_3 , Y, B) given by the simple quark model in which mesons are $(q\bar{q})$ and baryons are (qqq) . In drawing a duality

diagram for a given process, each external particle is represented by a line for each component quark, with q lines running in the direction of the particle and \bar{q} lines running oppositely. During the interaction the quark content rearranges itself among the particles. In the diagram, the quark lines, each retaining its identity, trace out this rearrangement and combine in groups to form the outgoing particles. If the diagram can be drawn so that no lines cross, the diagram is said to be planar and exhibits duality in the two channels shown. If the diagram contains lines that cross, it is nonplanar and will possess intermediate states that are "exotic." Planar duality diagrams lead to high energy amplitudes with imaginary parts, while nonplanar diagrams imply purely real amplitudes at high energies.*

Many, if not all, of the predictions based on duality diagrams can be obtained by use of exchange degeneracy, $SU(3)$, factorization, etc. It is a matter of taste which hypotheses one regards as more fundamental. Because the diagrams make no reference to characteristics

* The first use of what amounts to duality diagrams seems to have been made by Imachi et al. (1968) within the context of a semi-realistic Sakaton (quark) model. Arguing directly from the behavior of the high-energy data, as in Section 3(b) above, Imachi et al. conclude that what we have called planar duality diagrams (called H-type by them) lead to imaginary parts at high energies, while nonplanar diagrams (X-type) give purely real amplitudes.

such as spin, it is not clear how one goes beyond the implications of the optical theorem at $t = 0$. Rosner (1969) explicitly states that his derivation of the diagrams from $SU(3)$ couplings applies only to the $A'(v, t)$ amplitude of $(0^-, \frac{1}{2}^+)$ scattering, and requires purely f-coupling of the vector mesons and d-coupling of the tensor mesons to the pseudoscalar mesons in order to get connectedness of the quark lines. Harari (1969), on the other hand, says that he does not know how to include spin effects quantitatively. Nevertheless, he makes predictions about polarizations, implying that the diagrams should apply to all helicity amplitudes for a given process.

Two examples will illustrate the use and limitations of duality diagrams in their present form. For each example we also give arguments based on exchange degeneracy and factorization in order to compare assumptions and predictions. The first reaction is backward $\pi^- p \rightarrow K^0 \Lambda$, for which the experimental cross section and polarization are shown in Fig. 12 along with a Regge fit. The schematic Regge exchange diagram and the duality diagram are given in the top half of Fig. 26. The lower case letters (p, n, λ) denote the three quarks. The duality diagram is a planar one for s-u duality. The implication is thus that the s-channel resonances give an imaginary part to the u-channel Regge exchange amplitude at high energies. This is consistent with the existence of appreciable polarization of the Λ , as seen in Fig. 12, but does not require it. From the point of view of exchange degeneracy and factorization, we do not expect the $\pi \Lambda \rightarrow \Sigma_1$ vertex to satisfy any particular exchange degeneracy requirement because $\pi \Lambda \rightarrow \pi \Lambda$ has

resonances in all three channels. There is thus no expectation of a common overall phase for the A and B amplitudes in $\pi^-p \rightarrow K^0\Lambda$, and every expectation of polarization at high energies. The exchange degeneracy of the Σ_1 trajectories, assumed by Barger, Cline, and Matos (1969), is viewed here as an accident. In any event, their residue functions are far from exchange degenerate.

The second example is the polarization of the Λ in $K^-n \rightarrow \pi^-\Delta$ at forward angles. The relevant diagrams are shown in the bottom half of Fig. 26. The Regge exchanges are the $K^*(890)$ and $K^*(1420)$. The duality diagram is a nonplanar one and implies that the amplitude for $K^-n \rightarrow \pi^-\Lambda$ is purely real at high energies.* If we adopt Harari's viewpoint that both A' and B are real, then we expect no polarization at high energies. Unfortunately, experiments at 3 and 4.5 GeV/c show a large positive polarization of the Λ over a wide range of $|t|$ (Barloutaud et al., 1969; Yen et al., 1969). There are at least two ways out - only the A' amplitude is related to duality diagrams; 3 and 4.5 GeV/c are not high enough energies (unlikely!).

Now we look at this reaction with exchange degeneracy and factorization arguments. The extreme left-hand vertex in Fig. 27(b)

* This process is just one of many in which the transfer of a λ quark from an initial meson to a final baryon inevitably leads to the crossing of quark lines, e.g., $K^-p \rightarrow \pi^-\Sigma^+$, $K^-p \rightarrow \omega\Lambda$. See Table IV of Imachi et al. (1968) and Harari (1969).

presumably satisfies the requirements of exchange degeneracy because there are no $I = 3/2$ resonances in $K\pi$ scattering. For the other vertex ($p\bar{\Lambda} \rightarrow K_1^*$), the standard argument of Arnold (1965) on antibaryon-baryon scattering and no $B = 2$ resonances leads to the expectation of exchange degeneracy for this vertex, too. Then we are left with the same result as Harari. But it is possible that arguments on exchange degeneracy involving antibaryon-baryon scattering are suspect. The duality diagrams for such processes always involve more quarks in the intermediate states than $(q\bar{q})$ or (qqq) , even if lines do not cross. (See Lipkin (1969) for a discussion of these points.) If one considers only duality for meson-meson and meson-baryon scatterings, it is impossible to deduce anything about the $K^*(890)$ ΛN couplings relative to the $K^*(1420)$ ΛN couplings without further assumptions, e.g. d/f ratios for the vector and tensor mesons. We do have the evidence from FESR of the approximate exchange degeneracy of the (ρ, A_2) and (ω, P') residues (Section 1(c)(iv) above) to argue for $(K^*(890), K^*(1420))$ exchange degeneracy by $SU(3)$ analogy. The data quoted above seem to say that this is not true.

5. Duality, The Deck Effect, and Multiperipheralism

The production of a low mass enhancement in the $\pi\rho$ system in the reaction $\pi N \rightarrow \pi\rho N$ by means of a double peripheral mechanism, known as the Deck effect, has made difficult the analysis of the A_1 and A_2 mesons and has occasionally cast doubt on the very existence of the A_1 . Chew and Pignotti (1968a), who coined the name "duality",

observed that this concept makes empty a discussion of whether there is an A_1 or just an enhancement by some peripheral mechanism. Resonances generate and are generated by peripheral exchanges. The Regge (or elementary) pion exchange amplitude is the appropriate high-energy description of the $\pi\rho$ system. When extended down to threshold it provides an average description of that mass region. If the smooth average is large at low mass, duality requires the existence of resonances.

There is an interesting point here in connection with duality and pion exchange (private communication from E. L. Berger, G. F. Chew, and G. Ranft). The Schmid circles that correspond to resonances are generated mainly by the changing phase $e^{-i\pi\alpha(t)}$ in the signature. For pion exchange, however, the immediate proximity of the pion pole to the physical region means that the partial wave projections come from the very small t region and the phase does not change appreciably. The amplitude is mainly real where it matters. This could imply that the A_1 and similar objects (e.g., L meson) generated by pion exchange and having zero orbital angular momentum are less fully developed as resonances than objects like the ρ or the f^0 . They could conceivably be "virtual bound states", that is, poles on the real energy axis of the unphysical sheet, below threshold.

Chew and Pignotti make another point of interest to theorists who wish to calculate the gross properties of multiparticle processes, or who are interested in the effects via unitarity of multiparticle channels on elastic scattering. One of the concerns in the use of Regge

exchanges in multiperipheral models is their lack of validity for small sub-energies where there are known resonances. Duality assures that the Regge exchange represents the low energy behavior, at least in an average sense, and makes it unnecessary even to inquire into the details of the usually messy low mass regions. Duality does even better than that. If the peripheral Deck diagram for the $\pi\rho$ system can give an average description of the A_1, A_2, \dots region, then in the same way a peripheral link between the two pions in the ρ can give an average description of that resonance and its recurrences. Thus, if only average effects are relevant, a complicated n-particle final state involving numerous heavy resonances can be replaced by a multiperipheral Regge exchange diagram involving only the lightest particles in the final state, as indicated in Fig. 27 for a relatively simple example. This allows an enormous simplification in calculation of multiparticle effects.

VI. VENEZIANO MODELS

The single most striking development in high energy theory in the past year is the creation of Veneziano models. With hints gleaned from his participation in extensive work on a FESR bootstrap of $\pi\pi \rightarrow \pi\omega$ (Ademollo et al., 1968), Veneziano (1968) wrote down a relatively simple closed form (Euler's beta function!) for the invariant amplitude for $\pi\pi \rightarrow \pi\omega$. The remarkable properties of this amplitude include possession of resonances at low energy in every channel, Regge behavior at high energies, duality, and crossing symmetry. Despite some limitations to be mentioned below, Veneziano's amplitude answered so many prayers that there has been veritable explosion of papers on the subject, with generalizations and modifications in every conceivable direction. Clearly a proper review cannot be made of such a rapidly developing subject. I can only discuss some of the basic ideas and comment on some of the directions being explored. Here again I am fortunate in being able to refer the reader to Jacob's paper at Schladming (Jacob, 1969), and also to the thorough unpublished notes of Yellin (1968, 1969a) and Sivers and Yellin (1969a).

1. Pion-pion Scattering

While the reaction $\pi\pi \rightarrow \pi\omega$, considered by Veneziano, has the considerable advantage of being purely $I = 1$ and identical in all three channels, it suffers from being difficult to study experimentally and of having the slight complication of spin (of the ω). Of more immediate interest is pion-pion scattering where some of the predictions

Veneziano model can be compared with experiment. The $\pi\pi \rightarrow \pi\pi$ problem has been discussed by Shapiro and Yellin (1968), Lovelace (1968), Shapiro (1969), Kawarabayashi, Kitakado, and Yubuki (1969), Yellin (1969b), and Sivers and Yellin (1969b).

(a) Resonances and Regge behavior

When Bose statistics, isospin conservation, and crossing symmetry are taken into account, the s-channel isospin amplitudes can be written

$$\begin{aligned}
 A_0^s &= \frac{3}{2} \left[F(s, t) + F(s, u) \right] - \frac{1}{2} F(t, u) \\
 A_1^s &= F(s, t) - F(s, u) \\
 A_2^s &= F(t, u)
 \end{aligned}
 \tag{VI.1}$$

where $F(t, u)$ is symmetric in t and u . The presence of only even ℓ values in A_0 and A_2 , and only odd ℓ values in A_1 , is evident from the symmetry or antisymmetry in t and u . If there are to be no $I = 2$ resonances, $F(t, u)$ must not possess poles for positive s , but it can and will possess poles in t and u , corresponding to $I = 0$ and $I = 1$ resonances in the t - and u -channels.*

If exchange degeneracy is assumed, all the resonances lie on one trajectory which is the same for all channels. One further assumes that the trajectory is linear and entirely real (at least at low energies). The resonances are thus approximated by poles on the real axis. This is

* In all of this the Pomeron is ignored, in conformity with the Freund-Harari hypothesis described in Section V,3(c), above.

called the zero-width approximation, and is at odds with the requirements of unitarity. The Veneziano ansatz for $F(s, t)$ is

$$F(s, t) = \frac{-\beta}{\pi} \frac{\Gamma(m - \alpha(s)) \Gamma(n - \alpha(t))}{\Gamma(m + n + p - \alpha(s) - \alpha(t))} + (m \leftrightarrow n), \quad (\text{VI.2})$$

where β is a constant, $m, n, (m \geq n)$ and p are integers chosen so that the amplitude does not possess double poles, and $\alpha(s) = a + bs$ is the real linear trajectory. The ratio of gamma functions in (VI.2) can be written as a polynomial (in the numerator or denominator) times a beta function, and is a trivial generalization of Veneziano's use of the beta function itself. Inspection of (VI.2) shows that when $\alpha(s) = N$ (N a positive integer). $F(s, t)$ has a simple pole in s with a residue that is a real polynomial in $\alpha(t)$ of degree N at most, provided $-n \leq p \leq 0$. Since $\alpha(t)$ is linear in t and t is linear in $\cos \theta_s$, this real polynomial corresponds to resonant partial waves in the s -channel with $L \leq N$. The resonant content of (VI.2) is therefore as shown in Fig. 28. The trajectory $\alpha(s)$ is the leading Regge trajectory with equally-spaced (in M^2) resonances having $L = N$. Accompanying each of these resonances are N other simultaneously resonant partial waves with $0 \leq L < N$. These secondary resonances are loosely called daughters, even though they occur in an equal mass problem where daughters of the Freedman-Wang variety decouple.

In the $\pi\text{-}\pi$ problem the requirement of no resonance at $\alpha(s) = 0$ and a p -wave resonance at $\alpha(s) = 1$ restricts the integers

in (VI.2) to $n = -p = 1$. For simplicity we will also put $m = 1$. It should be remembered, however, that sums of terms like (VI.2) can be used, giving great flexibility (and arbitrariness) in the properties of the daughter trajectories.* For our purposes then, we consider as typical the amplitude, appropriate for $\pi^+\pi^-$ elastic scattering,

$$F(s, t) = -\frac{\beta}{\pi} \frac{\Gamma(1 - \alpha(s)) \Gamma(1 - \alpha(t))}{\Gamma(1 - \alpha(s) - \alpha(t))} \quad (\text{VI.3})$$

The symmetry in s and t means that there is a spectrum of resonances of the form indicated in Fig. 28 in both the s - and the t -channels, but no resonances in the u -channel. The asymptotic behavior of (VI.3) can be inferred from

$$\lim_{|x| \rightarrow \infty} \frac{\Gamma(x + a)}{\Gamma(x + b)} = (x)^{a-b} \quad (|\arg x| \leq \pi - \epsilon) \quad (\text{VI.4})$$

For large s and fixed t this implies the asymptotic form,

$$F(s, t) \xrightarrow[\substack{s \rightarrow \infty \\ t \text{ fixed}}]{} \frac{-\alpha(t) \beta [-\alpha(s)]^{\alpha(t)}}{\Gamma(\alpha(t) + 1) \sin \pi \alpha(t)}, \quad (\text{VI.5})$$

* See, for example, Mandelstam (1968b) for a model with trajectories spaced by two units in angular momentum.

provided we stay away from the real axis in s .^{*} Equation (VI.5) has been written in standard Regge high-energy form in order to display more clearly several features. The first is the power-law behavior, $s^{\alpha(t)}$. The second is the specification of the scale parameter s_0 in $(s/s_0)^{\alpha(t)}$ as the reciprocal of the slope of the trajectory. The third feature is the presence in $F(s, t)$ of the phase $e^{-i\pi\alpha(t)}$, as expected from duality arguments. A final aspect is the factor of $\alpha(t)$ in the numerator. This is the "ghost-killing" factor that eliminates a particle of spin-parity 0^+ from the leading trajectory. If $\alpha(t)$ is the ρ trajectory, this scalar particle would occur at negative t .

To see that the Veneziano construction contains the appropriate signature factors, consider the $I = 1$ t -channel amplitude,

$$A_1^t = F(t, s) - F(t, u) \quad (VI.6)$$

At large s and fixed t this should go over into the standard ρ -exchange Regge amplitude. The asymptotic form of the first term in (VI.6) is given by (VI.5). For the second term we merely note that, with linear trajectories, $\alpha(s) + \alpha(t) + \alpha(u) = D$, where $D = 3a + 4b\mu^2$ is a constant. For large s and fixed t , $\alpha(u) \rightarrow -\alpha(s)$. The

* There are equally spaced poles on the real s -axis out to infinity. This is a flaw of the zero-width approximation. With finite widths these poles would move off on the unphysical sheet and result in smooth behavior above the physical cut at large enough s .

asymptotic form of (VI.6) is therefore

$$A_1^t \xrightarrow[\substack{s \rightarrow \infty \\ t \text{ fixed}}]{\quad} \frac{\alpha(t) \beta}{\Gamma(\alpha(t) + 1)} \left[\frac{1 - e^{-i\pi\alpha(t)}}{\sin \pi\alpha(t)} \right] [\alpha(s)]^{\alpha(t)} \quad (\text{VI.7})$$

This amplitude is the standard ρ -exchange amplitude with negative signature, but with an additional factor $\alpha(t)$ that is present because of exchange degeneracy. The $I = 0$ amplitude in the t -channel has the same form as (VI.7), but with the opposite signature and a numerical coefficient $(-3/2)$.

(b) Detailed properties

We now turn to some of the subtleties of the Veneziano model. The first of these is the question of the elastic widths of the resonances. For $\alpha(s) = N$ the residue of the pole is a polynomial of N th degree in $\alpha(t)$ and therefore in $\cos \theta_s$. This polynomial can be expanded in Legendre polynomials of order $L \leq N$. The coefficients of each $P_L(\cos \theta_s)$ is related to the elastic width of the resonances with angular momentum L at $\alpha(s) = N$. Consequently the relative values of the partial widths for decay into two pions can be determined for all the resonances, even though the total width of each state has been taken to be zero.* The results of one such calculation are shown in Fig. 28,

* This is exactly what one does in calculating to lowest order the decay of an unstable particle, e.g. $K \rightarrow \pi\pi$.

where a reasonable trajectory was chosen (to give the very low energy π - π phase shifts) and the widths are scaled to an elastic width of 112 MeV for the ρ -meson (Shapiro, 1969).

Several things should be noted in this array. The most glaring is a negative width for the $N = 2, L = 0$ state. When one thinks about it, it is obvious that there is no a priori reason why the polynomial in $\cos \theta_t$ should yield a positive coefficient for every Legendre polynomial. I have not seen a completely rigorous proof yet, but it can be shown that if $\alpha(0) > 0.496$ (for physical pion and ρ -meson masses) the $L = 0$ widths are all positive (Shapiro, 1969). For large N and $L < [N \ln N]^{\frac{1}{2}}$ the elastic widths go as

$$b_{N,I}^M \Gamma(N, L) \simeq \frac{C_I \beta N^{a-1}}{\pi \Gamma(a) \ln N} \exp(-L^2/N \ln N), \quad (\text{VI.8})$$

where $C_I = \frac{3}{2}, 1, 0$ for $I = 0, 1, 2$. For $L \gtrsim [N \ln N]^{\frac{1}{2}}$, the behavior of the width is complicated, but it can be shown to fall exponentially towards the value for the leading trajectory, which can be exhibited in closed form (Yellin, 1968) and is asymptotically,

$$b_{N,I}^M \Gamma(N, N) \rightarrow \frac{C_I \beta}{\pi(8)^{\frac{1}{2}}} e^{-(a+4b\mu^2)} \left(\frac{e}{4}\right)^N. \quad (\text{VI.9})$$

For large fixed N , we see that the widths decrease monotonically from $L = 0$ to $L = N$. Thus the positivity of the s -wave widths assures the

positivity of all the partial widths.* Figure 28 shows the beginnings of the decrease in widths as $N \rightarrow \infty$ for fixed L and also along the leading trajectory. In passing, we note that the expressions (VI.8) and (VI.9) imply that the r.m.s. value of L increases with energy as $(s \ln s)^{\frac{1}{2}}$, as is appropriate for a Regge diffraction amplitude.

Another significant aspect of the tabulated values in Fig. 28 is the very large width for the $I = 0$ s-wave resonance at the position of the ρ . This s-wave $\pi\text{-}\pi$ phase shift is known to resonate close to the mass of the ρ -meson, but its width is a subject of some controversy (see Section VIII,1 below). One serious difficulty of the simple Veneziano formula (VI.3) is the prediction of an $I = 1$ p-wave resonance (ρ') at the position of the $f^0(1260)$ with an elastic width roughly equal to that of the ρ -meson. Examination of the center column of Fig. 8, which shows the $\pi\text{-}\pi^0$ mass distribution and Legendre coefficients for the data of Crennell et al. (1968), shows no evidence for a p-wave resonance between the ρ and the g peaks. Estimates of production indicate that if the ρ' is largely elastic it would have been visible in the data shown in Fig. 8 if its width were greater than roughly 15 MeV (Shapiro, 1969). The only escape seems to be that its total width is so large that it is not seen as a discernable bump in Fig. 8. This does not seem very plausible.

* It has been remarked by Yellin (1969b) that, except for (VI.3), each term of the form (VI.2) individually contains an infinite number of resonances with negative elastic widths.

The high energy behavior has been exhibited in (VI.5) and (VI.7). In order to show clearly the interplay of the resonances and the Regge behavior, that is, duality, we display in Fig. 29 the Dalitz-Mandelstam diagram for $F(t,u)$. There are poles in t and poles in u . There are also lines of zeros at negative s , arranged so that there are no double poles simultaneously in t and u . The asymptotic behaviors in the six directions are indicated. Since there are resonances in the t and u channels, the amplitude for large t and fixed u , or large u and fixed t , has an imaginary part to its Regge behavior. For large s and fixed t or u , on the other hand, the Regge amplitude is real because the s -channel has no resonances. For large u or t , and fixed s , the amplitude vanishes faster than any power because there are no Regge poles to be exchanged in the s -channel.

(c) Soft pion results

Although it is somewhat far from models of high energy processes, brief mention should be made of the relation of the Veneziano model of π - π scattering to the low-energy or soft-pion results of current algebra. A remarkable feature of the simple form, (VI.3), is that $F(0,0) = 0$ for $a = \frac{1}{2}$ and $F(4\mu^2, 0) = 0$ for $a = \frac{1}{2}(1 - 4\mu^2/b)$. This means that both A_0^s and A_2^s have zeros near threshold ($s = 4\mu^2$, $t = u = 0$), provided $a \simeq \frac{1}{2}$. This is just the self-consistency condition of Adler (1965). Lovelace (1968) extrapolates (VI.3) off the mass shell in order to conform exactly to Adler's requirements, and then determines the ratio of the $I = 0$ to $I = 2$ scattering lengths in

agreement with the results of current algebra. Since the ratio depends very sensitively on the value of a and the literal off-mass-shell extrapolation can be questioned in view of the approximate nature of (VI.3) as a representation of reality, it may be best to be content with the self-consistency condition alone. A current algebra result that is relatively insensitive to a is the combination of scattering lengths, $L = (2a_0 - 5a_2)/6$. Weinberg's result is $L = 0.10/\mu$ (Weinberg, 1966), while (VI.3) gives $L = 0.11/\mu$ (Shapiro and Yellin, 1968; Shapiro, 1969). Yellin (1969b) discusses these results and a number of other aspects of the connection between the Veneziano model and the algebra of charges and finite energy sum rules.

Lovelace (1968) and subsequently Kawarabayashi, Kitakado, and Yabuki (1969) and Ademollo, Veneziano, and Weinberg (1969) applied the self-consistency condition to deduce mass formulas and coupling constant ratios in general agreement with experiment. In particular, by considering the process, $\pi + A \rightarrow B + C$, Ademollo, Veneziano, and Weinberg showed that Regge trajectories of opposite parity sequences than can be connected by pion emission (e.g., ρ and π , Δ and N) should have the same slope and differ in intercept by an odd half integer. There are several examples that seem to work.

2. Generalizations to n Particles

A number of workers have generalized the Veneziano model to more than four external particles. The essential idea for the generalization to n particles is contained in the 5-point amplitude, found by

Bardakci and Ruegg (1968) and Virasoro (1969). To indicate the idea we first consider the Veneziano model for the 4-point function in terms of the integral representation of the beta function:

$$B(x, y) = \frac{\Gamma(x) \Gamma(y)}{\Gamma(x+y)} = \int_0^1 du u^{x-1} (1-u)^{y-1} \quad (\text{VI.10})$$

In Veneziano's original example, $x = 1 - \alpha(s)$, $y = 1 - \alpha(t)$, but the essential point is that x and y are related to $-\alpha$. The beta function has simple poles in x and y at zero and the negative integers, and no double poles. In terms of the integral representation these poles develop at the ends of the range of integration. They can be exhibited explicitly by integration by parts.

For the 5-particle amplitude there are five independent kinematic invariants. These can be chosen as the squares of the sum of adjacent pairs of the 4-momenta shown on the left in Fig. 30. The requirements of the generalization are that (i) it possess resonances (simple poles) in all possible channels and have crossing symmetry, (ii) it possess simultaneous poles only in those invariants for which a suitable Feynman diagram can be drawn, e.g. the right-hand side of Fig. 30 shows a diagram which can have simultaneous poles in s_{12} and s_{45} , (iii) the residues of poles be finite polynomials in the other invariants (so that there will be a leading trajectory and possibly daughters), (iv) it possess Regge behavior when one or two subenergies become large and the momentum transfers remain fixed.

The recipe for the amplitude is a multiple integral with as many variables as there are allowed simultaneous poles (two for the 5-particle amplitude) and the integrand consisting of a product of factors each of which varies from zero to one on the range of integration, each raised to the power $[-1 - \alpha(s_i)]$, there being as many factors as there are independent subenergies. The 5-particle amplitude is

$$B_5(x_1, x_2, x_3, x_4, x_5) = \int_0^1 du_1 \int_0^1 du_4 \frac{1}{u_5} u_1^{x_1} u_2^{x_2} u_3^{x_3} u_4^{x_4} u_5^{x_5}, \quad (\text{VI.11})$$

where $u_2 = (1 - u_1 u_3)$, $u_3 = (1 - u_2 u_4)$, $u_5 = (1 - u_4 u_1)$, and $x_i = -1 - \alpha(s_{i,i+1})$. The verification of all the duality properties of a Veneziano-style amplitude is left to the reader in consultation with the original literature.

For the general n-particle amplitude methods of construction have been given by Chan (1969), Chan and Tsan (1969), Hopkinson and Plahte (1969), Goebel and Sakita (1969), and Koba and Nielsen (1969). The method of Hopkinson and Plahte is noteworthy because it is an iterative construction and may be useful for approximate forms when n is large.

While the n-particle amplitude is elegant in its manner of exhibiting duality, it is sufficiently complicated that little in the way of application has been made for anything but $n = 4$ (to be discussed below). For the 5-particle amplitude, Białas and Pokorski (1969) have studied the high energy behavior of the amplitude in detail, while Bardakci and Ruegg (1969) have examined processes like $K\bar{K} \rightarrow \pi\pi\pi$ and

$\bar{K}K \rightarrow \bar{K}K\pi$. Bardakci and Ruegg show that the 4- and 5-particle Veneziano amplitudes give consistent results, including the standard mixing angles for ω and ϕ , f and f' , a universal relation for 2^+ and 1^- meson decays, and pure F coupling for the decay $2^+ \rightarrow 1^- 0^-$.

3. Attempts at Unitarization

The most immediate difficulty in applying the Veneziano formula and its generalizations to the real world is the presence of poles on the real energy axis. The zero-width approximation can be employed in limited regions, for example near threshold in the $\pi\pi$ problem where the $I = 0, 1, 2$ phase shifts can be reproduced approximately (Shapiro, 1969; Kawarabayashi, Kitakada, and Yabuki, (1969). If the energy range spans one or more resonances, however, there is obvious trouble. One recipe is to give the trajectory function $\alpha(s)$ an imaginary part (Lovelace, 1968). This generates resonances with finite total widths, as desired, but causes the amplitude to possess resonances simultaneously in all partial waves (ancestors, as well as daughters!), something not desired. Such a procedure is quite ad hoc. It gives equal total widths to all partial waves that resonate at the same mass. An alternative approach to unitarity is to treat the partial wave projections of the Veneziano amplitude as the K-matrix. This suggestion, also due to Lovelace, is in direct analogy with nuclear reaction theory. Unitarity is satisfied in one channel, but at the expense of crossing symmetry (see also Arbab, 1969, for a related proposal for unitarization).

Another attack at the problem of a unitary theory based on Veneziano-like amplitudes has been made by Kikkawa, Sakita, and Virasoro (1969). These authors attempt to develop a diagrammatic approach in which the basic Veneziano amplitude is equivalent to the lowest order term in the normal Feynman calculus. Details are inappropriate at this point. There may, in fact, be very serious shortcomings to this perturbative approach (Bardacki, Halpern, and Shapiro, 1969).

Still another treatment of unitarization is that of Atkinson et al. (1969), details of which are to be presented here at Lund. This is a "nuts and bolts" approach in which the lowest pole or lowest few poles are replaced by a finite cut on the energy axis, the discontinuity across the cut satisfying unitarity. The resulting nonlinear equation is solved by the N/D method. While not entirely ad hoc, this method is likely to lead so far from the original Veneziano amplitude as to make the starting point forgotten (or forgettable).

The most elegant approach to unitarization of the 4-particle Veneziano amplitude is that of Martin (1969). He smears the Veneziano amplitude (VI.3) as follows:

$$\bar{F}(s, t) = \int_{x_m}^1 dx \phi(x) \frac{\Gamma(1 - a - bxs) \Gamma(1 - a - bxt)}{\Gamma(1 - 2a - b(s + t)x)}, \quad (\text{VI.12})$$

where $\phi(x)$ is a positive function that vanishes at the end points of integration. Note that the crossing symmetry is preserved. Martin shows that for a suitable class of functions $\phi(x)$ the poles on the real

axis is s or t move off onto the second sheet, as required. At high energies, the integral in (VI.12) correspond to Eq. (IV.21) with a particular discontinuity function across the cut in the J -plane. The unitarized amplitude thus shows power-law behavior modified by logarithmic corrections, as discussed in Section IV, 3, rather than pure pole behavior.

Clearly the last word has not been said on the creation of a unitary replacement for the Veneziano amplitude, but perhaps the first has. I am personally attracted to Martin's idea, not the least because it leads to cuts in the J -plane.

4. Applications

The applications of the Veneziano model are legion and growing. We give only a sampling. The applications to pseudoscalar meson elastic scattering have been described above. Some other applications are

- (i) $\bar{p}n \rightarrow \pi\pi\pi$ (Lovelace, 1968);
 $\bar{p}p \rightarrow \pi\pi\pi$ (Jengo and Remiddi, 1969).
- (ii) $\pi N \rightarrow \pi N$ (Igi, 1968);
 $KN \rightarrow KN, \bar{K}N \rightarrow \bar{K}N$ (Igi and Storrow, 1969);
- (iii) $\pi N \rightarrow \pi\pi N$ (Wagner, 1969; Roberts and Wagner, 1969);
- (iv) $\pi N \rightarrow \omega\pi N$ (Bender and Rothe, 1969).

The annihilation process $\bar{p}n \rightarrow \pi\pi\pi$ can be viewed as the decay of an isovector pseudoscalar particle of mass $2m_N$ into three pions and hence describable in terms of the Veneziano amplitudes for $\pi\pi$

scattering, suitably extrapolated in the mass of one of the pions. Since the Veneziano form, (VI.2) or (VI.3), depends explicitly only on the linear trajectories, it is natural to assume that the extrapolation is done by altering the connections, $s + t + u = 4\mu^2$, to $s + t + u = \Sigma$, where Σ is the sum of the actual masses involved. The coefficient β of each term can depend on the external masses, of course, but for a single term this represents only a scale change. In analyzing $\bar{p}n \rightarrow \pi^+ \pi^- \pi^-$, Lovelace initially considered a two-term formula,

$$A = -\beta \frac{\Gamma(1 - \alpha(s)) \Gamma(1 - \alpha(t))}{\Gamma(1 - \alpha(s) - \alpha(t))} + \gamma \frac{\Gamma(1 - \alpha(s)) \Gamma(1 - \alpha(t))}{\Gamma(2 - \alpha(s) - \alpha(t))}, \quad (\text{VI.13})$$

but ended up setting $\beta = 0$ in his comparison with experiment. The coefficient of β is our standard $\pi\text{-}\pi$ amplitude (VI.3). The coefficient of γ is a "satellite" term in which the leading trajectory (ρ, f, \dots) is suppressed. Lovelace felt compelled to eliminate the coupling to the ρ and f in this annihilation process because of the apparent absence of an appreciable ρ signal in the data (Anninos et al., 1969).

Figures 31 and 32 show comparisons of some representative aspects of the data with Lovelace's model and with an alternative fit (private communication from E. L. Berger). Both calculations use Lovelace's ansatz for the trajectory function $[\alpha(s_j) = 0.483 + 0.885 s + i 0.28(s_j - 4\mu^2)^{\frac{1}{2}}]$. Lovelace has $\beta = 0$

in (VI.13), while Berger puts $\beta = -1$, $\gamma = 1.95$.^{*} Figure 31 is the mass distribution for the $Q = 0$ combination of $\pi\pi$; it shows peaking at the ρ and f^0 masses, although in Lovelace's model the peaks are caused by the daughters (ϵ and ρ' , ϵ'). Figure 32 shows the decay angular distribution for the $\pi^+\pi^-$ system in the f^0 mass region. There are several points to be made in the comparison of the two models with the data. Firstly it is not surprising that Berger obtains somewhat better fits to the various distributions - he has more parameters. Secondly the experimental data of Fig. 32 show a sharp forward peak that needs an $L = 2$ contribution, present in Berger's model, but absent in Lovelace's. A third point is that neither model does very well in fitting the decay angular distribution in the mass region of the ρ . Finally, without entering into questions of taste, one can say that these figures indicate a certain degree of arbitrariness in the use of sums of terms of the general form (VI.2) in fitting data. Considerably more work needs to be done before we learn how much of the detailed partial wave content of the Veneziano amplitude is really necessary in fitting $\pi-\pi$ distributions in inelastic processes. It is probably significant, however, that the lines of zeros shown in Fig. 29 and the general increase in the amplitude away from the center of the diagram seem to be reflected in the experimental data.

The work of Igi and others on πN and KN elastic scattering is an ambitious attempt to compare the Veneziano model with the great

* Changes in the coefficient of the imaginary part of α by 30% in either direction can be compensated by changes in the ratio β/γ without destroying the fit.

abundance of data available. Many trajectories are necessary and consequently numerous beta functions must occur. There are problems of parity doubling here, as in other applications with spin (e.g. Abers and Teplitz, 1969).

The identification of the partial waves in the Veneziano amplitude with the K-matrix elements is the approach used by Wagner and Roberts and Wagner in their treatment of $\pi N \rightarrow \pi \pi N$. The peripheral production process involves the scattering $\pi \pi \rightarrow \pi \pi$ with one of the pions virtual. The off-mass-shell extrapolation is done as suggested by Lovelace, with the momentum transfer to the nucleon, Δ^2 , appearing only in the expression for t (of the $\pi \pi$ scattering):

$$t = -\frac{1}{2} (s - 3\mu^2 + \Delta^2 - 4q_{\text{on}} q_{\text{off}} \cos \theta) .$$

A direct consequence of this assumption is that the off-mass-shell corrections of the π - π partial wave amplitudes, while more or less standard for $l \neq 0$, are different from unity for the s-waves and not the same for $I = 0$ and $I = 2$. Wagner's paper contains numerous comparisons with experiment for both $\pi^- p \rightarrow \pi^- \pi^0 p$ and $\pi^- p \rightarrow \pi^+ \pi^- n$. There is general agreement with experiment (after adjustment of an arbitrary form factor in Δ^2 and one other parameter in the unitarization procedure). Evidence is presented for the necessity of the specific off-mass-shell corrections for the s-waves at low π - π masses.

VII. SOME ASPECTS OF MULTIPERIPHERALISM

Multiperipheralism has two major aspects - one is as a model for the analysis of many-particle ($n > 2$) final states in high energy collisions and the other is as a model for the $2 \rightarrow n$ amplitude used in the unitarity equation to generate self-consistent Regge singularities for high-energy elastic amplitudes. Both ideas date back to 1962 or 1963, but they have received renewed attention as significant amounts of data on many-particle final states began to accumulate. Present versions of the model involve a chain of Regge pole exchanges, as indicated on the right-hand side of Fig. 27. The experimental and theoretical aspects of many-particle final states and the multi-Regge-exchange model were treated in detail by Chan, Czyzewski, Turkot, and Ratti at the 1968 Cern Conference. In addition, at Vienna Czyzewski (1968) presented a very complete review, while Chan (1968) summarized the salient features deduced from comparison of the model with experiment. Accordingly, I comment only briefly on some of the applications published mainly in the last year. On the subject of multiperipheralism and the generation of self-consistent Regge singularities, my remarks are also brief, partly because Frazer (1968) covered some aspects at Vienna, partly because the technical details are difficult, and partly because results are just beginning to emerge.

1. Three-body and Quasi-three-body Final States

The simplest multi-Regge process is $2 \rightarrow 3$, indicated in Fig. 33. Numerous comparisons between theory and experiment have been made for

this configuration. Examples of the more recent ones are listed below. Before going into specifics, however, a few qualitative observations are in order. The Regge exchanges, a and b , in Fig. 33 are in general different trajectories. Let us suppose that the slopes of the trajectories are not wildly different, but that $\alpha_a(0) < \alpha_b(0)$. It is not difficult to show that the form of the multi-Regge amplitude and the kinematics are such as to cause the mass distribution of particles 3 and 4 to peak near threshold, and the corresponding distribution for particles 4 and 5 to be considerably broader and perhaps peak at higher masses. This is a general effect - it is, of course, the basis of the original calculation of the Deck effect where $a = \pi$, $b = P$, $3 = \rho$, $4 = \pi$, and $2 = 5$. Ranft (1969) has investigated a number of examples in detail, using the duality arguments of Chew and Pignotti (1968) to justify the use of the asymptotic Regge form down to threshold (see Section V, 5). Her specific examples verify the qualitative picture stated above.

If particles 2 and 5 are the same and so are a and 4 , the possibility arises of using either on-mass-shell elastic scattering data or some suitable off-mass-shell extrapolation, instead of the Regge exchange(s) b . This has been done in a number of the calculations and fits nicely into the framework of the multi-Regge model via duality.

Table III contains a representative sample of three-body and quasi-three-body final states which have been analyzed in terms of the double-Regge-exchange model. The configurations and exchanges of

Fig. 33 are tabulated. In some reactions (e.g., $K^+p \rightarrow K^+\omega p$) several diagrams are used; the one listed is then merely an example. The main features to emerge from these comparisons are that use of a Regge amplitude for the pion enhances the peaking at low masses for the two particles on either side of the pion link, and gives rise to appreciable modulations in the Treiman-Yang angular distributions. Both features are in general accord with experiment and are not given by elementary pion exchange. The reader is referred to the references for the numerous mass plots and angular correlations for each reaction.

2. Four Bodies and More in the Final State

The work of Chan and his collaborators at CERN on comparison of the multi-Regge-exchange model with various experiments has resulted in a long series of papers. I mention only the applications to $\pi N \rightarrow N (n-1)\pi$ and $\bar{K}N \rightarrow \Lambda (n-1)\pi$ by Chan, Loskiewicz, and Allison (1968), to $\bar{p}p \rightarrow \pi^+\pi^+\pi^-\pi^-$ by Ranft (1968), and the incorporation of low energy resonances into the model by Plahte and Roberts (1969). A comparison of data on 3, 4, 5, and 6-body final states from K^+p interactions at 5 GeV/c. with the multi-Regge model has been made by Bassompierre et al. (1969). When resonances are included the model agrees reasonably well with experiment.

Two examples of experiments on four-body final states should be cited. The first is the work of Rushbrooke and Williams (1969) on $pp \rightarrow pp\pi^+\pi^-$ at 16 GeV/c. These authors interpret their data in terms of a multi-Regge diagram with the protons as the outer legs and the

pions as the inner legs. The Regge link between the pions is taken as a pion, while the outer links are replaced by the elastic scattering amplitude for $\pi^{\pm}p \rightarrow \pi^{\pm}p$. The various mass plots and momentum-transfer dependences are not sensitive to whether the exchanged pion is elementary or a Regge pole, but the sizeable variation in intensity as a function of Treiman-Yang angle favors the Regge pole description, in agreement with the results on the three-body final state.

The other four-body final state occurs in the reaction, $\pi^{-}p \rightarrow \pi^{-}\pi^{+}\pi^{-}p$, studied by Lipes, Zweig, and Robertson (1969) at 25 GeV/c. The data are searched for evidence of the double-Regge-exchange diagram of Fig. 33 with $1 = 3 = \pi^{-}$, $2 = 5 = p$, and particle 4 decaying into $\pi^{+}\pi^{-}$. The data favor $\alpha_a(0) \simeq \frac{1}{2}$, $\alpha_b(0) \simeq 1$, consistent with known trajectories $(\rho, P'; P)$, and definitely rule out double P exchange as a dominant mechanism. The presence or absence of multiple P exchange bears on unitarity and the multi-peripheral bootstrap, as will be mentioned below.

Before leaving n -particle final states I draw attention to the work of Van Hove (1969) on a new type of phase space plot for longitudinal momentum in multiparticle processes. These new constructions aid in handling the complicated kinematics of a many particle state and exhibiting various aspects of multi-Regge behavior.

3. Particle Spectra in Inelastic Proton-proton Collisions

Our final example of the use of multi-Regge models is the work of Caneschi and Pignotti (1969) on the energy and angular distributions of the pions and protons produced in multi-particle pp

collisions. This application is complementary to the calculations for a specific number of particles in the final state since it is concerned with the inelastic spectra of one particle, summed over all final states kinematically available. Caneschi and Pignotti include both meson and baryon links in their multi-Regge chain and find empirically that the baryon exchanges account for roughly half the cross section.

The relevant diagrams and kinematic quantities are shown in Fig. 34. Diagram (a), at upper left, represents the meson exchange contribution to the proton spectra. The laboratory cross section for this diagram is

$$\frac{d^2\sigma}{dp'd\Omega} \propto \frac{p'^2}{E'p} e^{at} \left(\frac{s}{s'}\right)^{2\alpha_M(t)} \left(\frac{s'}{m^2}\right)^{\alpha_P(0)}, \quad (\text{VI.1})$$

where (E, p) and (E', p') are the incident and outgoing energy and momentum of the proton in the laboratory, t is the momentum transfer squared to the proton and $s' = m^2 + t + 2m(E - E')$ is the mass squared of the unobserved particles. The factor $\exp(at)$ describes the behavior of the Regge residue; the next factor is the Regge propagator of the exchange meson; the last factor describes the Pomeron behavior of the meson-proton total cross section at energy s' (resulting from an approximate summing of all the different final states accessible at energy s'). Equation (VI.1) can fit the small-angle, small-energy-loss region of the proton spectra, but falls off much too rapidly at large momentum transfers.

Large momentum transfers to the proton can be generated by a diagram of the type shown in Fig. 34 (b). The resulting formula for the cross section has the appearance of the product of two expressions like (VI.1), one for the right-hand and one for the left-hand side of diagram (b). The left-hand part is just the same as before, while the right-hand part has the meson trajectory $\alpha_M(t)$ replaced by the baryon trajectory $\alpha_B(t)$ and the Pomeron $\alpha_P(0)$ replaced by $\alpha_A(0)$, a trajectory intercept appropriate for the energy dependence of the total annihilation cross section of a baryon and antibaryon. To obtain the proton spectra a numerical integration over the "masses" squared, s'_ℓ , and s'_r must be performed.

In the interests of simplicity the authors neglect interference terms in the cross section and determine empirically the relative amounts of the two diagrams (a) and (b) necessary to fit the 30 GeV/c data of Anderson et al. (1967). Their choices of the various trajectories are $\alpha_P(0) = 1$, $\alpha_A(0) = 0.5$, $\alpha_M(t) = 0.55 + 0.85 t$, $\alpha_B(t) = -0.38 + 0.2 t$. The resulting fits to the proton momentum spectra at various angles are shown in the upper left-hand corner of Fig. 35. The corresponding spectra for π^\pm at 30 GeV/c, calculated from the lower two diagrams in Fig. 34, are shown at bottom left in Fig. 35. At upper right are some of the same data and calculations, this time displayed as a function of longitudinal momentum for fixed values of perpendicular momentum. The general agreement is quite satisfactory over several orders of magnitude. The very flat

longitudinal momentum distribution for the protons at fixed p_{\perp} is a result, in the model, of a rising contribution from the meson-exchange part and a decreasing contribution for the baryon-exchange term. Since a certain number of parameters have been fed in, it is useful to test the model at other incident energies. The lower right-hand plot in Fig. 35 shows calculations of proton spectra at lower and higher energies. The comparison at 18 GeV/c is reasonable. Predictions are then shown for fixed angle (10 mrad) at 70 and 200 GeV/c.

The success of this particular model hinges on the inclusion of baryon exchanges in the sense shown in Fig. 34. This seems surprising at first, but Caneschi and Pignotti argue that, because multiplicities increase with increasing energy, sub-energies stay roughly constant on the average and hence allow lower-lying trajectories to compete with the leading ones. This leads to a plausible picture of high-energy collisions with forward and backward "fireballs" consisting of a nucleon and an energy-independent number of mesons emitted by the baryon links in the multi-Regge chain, and a cloud of pions originating from the meson links and growing in number logarithmically.

4. Self-consistent Regge Singularities and the Pomeron

The idea that s-channel unitarity can be used to determine in a self-consistent way the parameters of a t-channel Regge exchange is very attractive and has been worked on by many people. Since the original multiperipheral calculations of Amati, Stanghellini, and Fubini (1962) there has been the question of cuts in the J-plane

accompanying the poles. Initially unwanted and proved spurious, the ASF cuts, or at least their counterparts in multi-Regge theory, are with us again and are now respectable. They seem necessary, in fact, as we have already discussed in Chapter IV. Present attempts at the problem divide into two groups, those that try to make the input Regge poles emerge in a self-consistent or bootstrap way and those that aim to generate the Pomeron singularity from the exchange of mesons. Inside each group there is a diversity of techniques. On the technical side we note the generalization of the ASF integral equation to a form suitable for the more complicated dependence on the kinematics that accompanies the multi-Regge exchanges (Chew, Goldberger, and Low, 1969).

In the first category are the works of Halliday and Saunders (Halliday, 1969; Halliday and Saunders, 1969b) and of Chew and Pignotti (1968b) and Chew and Frazer (1969). The first named authors base their calculations on high-energy approximation to the unitarity equation in terms of Sudakov variables (Halliday and Saunders, 1969a; Sudakov, 1956). Chew and collaborators give approximate solutions to the generalized ASF integral equation at $t = 0$. Chew and Pignotti, using the duality ideas described in Section V,5, show that the total cross section arising from a multi-Regge chain with average trajectory intercept $\bar{\alpha}$ has an energy dependence,

$$\sigma_t \propto s^{2(\bar{\alpha}-1)+g^2},$$

where g^2 is a coupling strength characteristic of the internal vertices (averaged over momentum transfers) and related to the average

multiplicity by $\langle n \rangle \approx g^2 \ln s$. If $\bar{\alpha}$ is associated with multiple Pomeron exchange ($\alpha_P(0) \simeq 1$), the constancy of high-energy total cross sections can only be understood if g^2 is very small. Data on multiplicities indicate $g^2 \sim 1$ and therefore imply $\bar{\alpha} \sim 1/2$. If this model has even approximate validity, the conclusion is that multiple Pomeron exchange is not significant.

The incorrect energy dependence accompanying multiple Pomeron exchange has been known for some time (see, for example, Verdiev, Popova, and Ter-Martirosyan, 1964). Kajantie (1968) and Finkelstein and Kajantie (1968) have re-examined the energy dependence of the n-particle production cross sections for both Regge and elementary particle exchanges. For fixed poles ($\alpha_i' = 0$) and for α_{\max} occurring m times in the chain, the energy dependence of the n-particle cross section is

$$\sigma_n \propto (\ln s)^{m-1} s^{2(\alpha_{\max}-1)}$$

For the analogous situation with Regge exchanges ($\alpha_i' \neq 0$),

$$\sigma_n \propto \frac{[\ln(\ln s)]^{m-1}}{\ln s} s^{2(\alpha_{\max}-1)}$$

The energy dependence of σ_n (let alone σ_t) is seen to be unreasonable if the Pomeron is a fixed pole at $\alpha_P = 1$ and it occurs in the chain at all. If the slope of the Pomeron trajectory is finite, σ_n decreases even if $\alpha_P(0) = 1$, and independently of the value of m.

But this decrease is so slow with energy that there will certainly be difficulties with the total cross section. All these arguments favor a limited number of P exchanges, e.g. one. Many physicists favor this conclusion because of an intuitive feeling that the physics attributed to the Pomeron pole is a complicated shadowing phenomenon that should, almost by definition, occur only once in any collision process.

The properties of the output pole and its associated cut in the J-plane are considered by Chew and Frazer (1969). They find a self-consistent solution for the Pomeron pole at $\alpha(0) = 1 - a$ where $a \gtrsim 0.01$, with the end point of the cut at $\alpha_c(0) = 1 - 2a$. The importance of the cut relative to the pole can be expressed in terms of the integral of the discontinuity along the cut relative to the residue of the pole. The ratio of cut to pole is roughly the ratio, $\sigma_{\text{elastic}}/\sigma_{\text{inelastic}}$, which is 20% or less. A similar conclusion about the relative importance of cuts and poles in elastic scattering has been reached by Freund and O'Donovan (1968). The model of Chew and Frazer, with the input a pure pole, generates a pole accompanied by a cut in the J-plane with the sign appropriate for a unitarity correction, rather than an absorptive correction. As already mentioned in Section IV,5, Caneschi (1969) has shown that, if poles, modified by absorptive corrections, are used as input in the production amplitudes, the sign of the cut contribution in the elastic amplitude is that given by the absorptive model. This leads to the hope that a self-consistent set of J-plane singularities can be generated with features in accord with the suggestions from experiment.

Examples of the second category, generation of the Pomeron singularity by multiple meson exchange, are the original work of Amati, Stanghellini, and Fubini (1962), very recent attempts, still in progress, by Chew, Rogers, and Snider with essentially the ASF model, and the work of Freund (1969). This last is noteworthy for its use of duality in sense opposite from that described in Section V,5. Freund uses duality arguments to replace n-particle intermediate states in the unitarity equation by quasi-two-body channels involving towers of resonances! (He goes from right to left in Fig. 27, whereas Chew and Pignotti go from left to right.)

A final remark concerning the t-dependence of the diffractive elastic scattering can be made. Attempts to generate the forward diffraction peak, e^{At} , with $A \sim 8(\text{GeV}/c)^{-2}$, via the unitarity equation have succeeded only when the multiparticle amplitude possesses rapidly varying phases (Michejda, 1968). In particular, a multi-Regge-exchange model with a phase given by the product of phase factors, $\exp(-i\pi\alpha_1(t_1)/2)$, one for each link in the chain, yielded reasonable agreement with experiment. The same model without the phases yields $A \simeq 1.5 (\text{GeV}/c)^{-2}$ (Michejda, Turnau, and Biañas, 1968). An interesting by-product of this work is the result that contributions to the imaginary part of the elastic amplitude from larger and larger multiplicities show steeper and steeper t-dependences. This suggests that higher multiplicity states are produced more peripherally than low multiplicities, an idea that runs counter to intuitive belief that central

collisions are "hard" and peripheral collisions "soft." With what turns out to be considerable foresight, Michejda emphasizes that these results are not conclusive. A contribution to this conference by Ajduk and Stroynowski shows that the neglect of spin in the previous work is a serious deficiency. Spin effects can give roughly the observed value of A , without the necessity of Regge phase factors, and they may well make the behavior in t for different multiplicities agree with our intuitive ideas.

VIII. MISCELLANEOUS ASPECTS OF PRODUCTION PROCESSES

1. Pion-pion phase shifts

The extraction of the physical pion-pion scattering phases from experimental data on the production process $\pi N \rightarrow \pi\pi N$ has a long history, dating from the days of the Goebel-Chew-Low extrapolation idea and the discovery of the ρ -meson. In relatively recent years there has been a gradual refinement of the method of analysis and the accumulation of very large numbers of events. About two years ago the beginnings of a reasonably consistent picture emerged with the analyses of Baton, Laurens, and Reignier (1967) for the $I = 1$ and $I = 2$ phase shifts, and of Gutay et al. (1967), Walker et al. (1967), and Malamud and Schlein (1967) for the $I = 0$ and $I = 1$ phases.

The treatment of the peripheral production data can be understood from Fig. 36. At small momentum transfers the one-pion-exchange diagram can be assumed to dominate. Then the amplitude for $\pi N \rightarrow \pi\pi N$ can be factored into a $NN\pi$ vertex and a $\pi\pi \rightarrow \pi\pi$ amplitude, connected by a pion propagator. The various methods of analysis (Schlein, 1967; Baton, Laurens, and Reignier, 1967; Marateck et al., 1968; Gutay, 1969) differ in their treatment of the $\pi\pi$ amplitude and the $NN\pi$ vertex, but all depend on the idea of factorization of the production amplitude, at least implicitly. Below 1 GeV it is safe to assume that only s- and p-waves are significant.

For the $I = 1$ and $I = 2$ phase shifts the analysis is fairly straightforward. The ρ -resonance is predominantly elastic and known to be $J^P = 1^-$. Its unitarity limit of $12\pi\lambda^2$ is therefore a

check on the normalization or extrapolation procedures. Figure 37 shows the results of Baton and Laurens (1968) for $\sin^2 \delta$ in the $I = 1$ p-wave and the s-wave phase shift for $I = 2$. These phases were obtained by extrapolation to the pion pole, in the classic manner of Chew and Low. The p-wave phase is fitted by a nonrelativistic Breit-Wigner resonance with $\Gamma = 110 \pm 9$ MeV and $M_0 = 755 \pm 5$ MeV. This is consistent with other determinations of the parameters of the ρ -meson.

For the $I = 0$ s-wave deduced from the $\pi^+\pi^-$ system there are ambiguities in practice, although not in principle, as first pointed out by Gutay et al. (1967). The angular distribution of the pions can be written, assuming only s- and p-waves, as

$$\frac{dW}{d\Omega} = A(m_{\pi\pi}^2, \Delta^2) + B(m_{\pi\pi}^2, \Delta^2) \cos \theta + C(m_{\pi\pi}^2, \Delta^2) \cos^2 \theta$$

where θ is the "scattering" angle of one of the pions, measured relative to the incident pion's direction in the rest frame of the two pions in the final state. The coefficients A, B, C depend on the invariant mass of the two pions ($m_{\pi\pi}$) and the momentum transfer to the nucleon (Δ^2), as well as the incident momentum and the Treiman-Yang angle. For small momentum transfers, the distribution in the azimuthal Treiman-Yang angle is isotropic, consistent with the pion exchange shown in Fig. 36. Extrapolation of the observed values of A, B, C to the point $\Delta^2 = -\mu^2$ should give an unambiguous determination of both s and p-wave phases. Because of relatively rapidly varying corrections to A , it is not possible to make a useful extrapolation of this coefficient which, at the pion pole, involves only the s-wave phase shifts. An indirect method is necessary. The ratio B/C at the pion pole yields the $I = 0$

s-wave phase shift, provided the $I = 2$ s-wave phase (which enters B along with the $I = 0$ s-wave) and the $I = 1$ p-wave (present in B and C) are known. By extrapolation of B and C separately, or better, as a ratio B/C , the $I = 0$ s-wave phase can thus be determined as a function of $m_{\pi\pi}$. Unfortunately, there is a two-fold ambiguity, δ_0^0 and $(\delta_0^0)' = \delta_1^0 - \delta_0^0 + \pi/2$, as shown at top left in Fig. 38. Since δ_0^0 is near 90° at the position of the ρ there are four solutions, referred to as "up-up," "down-up," "up-down," and "down-down," depending on which branch below 750 MeV is connected with which branch above. The "down-up" solution corresponds to an s-wave resonance at roughly the ρ mass and a width of ~ 140 MeV, while the "up-down" solution represents a very broad s-wave enhancement, with a phase between 60° and 90° over the range, $500 \text{ MeV} < m_{\pi\pi} < 1000 \text{ MeV}$.

On the basis of a fitting of production amplitudes, Malamud and Schlein (1967) favored the "up-up" solution, while Marateck et al. (1968) preferred the "down-up" solution, shown separately at top right in Fig. 38. A further analysis has been made of basically the same compilation of data as used by Marateck et al., with the claim that a unique solution is determined (Scharenguivel et al., 1969). This analysis uses an extrapolation of the "front to back" ratio, $B/(2A + 2C/3)$, to $\Delta^2 = -\mu^2$, combined with a fit to the production amplitudes based on the factorization implied by Fig. 36. With nine parameters, a maximum likelihood fit strongly favors the "down-up" solution, corresponding to a relatively narrow s-wave resonance and agreeing closely with Marateck et al.

There are other experiments, however, that challenge the correctness of the "down-up" solution. Evidently the process, $\pi^+\pi^- \rightarrow \pi^0\pi^0$, with its amplitude $(f_0 - f_2)/2$, is an obvious reaction to study in order to elucidate the s-waves without the domination of the resonant p-wave. Published experiments have given conflicting results - Feldman et al. (1969), studying $\pi^-p \rightarrow \pi^0\pi^0n$ at 1.27 and 1.53 GeV/c, with spark chambers, favored a narrow resonance, while Braun, Cline, and Scherer (1968), with $\pi^+d \rightarrow \pi^0\pi^0p(p)$ at 2.15 GeV/c in a bubble chamber with tantalum plates, favored the "down" solution above 800 MeV. Both experiments suffer from limited statistics. A Karlsruhe-Cern contribution to this conference (Deinet et al., 1969) seems to point unambiguously(!) to the "up-down" solution, in exact opposition to the conclusion of Scharenguivel et al. (1969). The experiment is on $\pi^-p \rightarrow \pi^0\pi^0n$ at 1.77 GeV/c with a neutron time-of-flight spectrometer and thick plate spark chambers to detect the gammas from the π^0 decays. The number of events with $3\mu^2 < \Delta^2 < 15\mu^2$ is sufficient for a Chew-Low extrapolation for the total cross section for $\pi^+\pi^- \rightarrow \pi^0\pi^0$. The results are shown in the bottom half of Fig. 38, along with the $I = 0$ s-wave unitarity limit and the expectations of the various solutions shown at upper left in the same figure. There are, of course, possibilities for error in this experiment. The gamma rays are not fitted to the two π^0 's, and hence no Dalitz plot is available. Questions about reflections and interferences from a process like $\pi^-p \rightarrow \pi^0\Delta^0$ cannot be answered. Taken at face value, these data are in agreement with the predictions of the Veneziano model which has a broad s-wave resonance at the position of the ρ (see Fig. 28).

The question of the $I = 0$ s-wave phase shift is evidently still open, although the balance is shifting in favor of the "up-down" solution, or at least a phase shift that changes very little from 700 to 900 MeV. The contrary deduction from the experiments on $\pi^-p \rightarrow \pi^+\pi^-n$ may be caused by too heavy a dependence on a particular model for the production amplitudes.

2. K- π Phase Shifts

The same kinds of analysis that have been done on the pion production processes can be done with incident K mesons. Various aspects of the analysis of the three and four-body final states ($KN \rightarrow K\pi N$ and $KN \rightarrow K\pi\pi N$) have been given by Schlein (1968). The model used is that of one-pion-exchange with each vertex multiplied by a Dürr-Pilkuhn form factor (Dürr and Pilkuhn, 1965). For a process like $K^+p \rightarrow K^+\pi^-\pi^+p$ the events with small momentum transfers to the π^+p system are described by a differential cross section that has a product of the $K^+\pi^-$ and π^+p off-mass-shell scattering cross sections times suitable phase space factors and form factors, divided by the square of a pion propagator. A fit is made to the mass and t-dependences of the data by adjusting the radius parameters in the Dürr-Pilkuhn form factors, as well as the $K\pi$ and πN scattering amplitudes. For the 7.3 GeV/c data of Trippe et al. (1968) on $K^+p \rightarrow K^+\pi^-\Delta^{++}$ and $K^0p \rightarrow K^0\pi^0\Delta^{++}$, the results of such a fit are shown in Fig. 39. The lower curves display the t-dependences of the differential cross section for various mass cuts on the $K\pi$ system. From the left they are for the $K^*(890)$ region, the

$K^*(1420)$ region, below the $K^*(890)$, between the two resonances, and above the $K^*(1420)$. The upper half of the figure shows the $K_{\pi^+}^-$ and $K_{\pi^0}^0$ cross sections at small momentum transfers. The $K^*(890)$ and $K^*(1420)$ peaks are clearly visible. Since the spins, positions, widths, and elasticities of the $K^*(890)$ and $K^*(1420)$ are known reasonably reliably, the cross section can be processed to subtract out the p- and d-wave resonant contributions and leave a remainder. The insert in the upper right-hand corner of Fig. 39 shows this remainder now expressed as an elastic scattering cross section. It is suggestive that the data points approach the unitarity limit for an $I = \frac{1}{2}$ s-wave near 1 GeV. Trippe et al. state that these results imply the existence of an $I = \frac{1}{2}$ scalar resonance at 1.1 GeV. It is desirable to have confirmation of this resonance in other, preferably very different, experiments. The hazards of subtracting large contributions, parameterized in a particular way, to obtain a small remainder are obvious, even when, as in this instance, there are good normalization points on either side in the form of well-known resonances. I have presented these data, not so much as convincing evidence for a new resonance, but as an example of the type of analysis possible in pion-exchange processes where known resonances provide benchmarks for calibration of one's model.

3. On the Connection Between Production Mechanism and Decay of Resonances at High Energies

Five years ago Gottfried and I published a paper with the above title, pointing out that the density matrix for the spin population of an unstable resonance carried an imprint of the mechanism of production

(Gottfried and Jackson, 1964). Special examples had been known, of course, before that time. Since then many developments have occurred. Van Rossum (1968) gave a comprehensive review at the CERN Conference. I therefore restrict myself to a few comments. Mention should be made of the work in the Soviet Union, contemporary with our original work (Berkov, Nikitin, and Terent'ev, 1964) and subsequently (Kaidalov and Karnakov, 1966; Gribov, 1967a). Gribov suggested looking for the contributions from the Pomeron pole and the P-P cut in the decay correlations of $KN \rightarrow K N^*$. Unfortunately, even the highest energy data on this reaction show little if any evidence for the presence of Pomeron exchange.

In photoproduction of pions there is a famous theorem due to Stichel (1964) which states that the cross section for photons linearly polarized in (perpendicular to) the production plane corresponds to the exchange of unnatural (natural) parity in the t-channel. The general problem of circular and linear polarization of the photons in quasi-two-body photoproduction of mesonic and baryonic states of arbitrary spins and parities has been considered recently by Thews (1968) who discusses what can be learned about the t-channel exchanges from the polarization dependence of the cross section. Interesting theorems in a similar vein are presented by Ader, et al. (1968) who discuss in detail how to isolate the cross section corresponding to natural or unnatural parity exchanges by taking certain linear combinations of decay density matrix elements times the differential cross section.

I wish to issue a warning about the use of the theorems of Stichel, Thews, and Ader et al. They are only correct to leading order in powers of s . At present laboratory energies there can be sizeable corrections. An example is revealing. For vector meson production, e.g. $K^+ p \rightarrow K^{*+} p$, the combinations $(\rho_{11} + \rho_{1,-1})$ and $(\rho_{11} - \rho_{1,-1})$ measure the amounts of natural and unnatural parity exchanges, respectively, according to Ader et al. If only natural parity exchange occurs, then $\rho_{1,-1} = \rho_{1,1}$ is predicted. An elementary perturbation theory calculation using only vector meson exchange shows that this equality is only true as $s \rightarrow \infty$ (see Eq. (16) and Fig. 2 of Jackson and Pilkuhn, 1964). At 3 GeV/c, the ratio $\rho_{1,-1}/\rho_{11}$ at small momentum transfers ranges from 0.7 to 1.0, depending on the details of the couplings of the exchanged vector meson. In terms of Regge exchanges the reliability of these theorems will be especially poor when the "other" parity corresponds to Regge poles whose trajectories lie higher (typically by half a unit) than those appropriate to the parity being measured. In these circumstances the error will be of order $s^{-1+\Delta\alpha}$. In all of this it appears that the only theorem that holds without approximation is the original one on the vanishing of ρ_{00} for vector meson production when only natural parity is exchanged, plus some trivial extensions (Jackson, 1964).

Other developments on the use of decay correlations include quadratic relations among density matrix elements to test for single Regge pole exchanges (Ringland and Thews, 1968) or for certain classes of exchanges (Kaidalov, 1967). It should be noted that here again are relations valid only to leading order in s .

Calculations of cross sections and density matrix elements for the reaction $\pi N \rightarrow \rho N$, especially in the small t region, have been made by Dass and Froggatt (1968) using a Regge pole model. At small t the process is dominated by pion exchange and the density matrix elements and cross section have different behaviors at $t \rightarrow 0$, depending on whether one has an evasive pion or a pion conspiracy (or a conspiring cut). The limiting form of the different behaviors as $s \rightarrow \infty$ are as follows:

	<u>Evasive pion</u>	<u>Pion conspiracy</u>
$\rho_{00} \frac{d\sigma}{dt}$	$\frac{t}{(t - \mu^2)^2}$	$\frac{t}{(t - \mu^2)^2}$
$\rho_{11} \frac{d\sigma}{dt}$	t	constant
$\rho_{10} \frac{d\sigma}{dt}$	$t^{3/2}/(t - \mu^2)$	$t^{1/2}/(t - \mu^2)$
$\rho_{1,-1} \frac{d\sigma}{dt}$	t	t

For an evasive pion, the cross section dips toward $t = 0$ in the forward direction and ρ_{00} remains large. For a conspiring pion, the cross section stays finite at $t = 0$, while ρ_{00} goes to zero there. These very different behaviors can, in principle, be used to elucidate the types of t -channel exchanges. The situation does not look too promising

at the moment, however. The calculations of Dass and Froggatt show that the differences occur at extremely small t values ($|t| < \mu^2$). On the experimental side, data on $\pi^- p \rightarrow \rho^0 n$ indicates a finite cross section and a large value of ρ_{00} at $t = 0$. Perhaps this is just a reflection of corrections of order s^{-1} to the theory on the one hand, and of finite bin size in the experiment on the other.

CONCLUDING REMARKS

As a final comment on the state of our art and its development over the past 50 or 60 years I offer Figs. 40 and 41. Figure 40 is evidence for progress in theory. The top equation, taken from a paper in Phil. Mag. of 1910, is perhaps the first scattering cross section formula in particle physics; it is certainly the most famous. Since 1910 theory has progressed - the second cross section formula, typical of many in Phys. Rev. in 1968, shows that equations have become longer, more numerous, and, I fear, less famous. The experimental side, too, has changed drastically over the years. Progress of sorts is indicated by the acknowledgments shown in Fig. 41. In 1919 good physics was done with simple apparatus and an able assistant to help with the tedious work of observing a zinc sulphide screen, but the completion of almost any experiment in high energy physics fifty years later requires a galaxy of Professors, Ph.D. physicists, engineers, and technicians to assist, support and encourage an international team of researchers assembled from the far corners of the earth, as is attested by daggers, asterisks, and other symbols on almost every name.

What will the next 50 years bring?

BIBLIOGRAPHY

1. Conferences

Proceedings of the XIIIth International Conference on High-Energy Physics, Berkeley, August 31-September 7, 1966 (University of California, Berkeley).

Proceedings of the 1967 International Symposium on Electron and Photon Interactions at High Energies, Stanford Linear Accelerator Center, September 5-9, 1967 (Clearinghouse, Federal Sc. and Tech. Info., N.B.S., U. S. Dept. of Commerce, Springfield, Virginia).

Proceedings of the Heidelberg Conference on Elementary Particles, September 20-27, 1967, F. Filthuth, ed. (North-Holland, Amsterdam and John Wiley, N. Y.)

Topical Conference on High-Energy Collisions of Hadrons, CERN, 15-18 January, 1968, two volumes (CERN-68-7).

Proceedings of the 14th International Conference on High-Energy Physics, Vienna, 28 August-5 September, 1968 (CERN, Geneva).

Proceedings of the VIII Internationale Universitätswochen für Kernphysik der Universität Graz, Schladming, 24 February-8 March, 1969 (to be published).

2. References

Abarbanel, H. D. I., S. D. Drell, and F. J. Gilman, (1968). Phys. Rev. Letters 20, 280.

Abarbanel, H. D. I., S. D. Drell, and F. J. Gilman, (1969). Phys. Rev. 177, 2458.

- Abers, E. A. and V. L. Teplitz, (1969). Phys. Rev. Letters 22, 909.
- Abolins et al., (1969). Phys. Rev. Letters 22, 427.
- Ademollo et al., (1968). Phys. Rev. 176, 1904.
- Ademollo, M., G. Veneziano, and S. Weinberg, (1969). Phys. Rev. Letters 22, 83.
- Ader et al., (1968). Nuovo Cimento 56A, 952.
- Adler, S. L., (1965). Phys. Rev. 137, B1022.
- Alderholz et al., (1968a). Phys. Letters 27B, 174.
- Alderholz et al., (1968b). Nucl. Phys. B8, 485.
- Alexander et al., (1969). Phys. Rev. 177, 2092.
- Allaby et al., (1968a). Phys. Letters 28B, 67.
- Allaby et al., (1968b). Phys. Letters 28B, 229.
- Amati, D., A. Stanghellini, and S. Fubini, (1962). Nuovo Cimento 26, 896.
- Anderson et al., (1967). Phys. Rev. Letters 19, 198.
- Andersson et al., (1969). Phys. Letters 28B, 611.
- Andrews et al., (1969). Phys. Rev. Letters 22, 731.
- Ankenbrandt et al., (1968). Phys. Rev. 170, 1223.
- Anninos et al., (1968). Phys. Rev. Letters 20, 402.
- Ansel'm, A. A. and I. T. Dyatlov, (1967). Yad. Fiz. 6, 591, 603.
[Sov. J. Nucl. Phys. 6, 430, 439 (1968)].
- Arbab, F., (1969). Phys Rev. (to be published).
- Arbab, F. and R. C. Brower, (1968). Phys. Rev. 175, 1991.
- Arbab, F. and J. D. Jackson, (1968). Phys. Rev. 176, 1796.
- Arnold, R. C., (1965). Phys. Rev. Letters 14, 657.

- Arnold, R. C., (1967). Phys. Rev. 153, 1523.
- Arnold, R. C. and M. L. Blackmon, (1968). Phys. Rev. 176, 2082.
- Atkinson et al., (1969). ICTP/68/34 preprint.
- Baker et al., (1968). Phys. Letters 28B, 291.
- Baker et al., (1969). Nucl. Phys. B9, 249.
- Ball, J. S., W. R. Frazer, and M. Jacob, (1968). Phys. Rev. Letters 20, 518.
- Banaigs et al., (1969). Nucl. Phys. B9, 640.
- Bardakci, K. and H. Ruegg, (1968). Phys. Letters 28B, 342.
- Bardakci, K. and H. Ruegg, (1969). Phys. Letters 28B, 671.
- Bardakci, K., M. B. Halpern, and J. A. Shapiro, (1969). University of California, Berkeley, preprint (May, 1969).
- Barger, V., (1968). CERN, Vol. I., p. 3.
- Barger, V. and D. Cline, (1967). Phys. Rev. 155, 1792.
- Barger, V. and D. Cline, (1968). Phys. Rev. Letters, 21, 392.
- Barger, V., D. Cline, and J. Matos, (1969). Phys. Letters 29B, 121.
- Barger, V. and L. Durand, (1968). Phys. Letters 26B, 588.
- Barger, V. and R. J. N. Phillips, (1968). Phys. Letters 26B, 730.
- Barger, V. and R. J. N. Phillips, (1969). Phys. Rev. Letters 22, 116.
- Barloutaud et al., (1969). Nucl. Phys. B9, 493.
- Bassel, R. H. and C. Wilkin, (1967). Phys. Rev. Letters 18, 871.
- Bassompierre et al., (1969). Nucl. Phys. B9, 295.
- Baton, J. P. and G. Laurens, (1968). Phys. Rev. 176, 1574.
- Baton, J. P., G. Laurens, and J. Reignier, (1967). Nucl. Phys. B3, 349.
- Belletini, G., (1968). Vienna, p. 329.
- Bender, I. and H. J. Rothe, (1969). Heidelberg preprint (May 14, 1969).

- Beretvas, A. and N. E. Booth, (1969). Phys. Rev. Letters 22, 113.
- Berger, E. L., (1968a). Phys. Rev. 166, 1525.
- Berger, E. L., (1968b). Phys. Rev. Letters 21, 701.
- Berger, E. L., (1969). Phys. Rev. 179, 1567.
- Berger et al., (1968). Phys. Rev. Letters 20, 964.
- Berkov, A. V., Yu. P. Nikitin, and M. V. Terent'ev, (1964). Zh. Eksp. Teor. Fiz. 46, 2202. [Sov. Phys. JETP 19, 1487 (1964)].
- Bertocchi, L., (1967). Heidelberg, p. 197.
- Biazas, A., (1968). CERN, Vol. I., p. 218.
- Biazas, A. and K. Zalewski, (1968). Nucl. Phys. B6, 465.
- Biazas, A. and S. Pokorski, (1969). Nucl. Phys. B10, 399.
- Bietti et al., (1968). Phys. Letters 26B, 457.
- Blackmon, M. L. and G. R. Goldstein, (1969). Phys. Rev. 179, 1480.
- Böckmann et al., (1968). Phys. Letters 28B, 72.
- Booth, N. E., (1968). Phys. Rev. Letters 21, 465.
- Braun, K. J., D. Cline, and V. Scherer, (1968). Phys. Rev. Letters 21, 1275.
- Byers, N. and C. N. Yang, (1966). Phys. Rev. 142, 976.
- Caneschi, L., (1969). Santa Barbara preprint (to be published).
- Caneschi, L. and A. Pignotti, (1969). Phys. Rev. Letters 22, 1219.
- Capps, R. H., (1969). Phys. Rev. Letters 22, 215.
- Chan Hong-Mo, (1968). Vienna, p. 391.
- Chan Hong-Mo, (1969). Phys. Letters 28B, 425.
- Chan Hong-Mo and Tsou Sheung Tsun, (1969). Phys. Letters 28B, 485.
- Chan Hong-Mo, J. Łoskiewicz, and W. W. M. Allison, (1968). Nuovo Cimento 27A, 93.
- Chew, G. F. and W. R. Frazer, (1969). Phys. Rev. (to be published).
- Chew, G. F., M. L. Goldberger, and F. E. Low, (1969). Phys. Rev. Letters 22, 208.

- Chew, G. F. and A. Pignotti, (1968a). Phys. Rev. Letters 20, 1078.
- Chew, G. F. and A. Pignotti, (1968b). Phys. Rev. 176, 2112.
- Chien et al., (1969). Phys. Letters 28B, 615.
- Chiu, C. B. and M. Der Sarkissian, (1968). Nuovo Cimento 55A, 396.
- Chiu, C. B. and J. Finkelstein, (1967). Nuovo Cimento 48A, 820.
- Chiu, C. B. and J. Finkelstein, (1968a). Nuovo Cimento 57A, 649.
- Chiu, C. B. and J. Finkelstein, (1968b). Nuovo Cimento 59A, 92.
- Chiu, C. B. and J. Finkelstein, (1968c). Phys. Letters 27B, 510.
- Chiu, C. B. and A. Kotanski, (1969). Nucl. Phys. B8, 553.
- Chiu, C. B. and A. V. Stirling, (1968). Phys. Letters 26B, 236.
- Chou, T. T. and C. N. Yang, (1967). High Energy Physics and Nuclear Structure, ed. G. Alexander (North-Holland Publishing Co., Amsterdam), p. 348.
- Chou, T. T. and C. N. Yang, (1968a). Phys. Rev. 170, 1591.
- Chou, T. T. and C. N. Yang, (1968b). Phys. Rev. 175, 1832.
- Chu, S.-Y. and D. P. Roy, (1968). Phys. Rev. Letters 20, 958.
- Cohen-Tannoudji, G., A. Morel, and H. Navelet, (1967). Nuovo Cimento 48A, 1075.
- Colley, D. C., (1968). CERN, Vol. I., p. 60.
- Collins, P. D. B. and E. J. Squires, (1968). Regge Poles in Particle Physics, Springer Tracts in Modern Physics No. 45, (Springer-Verlag, Berlin).
- Crennell et al., (1968). Phys. Letters 28B, 136.
- Czyz, W. and L. C. Maximon, (1969). Annals of Physics (N.Y.) 52, 59.

- Czyzewski, O., (1968). Vienna, p. 367.
- Dance, D. R. and G. Shaw, (1968). Phys. Letters 28B, 182.
- Dass, G. V. and C. D. Froggatt, (1968). Nucl. Phys. B8, 661.
- Dass, G. V. and C. Michael, (1968a). Phys. Rev. Letters 20, 1066.
- Dass, G. V. and C. Michael, (1968b). Phys. Rev. 175, 1774.
- Dass, G. V., C. Michael, and R. J. N. Phillips, (1969). Nucl. Phys. B9, 549.
- De Baere et al., (1969). (To be published).
- Deinet et al., (1969). Paper submitted to the Lund Conference (to be published).
- de Lany et al., (1967). Phys. Rev. Letters 18, 149.
- Delbourgo, R., (1969). Trieste preprint ICTP/68/21.
- Delbourgo, R. and A. Salam, (1969). Phys. Letters 28B, 497.
- Derrick, M., (1968). CERN, Vol. I., p. 111.
- Dietz, K., (1969). Schladming, [Bonn preprint] (to be published).
- Di Lella, L., (1967). Heidelberg, p. 159.
- Di Vecchia et al., (1968a). Phys. Letters 27B, 296.
- Di Vecchia et al., (1968b). Phys. Letters 27B, 521.
- Dolen, R., D. Horn, and C. Schmid, (1967). Phys. Rev. Letters 19, 402.
- Dolen, R., D. Horn, and C. Schmid, (1968). Phys. Rev. 166, 1768.
- Donnachie, A. and R. G. Kirsopp, (1969). Nucl. Phys. B10, 433.
- Donnachie, A., R. G. Kirsopp, and C. Lovelace, (1968). Phys. Letters 26B, 161.
- Drell, S. D., and J. S. Trefil, (1966). Phys. Rev. Letters 16, 552, 832(e).
- Durand, L., (1968). Phys. Rev. 166, 1680.
- Durand, L. and R. Lipes, (1968). Phys. Rev. Letters 20, 637.
- Durr, H. P. and H. Pilkuhn, (1965). Nuovo Cimento 40, 899.

- Esterling et al., (1968). Phys. Rev. Letters 21, 1410.
- Feldman et al., (1969). Phys. Rev. Letters 22, 316.
- Finkelstein, J., (1969). Phys. Rev. Letters 22, 362.
- Finkelstein, J. and M. Jacob, (1968). Nuovo Cimento 56A, 681.
- Finkelstein, J. and K. Kajantie, (1968). Nuovo Cimento 56A, 659.
- Frautschi, S. and B. Margolis, (1968a). Nuovo Cimento 56A, 1155.
- Frautschi, S. and B. Margolis, (1968b). Nuovo Cimento 57A, 427.
- Frazer, W. R., (1968). Vienna, p. 415.
- Freund, P. G. O., (1968). Phys. Rev. Letters 20, 235.
- Freund, P. G. O., (1969). Phys. Rev. Letters 22, 565.
- Freund, P. G. O. and P. J. O'Donovan, (1968). Phys. Rev. Letters 20, 1329.
- Friedman, J. H. and R. R. Ross, (1969). Phys. Rev. Letters 22, 152.
- Gilman, F. J., (1969). Phys. Rev. (to be published) SLAC-PUB-576.
- Gilman, F. J., H. Harari, and Y. Zarmi, (1968). Phys. Rev. Letters 21, 323.
- Glauber, R. J., (1959). Lectures in Theoretical Physics, Vol. 1, ed. W. E. Brittin (Interscience Publishers, Inc, N. Y.), p. 315.
- Glauber, R. J., (1967). High Energy Physics and Nuclear Structure, ed. G. Alexander (North-Holland Publishing Co., Amsterdam), p. 311.
- Goebel, C. J. and B. Sakita, (1969). Phys. Rev. Letters 22, 257.
- Goldhaber et al., (1969). Phys. Rev. Letters 22, 802.
- Gribov, V. N., (1967a). Yad. Fiz. 5, 197. [Sov. J. Nucl. Phys. 5, 138 (1967)].
- Gribov, V. N., (1967b). Zh. Eksp. Teor. Fiz. 53, 654. [Sov. Phys. JETP

- 26, 414 (1968)]. Also papers submitted to the Vienna Conference.
- Gottfried, K. and J. D. Jackson, (1964). Nuovo Cimento 33, 309.
- Gutay, L. J., (1969). Purdue preprint C00-1428-126 (May 1969).
- Gutay et al., (1967). Phys. Rev. Letters 18, 142.
- Halliday, I. G., (1969). Nuovo Cimento 60A, 177.
- Halliday, I. G. and L. M. Saunders, (1969a). Nuovo Cimento 60A, 115.
- Halliday, I. G. and L. M. Saunders, (1969b). Nuovo Cimento 60A, 494.
- Harari, H., (1967). Stanford, p. 337.
- Harari, H., (1968a). Phys. Rev. Letters 20, 1395.
- Harari, H., (1968b). Vienna, p. 195.
- Harari, H., (1969). Phys. Rev. Letters 22, 562.
- Harari, H. and Y. Zarmi, (1969). Weizmann Institute preprint.
- Henyey, F. S., (1968). Phys. Rev. 170, 1619.
- Henyey et al., (1968). Phys. Rev. Letters 21, 946.
- Henyey, F., K. Kajantie, and G. L. Kane, (1968). Phys. Rev. Letters 21, 1782.
- Hopkinson, J. F. L. and E. Plahte, (1969). Phys. Letters 28B, 489.
- Horn, D., (1969). Schladming [Tel-Aviv preprint TAUP-77-69].
- Huang, K. and S. Pinsky, (1968). Phys. Rev. 174, 1915.
- Igi, K., (1962). Phys. Rev. Letters 9, 76. [See also Phys. Rev. 130, 820 (1963)].
- Igi, K., (1968). Phys. Letters 28B, 330.
- Igi, K. and S. Matsuda, (1967a). Phys. Rev. Letters 18, 625.
- Igi, K. and S. Matsuda, (1967b). Phys. Rev. 163, 1622.
- Igi, K. and J. K. Storrow, (1969). CERN preprint, TH. 993 (31 January 1969).
- Imachi et al., (1968). Prog. Theo. Phys. 40, 353.

- Jackson, J. D., (1964). Nuovo Cimento 34, 1644.
- Jackson, J. D., (1965). Peripheral Interactions, in High Energy Physics, Les Houches, 1965, ed. C. DeWitt and M. Jacob (Gordon and Breach, N.Y., 1966).
- Jackson, J. D. and H. Pilkuhn, (1964). Nuovo Cimento 33, 906.
- Jackson, J. D. and C. Quigg, (1969). Phys. Letters 29B, 236.
- Jacob, M., (1969). Schladming [CERN preprint TH. 1010]
- Jacob, M. and S. Pokorski, (1969). Nuovo Cimento 61A, 233.
- Jengo, R. and E. Remiddi, (1969). Lett. Nuovo Cimento 1, 637.
- Jones, C. E. and V. Teplitz, (1967). Phys. Rev. 159, 1271.
- Kaidalov, A. B., (1967). Phys. Letters 26B, 20.
- Kaidalov, A. B. and B. M. Karnakov, (1966). Yad. Fiz. 3, 1119.
[Sov. J. Nucl. Phys. 3, 814 (1966)]
- Kaidalov, A. B. and B. M. Karnakov, (1968). Yad. Fiz. 7, 1147.
[Sov. J. Nucl. Phys. 7, 685 (1968)]
- Kajantie, K., (1968). Nuovo Cimento 53A, 424.
- Kajantie, K. and P. V. Ruuskanen, (1969). Helsinki preprint No. 7-69.
- Kawarabayashi, K., S. Kitakada, and H. Yabuki, (1969). Phys. Letters 28B, 432.
- Kikkawa, K., B. Sakita, and M. A. Virasoro, (1969). Phys. Rev. (to be published).
- Koba, Z. and H. B. Nielsen, (1969). Nucl. Phys. B10, 633.
- Kofoed-Hansen, O., (1969). Nuovo Cimento 60A, 621.
- Kokkedee, J. J. J., (1969). The Quark Model, (W. A. Benjamin, N.Y.).
- Lea, A. T., B. R. Martin, and G. C. Oades, (1968). Phys. Rev. 165, 1770.
- LeBellac, M. (1967). Phys. Letters 25B, 524.

- Lipes, R., G. Zweig, and W. Robertson, (1969). Phys. Rev. Letters 22, 433.
- Lipkin, H. J., (1969). These Proceedings.
- Logunov, A. A., L. D. Soloviev, and A. N. Tavkhelidze, (1967). Phys. Letters 24B, 181.
- Lohrmann, E., (1969). These Proceedings.
- Lovelace, C., (1968). Phys. Letters 28B, 264.
- McClellan et al. (1969). Phys. Rev. Letters, 22, 377.
- Malamud, E. and P. E. Schlein, (1967). Phys. Rev. Letters 19, 1056.
- Mandelstam, S. (1963). Nuovo Cimento 30, 1127, 1148.
- Mandelstam, S., (1968a). Phys. Rev. 168, 1884.
- Mandelstam, S., (1968b). Phys. Rev. Letters 21, 1724.
- Mandelstam S. and L. L. Wang, (1967). Phys. Rev. 160, 1490.
- Marateck et al., (1968). Phys. Rev. Letters 21, 1613.
- Martin, A., (1969). CERN preprint, TH. 1037 (28 May 1969).
- Mathews, R. D., (1969). Nucl. Phys. (to be published) UCRL-18611.
- Matsuda, S., (1969). Nucl. Phys. B9, 113.
- Matsuda, S. and K. Igi, (1967). Phys. Rev. Letters 19, 928.
- [Erratum, Phys. Rev. Letters 20, 781 (1968)]
- Michael, C., (1968). Nucl. Phys. B8, 431.
- Michael, C., (1969). Phys. Letters 29B, 230.
- Michejda, L., (1968). Fort. der Physik 16, 707.
- Michejda, L., J. Turnau, and A. Bia~~l~~as, (1968). Nuovo Cimento 56A, 241.
- Michelini et al., (1969). (to be published).
- Oehme, R., (1968). Phys. Letters 28B, 122.

- Orear et al., (1968). Phys. Letters 28B, 61.
- Paschos, E. A., (1968). Phys. Rev. Letters 21, 1855.
- Phillips, R. J. N., (1967a). Phys. Letters 24B, 342.
- Phillips, R. J. N., (1967b). Nucl. Phys. B2, 394.
- Plahte, E. and R. G. Roberts, (1969). Nuovo Cimento 60A, 33.
- Raman, K. and K. V. Vasavada, (1968). Phys. Rev. 175, 2191.
- Ranft, G., (1968). Nuovo Cimento 58A, 425.
- Ranft, G., (1969). Nuovo Cimento 60A, 643.
- Regge, T., (1959). Nuovo Cimento 14, 951.
- Richter, B., (1968). Vienna, p. 3.
- Ringland, G. A. and R. L. Thews, (1968). Phys. Rev. 170, 1569.
- Rivers, R. J., (1968). Nuovo Cimento 58A, 100.
- Rivers, R. J. and L. M. Saunders, (1968). Nuovo Cimento 58A, 385.
- Roberts, R. G. and F. Wagner, (1969). CERN preprint TH. 1014 (3 April 1969).
- Rosner, J. L., (1969). Phys. Rev. Letters 22, 689.
- Roy, D. P. and S.-Y. Chu, (1968). Phys. Rev. 171, 1762.
- Rushbrooke, J. G. and J. R. Williams, (1969). Phys. Rev. Letters 22, 248.
- Salin, Ph., (1968). CERN, Vol. I, p. 478.
- Sawyer, R., (1968). Phys. Rev. Letters 21, 764.
- Scharenguivel et al., (1969). Purdue University preprint.
- Schlein, P. E., (1967). Phys. Rev. Letters 19, 1052.
- Schlein, P. E., (1968). Meson Spectroscopy, C. Baltay and A. H. Rosenfeld, ed. (W. A. Benjamin, N.Y.), p. 161.

- Schmid, C., (1968). Phys. Rev. Letters 20, 689.
- Schmid, C., (1969a). Lett. Nuovo Cimento 1, 165.
- Schmid, C., (1969b). Nuovo Cimento 61A, 289.
- Schrempp, F., (1968). Nucl. Phys. B6, 487.
- Sertorio, L. and L.-L. Wang, (1969). Phys. Rev. 178, 2462.
- Shapiro, J., (1969). Phys. Rev. 179, 1345.
- Shapiro, J. and J. Yellin, (1968). UCRL-18500 (September 26, 1968).
- Sivers, D. and J. Yellin, (1969a). Notes on $\pi\pi$ Scattering III. J Plane Phenomena UCRL-18665 (January 17, 1969).
- Sivers, D. and J. Yellin, (1969b). Annals of Physics (N.Y.) (to be published).
- Stichel, P., (1964). Zeit. für Physik 180, 170.
- Sudakov, V. V., (1956). Zh. Eksp. Teor. Fiz. 30, 87.
[Sov. Phys. JETP 3, 65 (1956)].
- Thews, R. L., (1968). Phys. Rev. 175, 1749.
- Tripp, R. D., (1968). Vienna, p. 173.
- Trippe, T. G. et al., (1968). Phys. Letters 28B, 203.
- Van Hove, L., (1966a). Proceedings of the Conference on High-Energy Two-Body Reactions, Stony Brook (unpublished); see also Particle Physics at High Energies, eds. T. W. Priest and L. L. J. Vick (Oliver and Boyd, Edinburgh, 1967).
- Van Hove L., (1966b). Berkeley, p. 253.
- Van Hove, L., (1969). Nucl. Phys. B9, 331.
- van Rossum, L., (1968). CERN, Vol. I., p. 161.

- Vasavada, K. V. and K. Raman, (1968). Phys. Rev. Letters 21, 577.
- Veneziano, G., (1968). Nuovo Cimento 57, 190.
- Verdiev, I. A., A. M. Popova, and K. A. Ter-Martirosyan, (1964). Zh. Eksp. Teor. Fiz. 46, 1295, 1700. [Sov. Phys. JETP 19, 878, 1148 (1964)].
- Virasoro, M. A., (1969). Phys. Rev. Letters 22, 37.
- Wagner, F., (1969). CERN preprint TH. 1012 (31 March 1969).
- Walker et al., (1967). Phys. Rev. Letters 18, 630.
- Weinberg, S., (1966). Phys. Rev. Letters 17, 616.
- White, J. N. J., (1968). Phys. Letters 27B, 92.
- Wu, T. T. and C. N. Yang, (1965). Phys. Rev. 137, B708.
- Yellin, J., (1968). Notes on $\pi\pi$ Scattering I. UCRL-18637 (November 21, 1968).
- Yellin, J., (1969a). Notes on $\pi\pi$ Scattering II. Sum Rules and Threshold Behavior UCRL-18664 (January 2, 1969).
- Yellin, J., (1969b). Phys. Rev. (to be published).
- Yen et al., (1969). Phys. Rev. Letters 22, 963.

Table I. High Energy Physics Research Effort as Evidenced by Publication in Two Letter Journals : EXPERIMENTAL PAPERS ON HADRONIC AND PHOTONIC PROCESSES

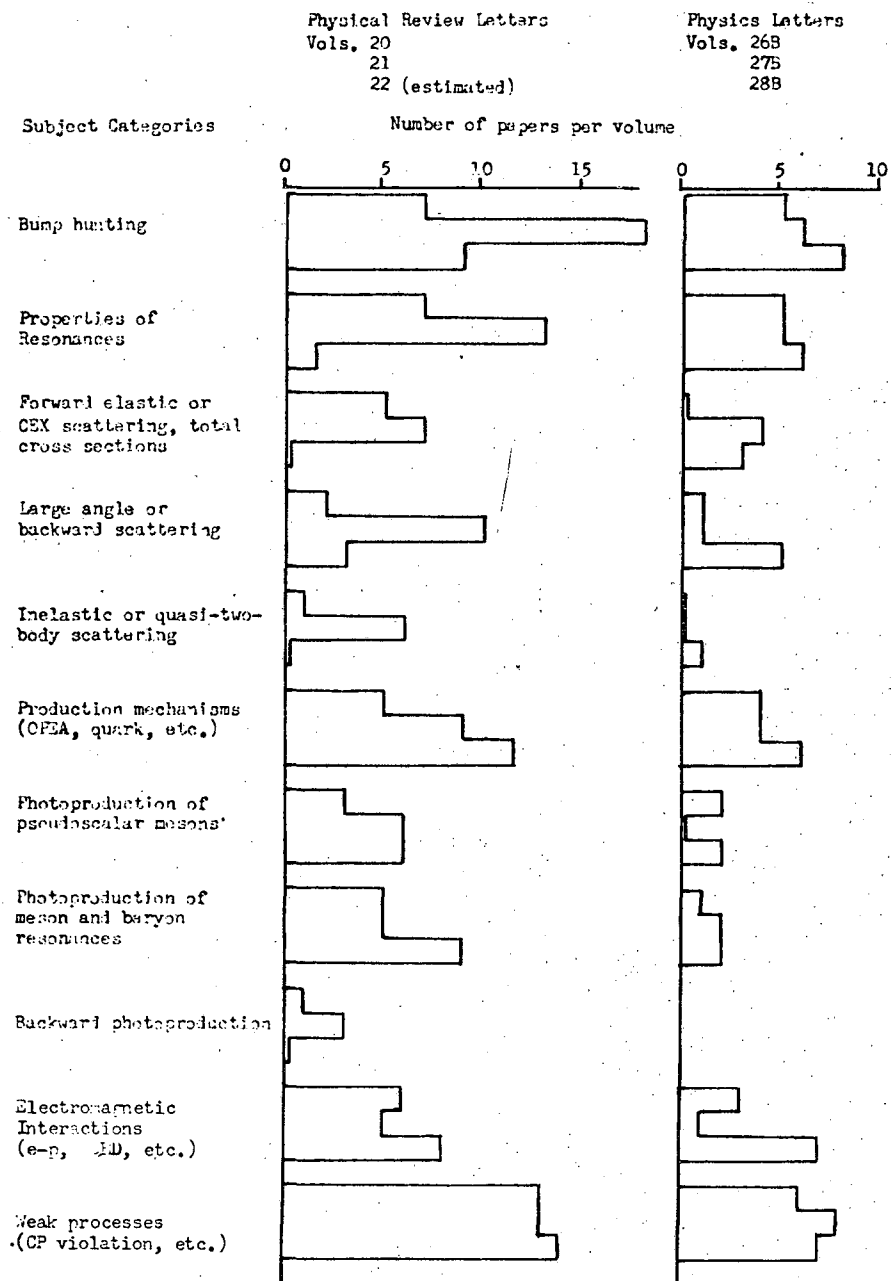


Table II. High Energy Physics Research Efforts as Evidenced by Publication in Two Letter Journals : THEORETICAL PAPERS ON HADRONIC AND PHOTONIC PROCESSES

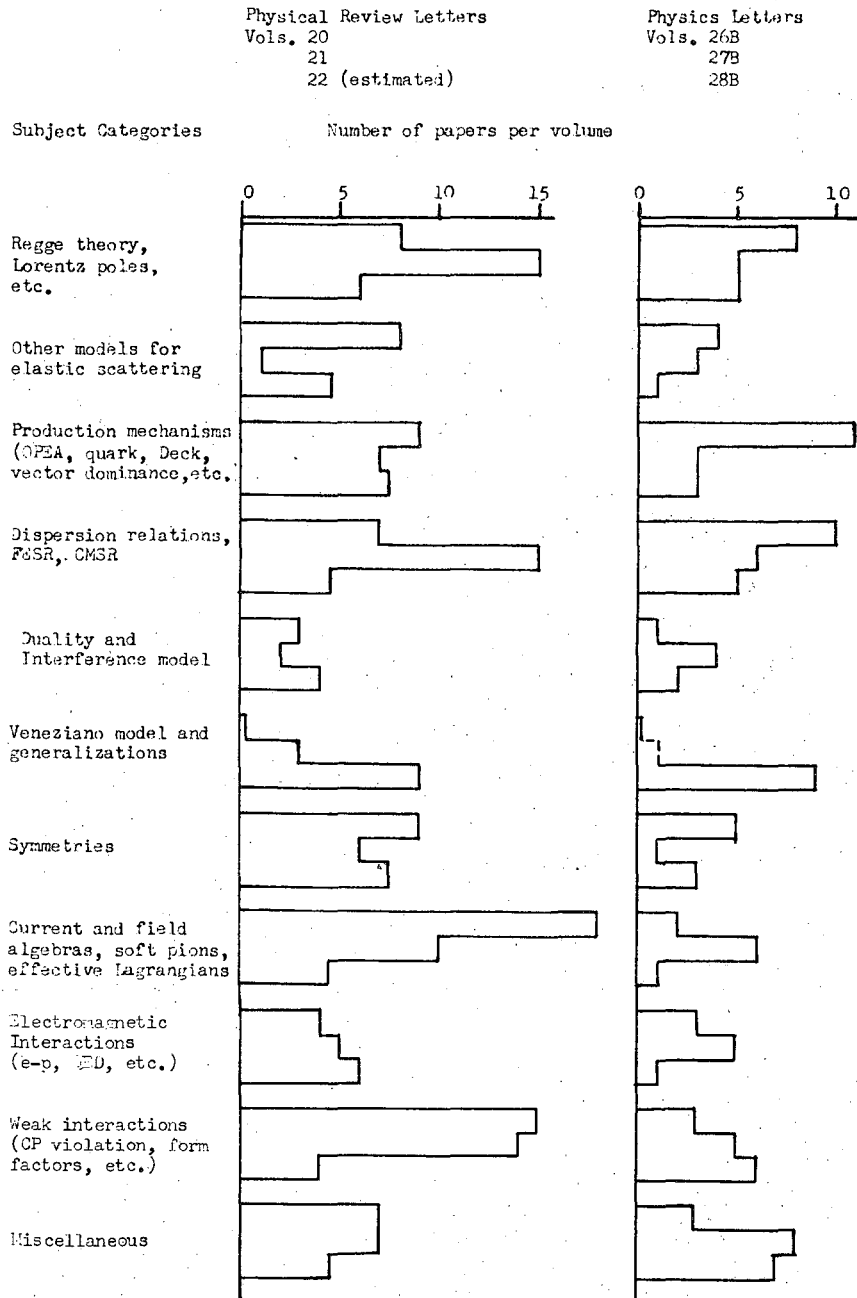


Table III

Examples of Double-Regge Exchanges

(See Fig. 33 for the notation)

P _{Lab} (GeV/c)	Particles					Regge exchanges		Reference
	1	2	3	4	5	a	b	
8,11	π	p	ρ	π	p	π	P	Berger (1968a)
28.5	p	p	n	π^+	p	π	P	Berger (1968b)
6.6	p	p	p	π^-	Δ^{++}	elastic data	π	Berger et al. (1968)
9	K^+	p	K^+	ω	p	ω	P	Alexander et al. (1969)
12.6	K^-	p	K^{*0}	π^-	p	π	P	Andrews et al. (1969)
	K^-	p	K^-	π^-	Δ^{++}	P	π	Andrews et al. (1969)
28.5	p	p	p	π^-	Δ^{++}	P	π	Berger (1969)

FIGURE CAPTIONS

- Fig. 1. Experimental and theoretical effort in high energy physics as evidenced by frequency of publication in letter journals (Physics Letters, Vols. 26B, 27B, 28B; Physical Review Letters, Vols. 20, 21, 22).
- Fig. 2. Differential cross section for elastic π^-p scattering at 9.7 and 13.6 GeV/c (from Orear et al., 1968).
- Fig. 3. Differential cross section for p-p elastic scattering at 19.2 GeV/c, along with results at other incident momenta (from Allaby et al., 1968a).
- Fig. 4. Differential cross section for \bar{p} -p elastic scattering at 5.9, 8.9, and 9.7 GeV/c (from Orear et al., 1968).
- Fig. 5. Differential cross sections for inelastic p-p scattering at 19.2 GeV/c compared with the elastic cross section of Fig. 3. The insert shows how the different inelastic contributions are defined (from Allaby et al., 1968b).
- Fig. 6. Polarization in π^+p and π^-p elastic scattering at 5.15 GeV/c (from Esterling et al., 1968).
- Fig. 7. Polarization in K^+p elastic scattering at 1.22 and 2.48 GeV/c (from Anderson et al., 1969).
- Fig. 8. Pion-pion mass distributions and Legendre polynomial coefficients for $\pi N \rightarrow \pi\pi N$ at 6 GeV/c. The left column is for $\pi^-p \rightarrow \pi^+\pi^-n(Q_{\pi\pi} = 0)$; the center column is for $\pi^-p \rightarrow \pi^-\pi^0p(Q_{\pi\pi} = -1)$; the right column is for $\pi^+p \rightarrow \pi^+\pi^+n(Q_{\pi\pi} = 2)$. (From Crennell et al., 1968).

Fig. 9. Comparison of experimental results on combined decay correlations in the process, $K^-p \rightarrow K^*\Delta$ at 2.6 GeV/c, with quark model predictions of class A. In each histogram the correlation predicted by the quark model is stated in terms of the direction cosines of the decay particles of the two resonances. The solid and open points refer to the left and right-hand sides of each equation. The abscissa in each diagram is the cosine of the production angle in the C.M. system (from Friedman and Ross, 1969).

Fig. 10. Energy dependence of the backward differential cross section $d\sigma/du$ at $u = 0$ for K^+p (solid points) and K^-p (open circles) elastic scattering. The dashed curves are the corresponding results for $\pi^\pm p$ scattering (from Baker et al., 1968).

Fig. 11. Backward differential cross section for π^+p elastic scattering at 5.2 and 6.9 GeV/c and π^-p at 6.9 GeV/c (from Baker et al., 1968).

Fig. 12. Backward differential cross section and polarization for $\pi^-p \rightarrow K^0\Lambda$ at incident momenta from 2 to 12 GeV/c. (Data from Michelini et al., 1969; figures from Barger, Cline, and Matos, 1969).

Fig. 13. Regge pole fits to $\pi^\pm p$ elastic scattering and polarization in the small and moderate $|t|$ region ($0 < |t| < 4(\text{GeV}/c)^2$) using cyclic residue functions (from Barger and Phillips, 1969).

Fig. 14. Tests of exchange degeneracy and SU(3) with the "elastic" reactions, $\pi^- p \rightarrow \pi^0 n$, $\pi^- p \rightarrow \eta^0 n$, and $K^- p \rightarrow \bar{K}^0 n$, and the inelastic processes, $\pi^+ p \rightarrow \pi^0 \Delta^{++}$, $\pi^+ p \rightarrow \eta^0 \Delta^{++}$, and $K^+ p \rightarrow K^0 \Delta^{++}$, at incident momenta from 3 to 5 GeV/c. The separate cross sections are shown at the left; the SU(3) components from π^0 and η^0 final states appear in the center; the sum of cross sections from the center are compared with the \bar{K}^0 and K^0 data at the right (from Mathews, 1969).

Fig. 15. Data at various momenta on the "elastic" and inelastic reactions of Fig. 14 are compared with a two-parameter Regge model based on $[U(6) \otimes U(6)] \times O(3)$ (from Delbourgo and Salam, 1969.)

Fig. 16. Differential cross section for p-p scattering predicted by the Chou-Yang model with a dipole electromagnetic form factor. Curve a is based on a purely imaginary scattering amplitude ($\Delta(\vec{q})$ real), while curve b includes a small real part. The trend of the data shown in Fig. 3 is displayed for comparison (from Durand and Lipes, 1968).

Fig. 17. Differential cross section for pp scattering predicted by the hybrid model at various incident momenta (from Chiu and Finkelstein, 1968b).

Fig. 18. Energy dependence of a Regge cut factor (see Eq.(IV-22)). The cross section for a pure pole goes as $\sigma \propto s^{2\alpha-2}$, while for a typical Regge cut amplitude goes as $\sigma \propto s^{2\alpha_c-2}/f(s)$. The dashed line is a power-law approximation corresponding to $\Delta\alpha = -0.25$.

- Fig. 19. Cross sections for a Regge pole exchange plus a Regge cut generated by absorptive corrections (schematic). The pole and cut amplitudes interfere to produce a dip, as seen in πN charge exchange (from Henyey et al., 1968).
- Fig. 20. Complex ν plane, showing poles, unitarity cuts and the contour used to obtain finite energy sum rules.
- Fig. 21. The integrands for the two sides of the finite energy sum rule (V. 4) for the crossing-odd forward scattering amplitude in πN scattering, $A^{(-)} + \nu B^{(-)}$, with $n = 0$ (from Igi and Matsuda, 1967a).
- Fig. 22. Residues of the P' Regge pole in the $A^{(+)}$ and $B^{(+)}$ amplitudes as functions of t for πN and KN scattering, as inferred from FESR (from Gilman, Harari and Zarmi, 1968).
- Fig. 23. FESR integrals vs. $\tau = -t$ for the t -channel pion photoproduction amplitudes $F_2^{(-)}(\varphi_2)$ and $F_3^{(-)}(\varphi_3)$. The solid curves are the low energy (left-hand) sides of (V.7), while the dashed curves are the high energy sides calculated from a model with an evasive pion plus absorptive corrections. The circles refer to a "pseudomodel" (see text) (from Jackson and Quigg, 1969).
- Fig. 24. Total cross sections for K^+p and K^-p interactions vs. ν , the K -meson energy in the laboratory. The dashed curve on the right is a rough Regge pole representation of the average cross section, $\sigma_t \simeq 17 + 16(\nu - m_K)^{-\frac{1}{2}}$ mb.

- Fig. 25. Argand diagrams for linear combinations of s-channel $I = 1/2$ and $I = 3/2$ partial wave amplitudes for πN scattering, corresponding to $I = 0$ and $I = 1$ in the t-channel (see Eq.(V.8)). The first seven partial waves are shown. (From Harari and Zarmi, 1969).
- Fig. 26. Regge exchange diagram and duality diagram for (a) $\pi^- p \rightarrow K^0 \Lambda$ (backward), and (b) $K^- n \rightarrow \pi^- \Lambda$ (forward). The upper duality diagram is a planar one, while the lower one is nonplanar.
- Fig. 27. Chew-Pignotti duality. The diffractive production of massive mesonic and baryonic states can be described in the average sense of duality by the multiperipheral diagram at the right, in which only the lightest mesons and baryons appear.
- Fig. 28. Trajectories and particle content of the Veneziano amplitude (VI.3) for $\pi-\pi$ scattering. With the leading trajectory given by $\alpha_\rho(t) = 0.48 + 0.90t$, the elastic partial widths (in MeV) are the numbers beside each dot, normalized to $\Gamma_\rho = 112$ MeV (after a table of Shapiro, 1969).
- Fig. 29. Dalitz-Mandelstam diagram for $F(t,u)$, (VI.3). The lines of poles in t and u are shown, as are the lines of zeros from the denominator. The asymptotic behavior in all six directions is indicated (from Shapiro, 1969).
- Fig. 30. Five-particle diagrams for the generalization of the Veneziano formula (from Bardakci and Ruegg, 1968).
- Fig. 31. Comparison of the Veneziano model (VI.13) with the $\pi^+ \pi^-$ mass distribution for $\bar{p} n \rightarrow \pi^+ \pi^- \pi^-$. The dash-dot curve is after

Lovelace (1968), with $\beta = 0$. The solid curve is the fit of Berger (private communication).

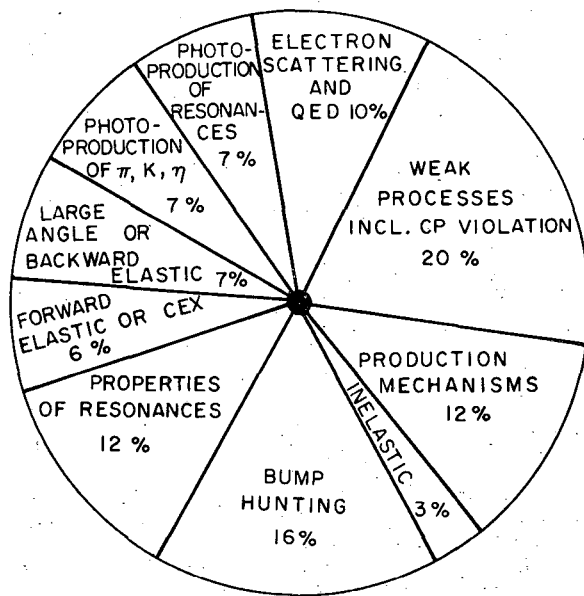
- Fig. 32. Decay angular distribution of the π^+ in the mass region of the f^0 for $\bar{p}n \rightarrow \pi^+ \pi^- \pi^-$, as shown by the shaded region on the Dalitz plot. The curves have the same meaning as in Fig. 31.
- Fig. 33. Double-Regge-exchange diagram for a three-body final state. a and b denote the Regge trajectories.
- Fig. 34. Multiperipheral diagrams considered by Caneschi and Pignotti (1969): (a) meson exchange for the proton spectra, (b) baryon exchange for the proton spectra, (c) and (d), corresponding diagrams for the pion spectra (from Caneschi and Pignotti, 1969).
- Fig. 35. Comparison of Caneschi-Pignotti model with the data of Anderson et al. (1967) on proton and pion spectra from inelastic p-p collisions at 30 GeV/c. Upper left: proton momentum spectra at various angles. Lower left: corresponding pion spectra (π^+ and π^-). Upper right: proton and pion longitudinal momentum spectra at fixed perpendicular momentum. Lower right: comparison of the model with proton data at 18.8 GeV/c, and predictions for 70 and 200 GeV/c. (From Caneschi and Pignotti, 1969).
- Fig. 36. Peripheral one-pion-exchange diagram for $\pi N \rightarrow \pi \pi N$ showing the decomposition into π - π scattering and πNN vertex. (From Gutay, 1969).
- Fig. 37. $I = 1$ and $I = 2$ pion-pion phase shifts. (a) $\sin^2 \delta$ for the $I = 1$ p-wave, (b) phase for $I = 2$ s-wave (from Baton and Laurens, 1968).

Fig. 38. Evidence concerning the $I = 0$ s-wave pion-pion phase shift. Top left: δ_0^0 vs $m_{\pi\pi}$ from s-wave-p-wave interference, showing the two-fold ambiguities above and below the ρ . Top right: The "down-up" solution preferred by Marateck et al. (1969) and Scharenguivel et al. (1969). Bottom: Cross section for $\pi^+\pi^- \rightarrow \pi^0\pi^0$ obtained by Chew-Low extrapolation, with curves based on the various solutions shown at top left and the s-wave unitarity limit. (Top figures from Marateck et al., 1968; bottom figure from Deinet et al., 1969.)

Fig. 39. Spectra for the reaction, $K^+p \rightarrow K\pi\Delta^{++}$ at 7.3 GeV/c. The upper histogram shows the cross section $d\sigma/dm$ for the $K^+\pi^-$ and $K^0\pi^0$ systems. The insert displays the elastic $K\pi$ scattering cross section after removal of the resonant p-wave ($K^*(890)$) and d-wave ($K^*(1420)$) by a subtraction. The lower histograms show the t-dependence of the production cross section for various cuts on the $K\pi$ mass spectrum (from Trippe et al., 1968).

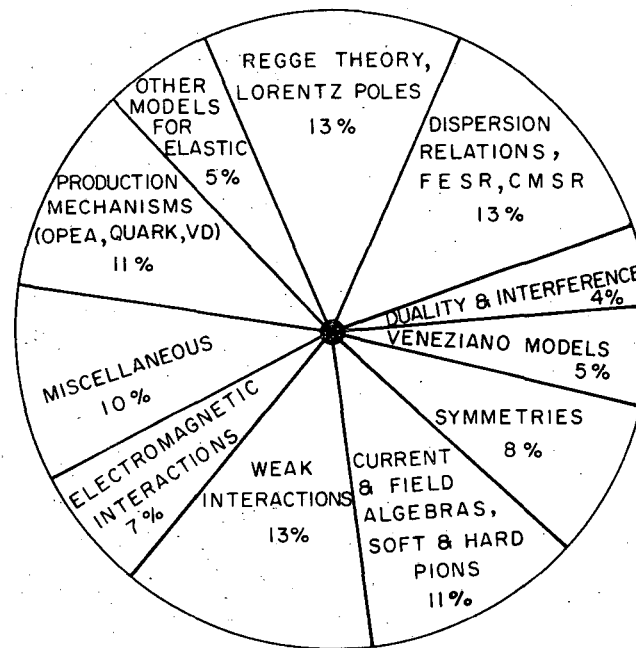
Fig. 40. Progress in Theory, 1910 \rightarrow 1968. Cross section formulas, then and now.

Fig. 41. Progress in Experiment, 1919 \rightarrow 1968. Acknowledgments, then and now.



EXPERIMENTAL

LETTER PUBLICATIONS

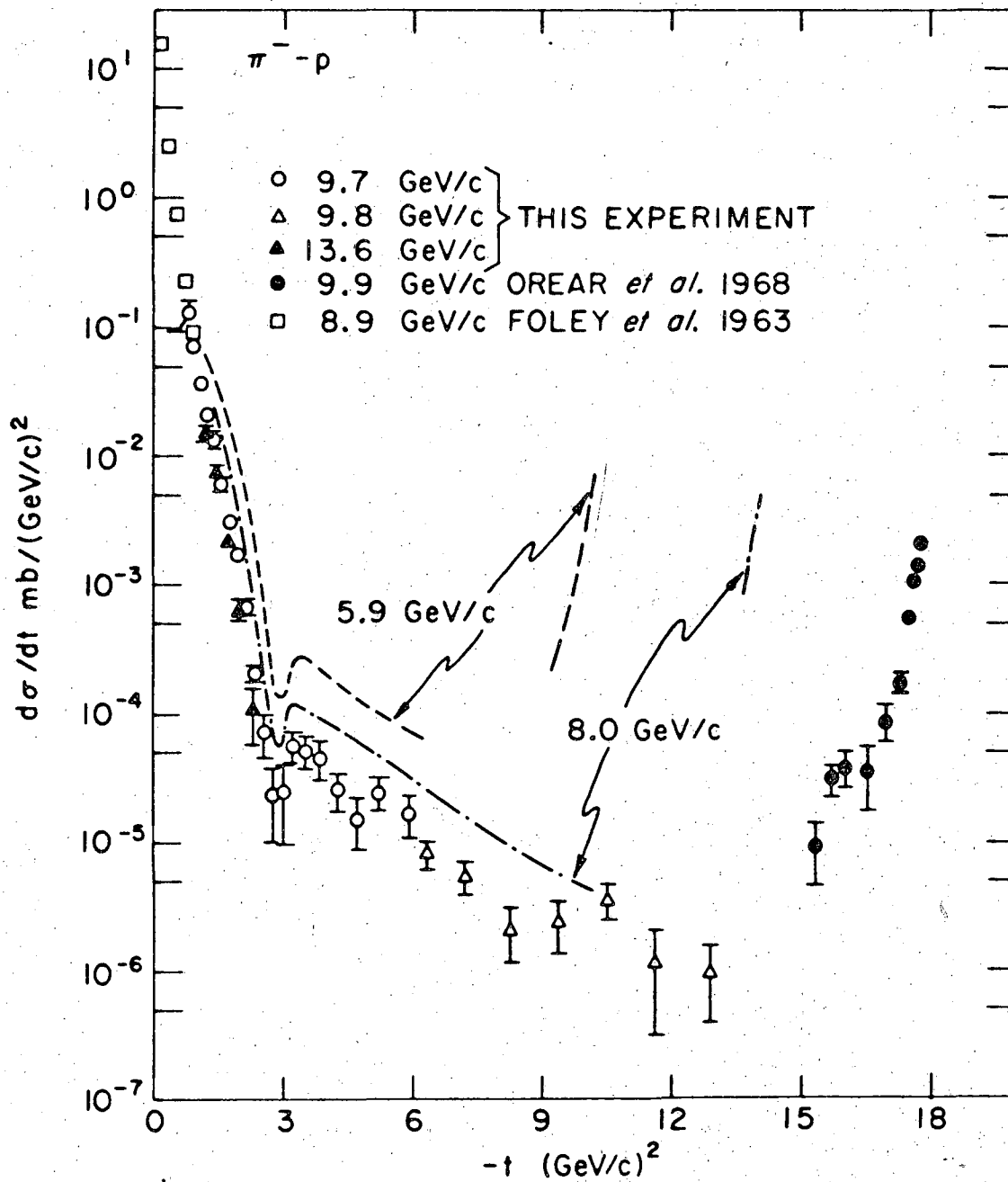


THEORETICAL

LETTER PUBLICATIONS

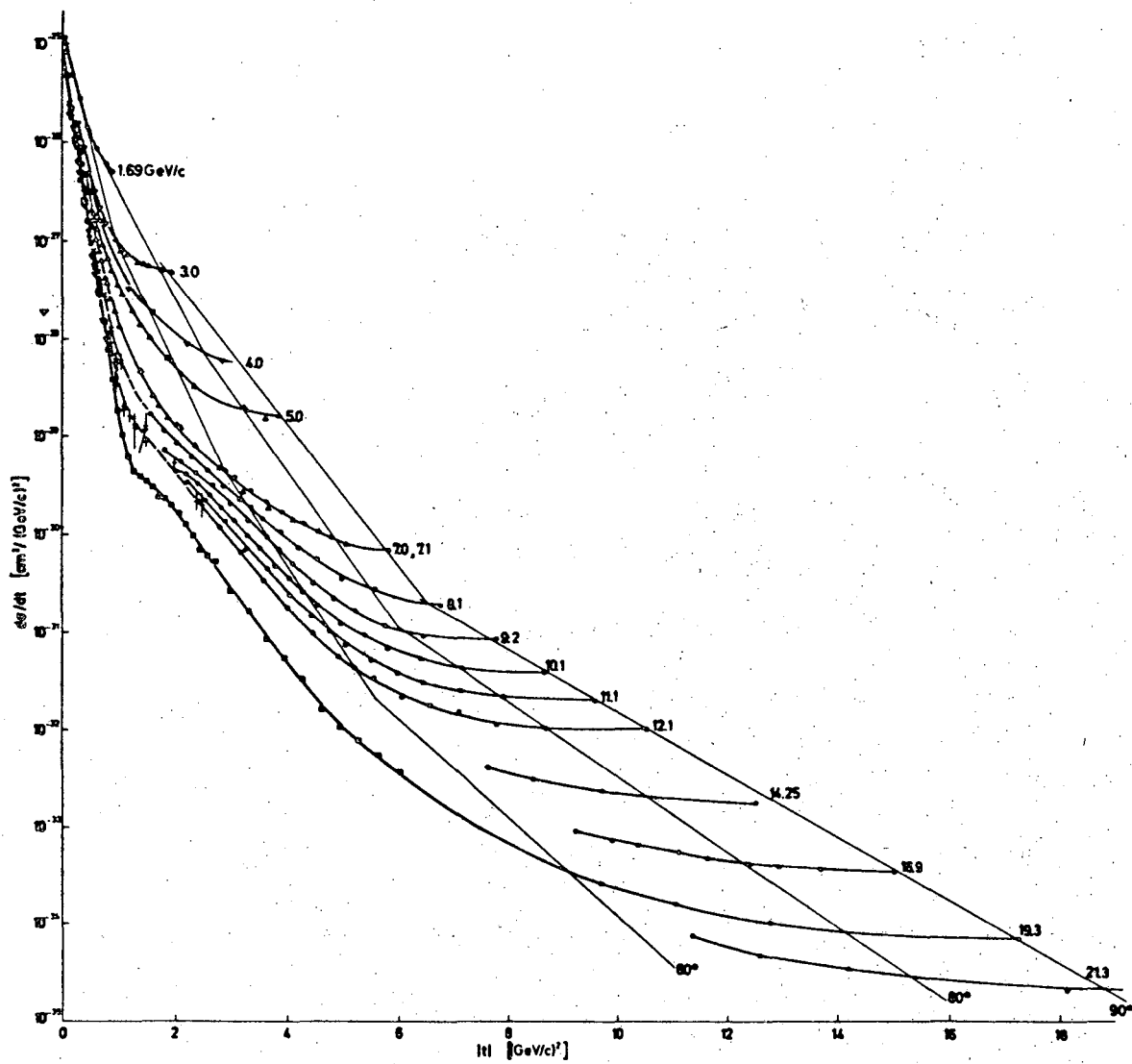
Fig. 1

XBL696-2928



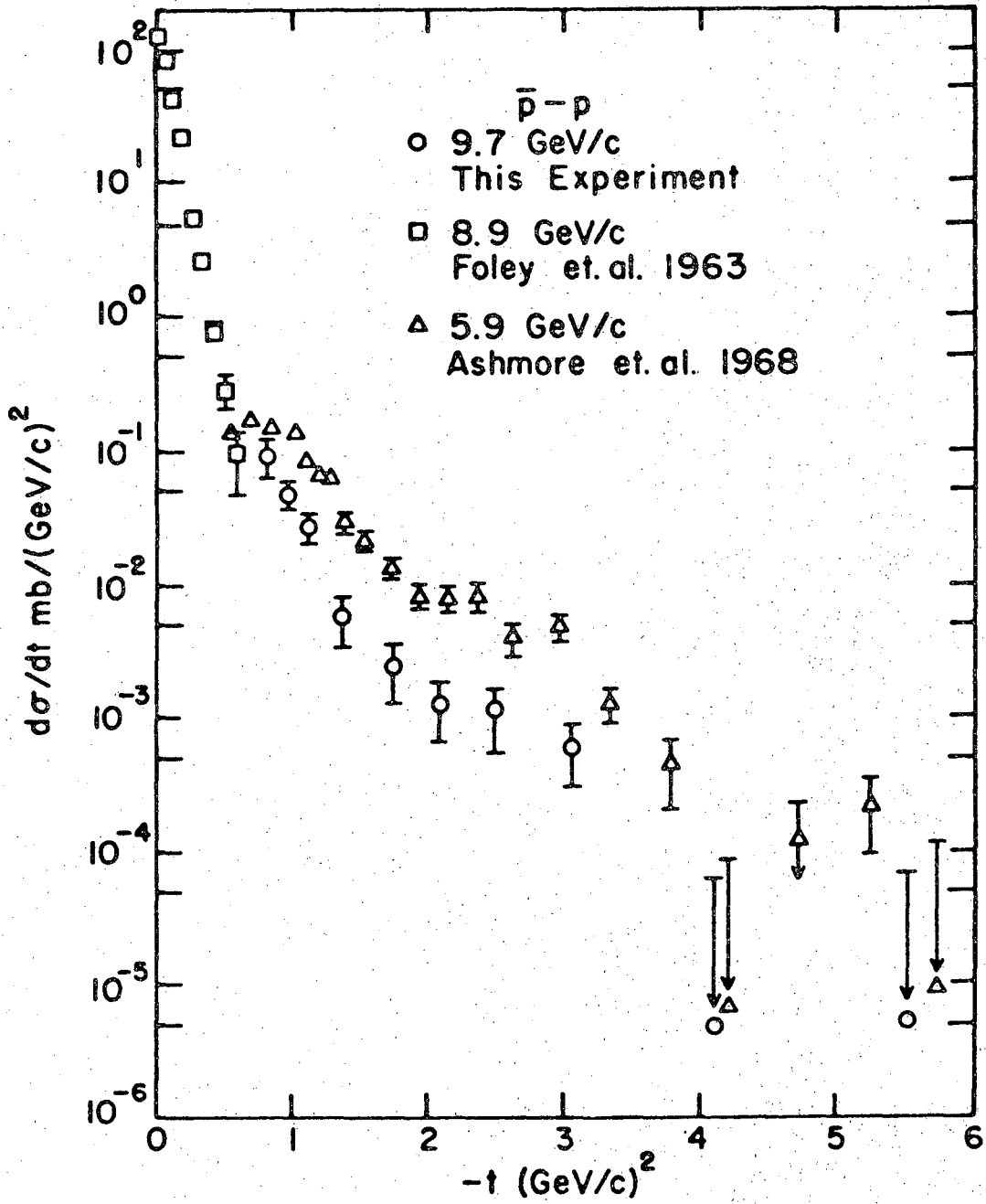
XBL 696-599

Fig. 2.



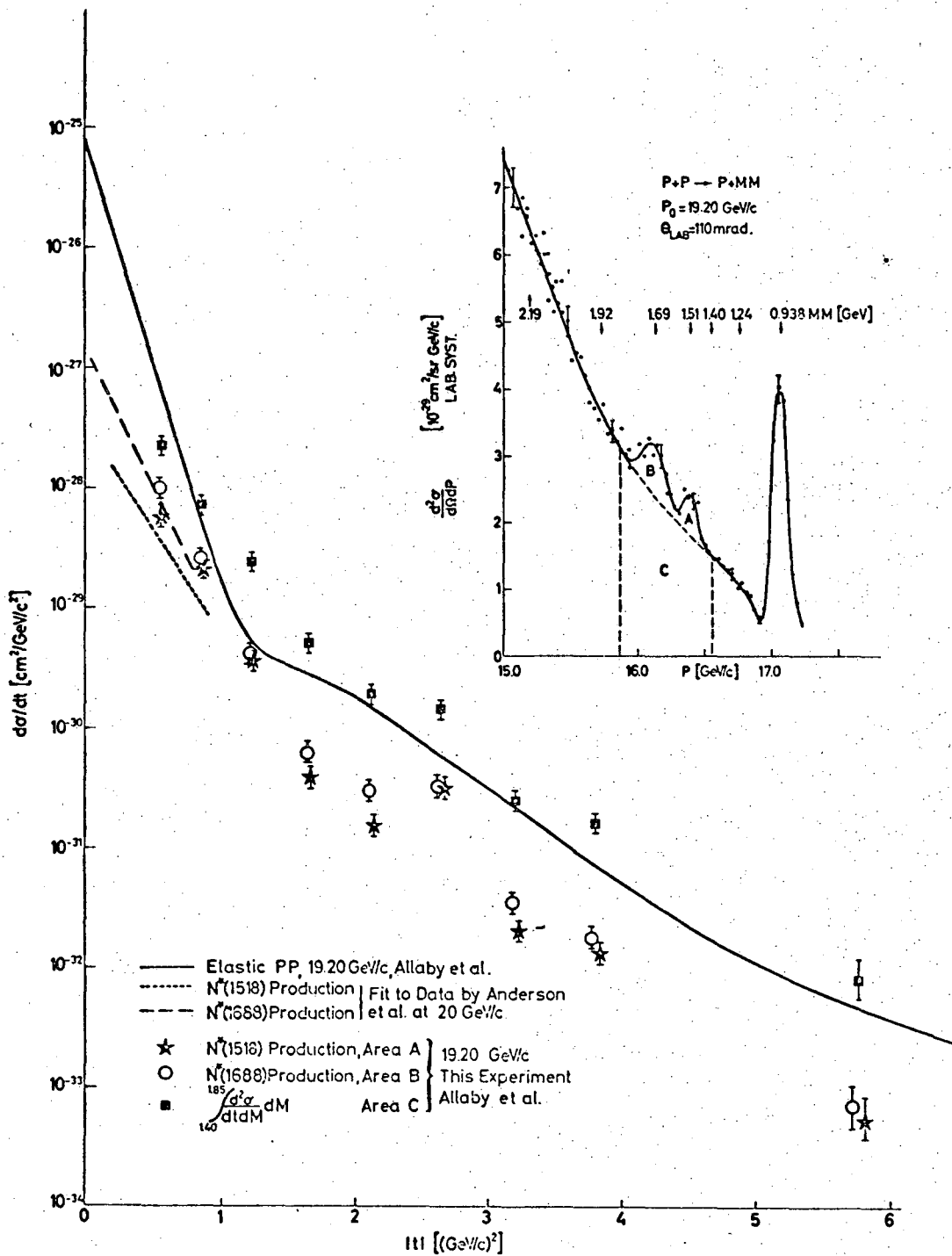
XBL 696-600

Fig. 3.



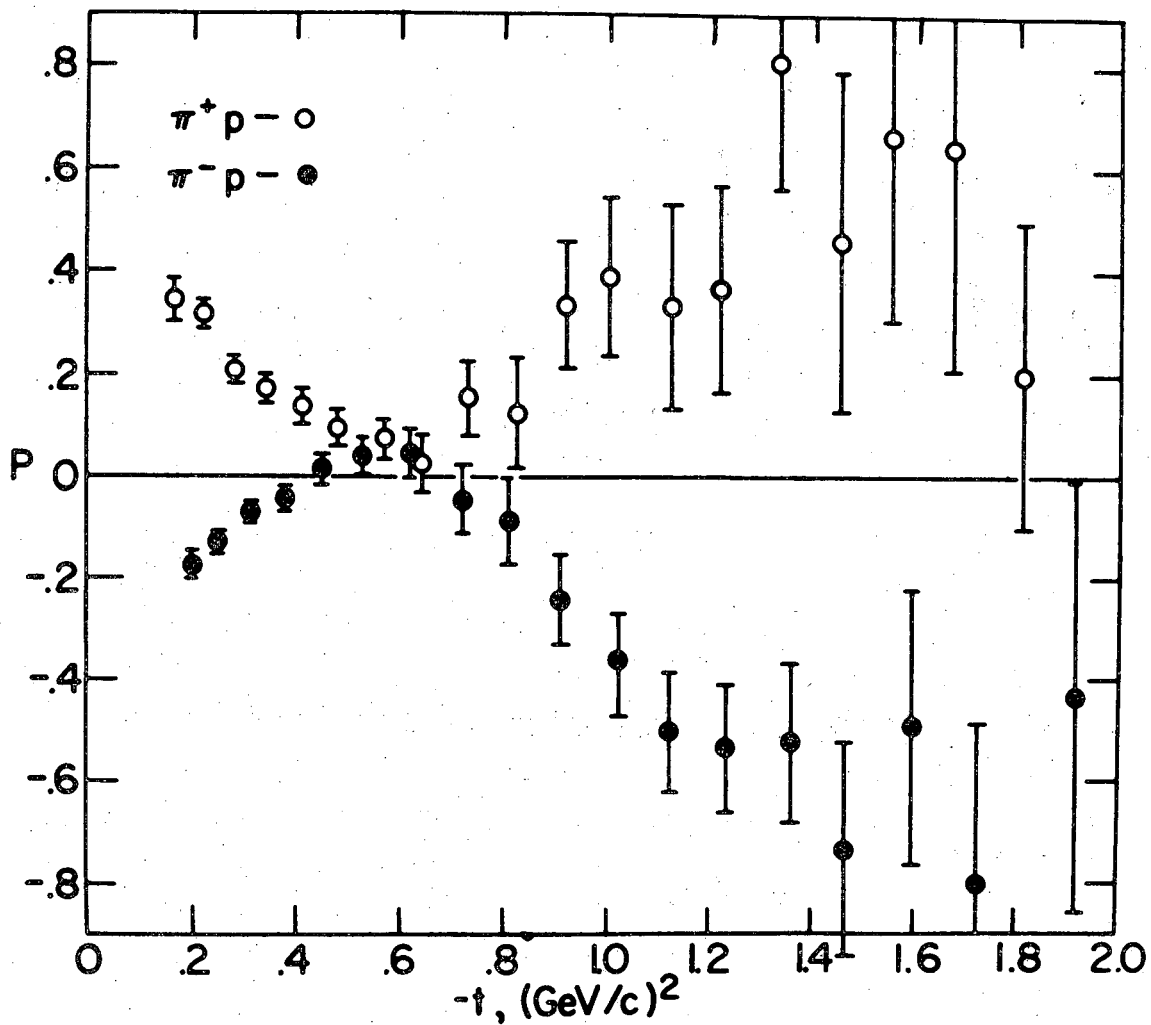
XBL 696-598

Fig. 4.



XBL 696-594

Fig. 5.



XBL 696-606

Fig. 6.

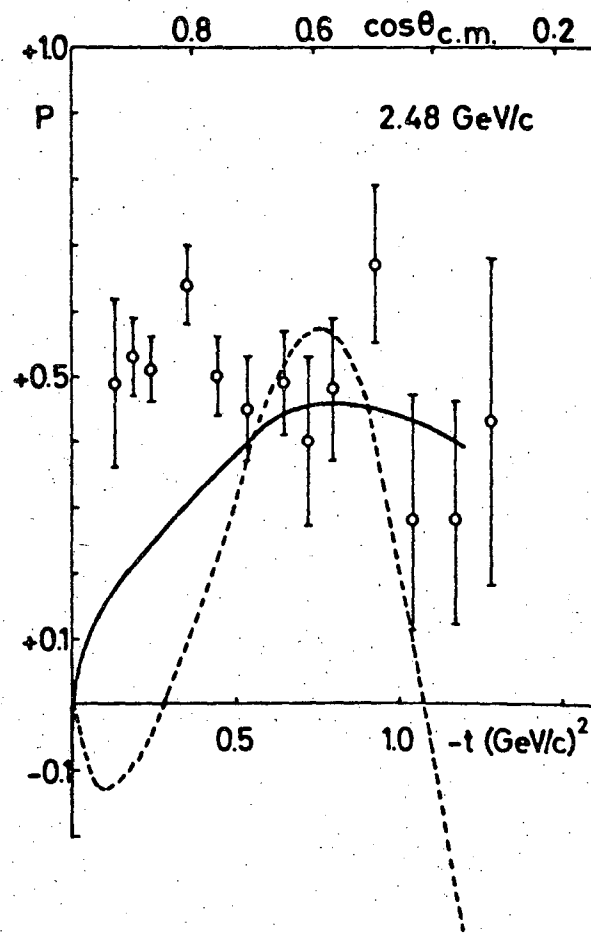
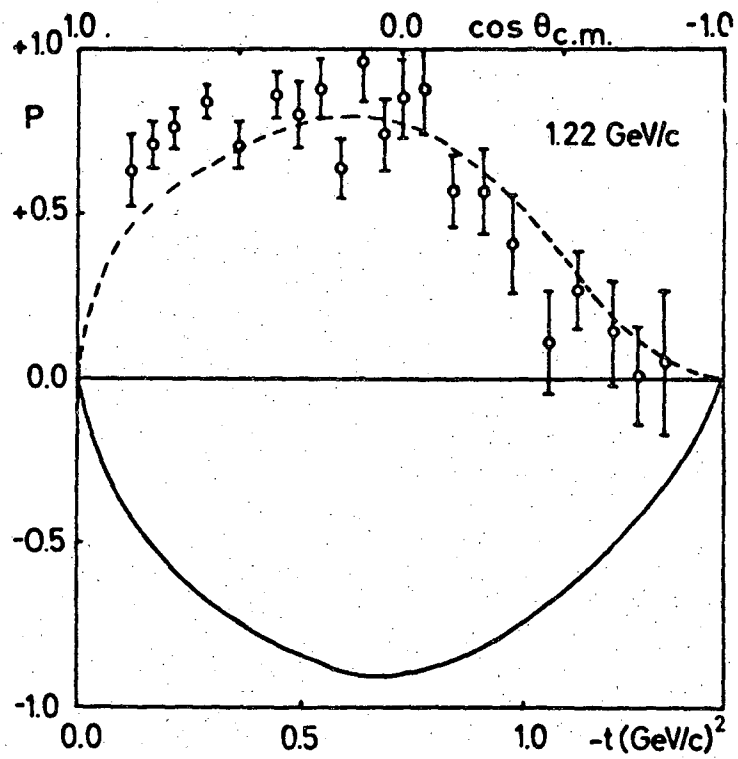
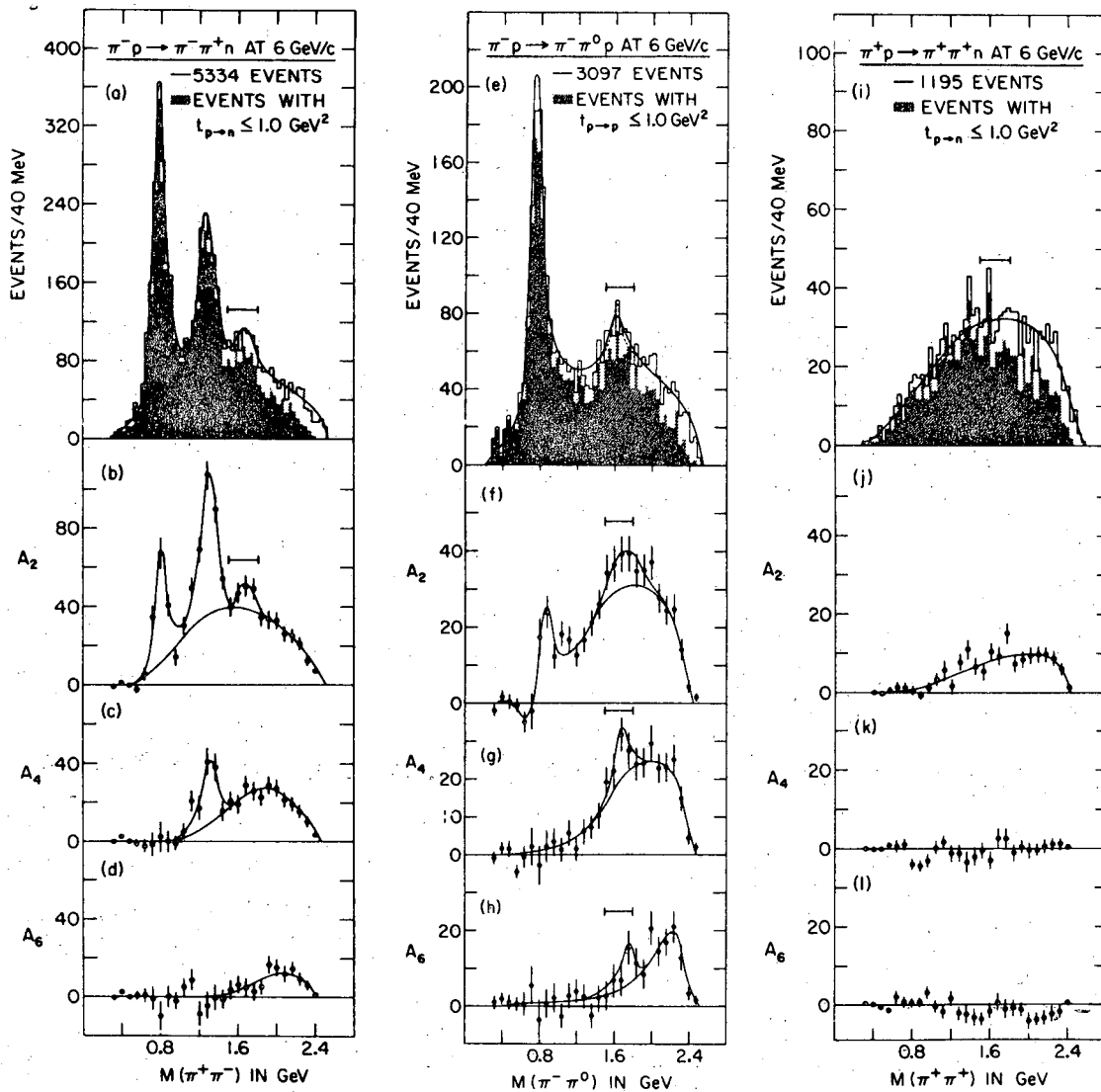


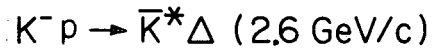
Fig. 7.

XBL 696-603

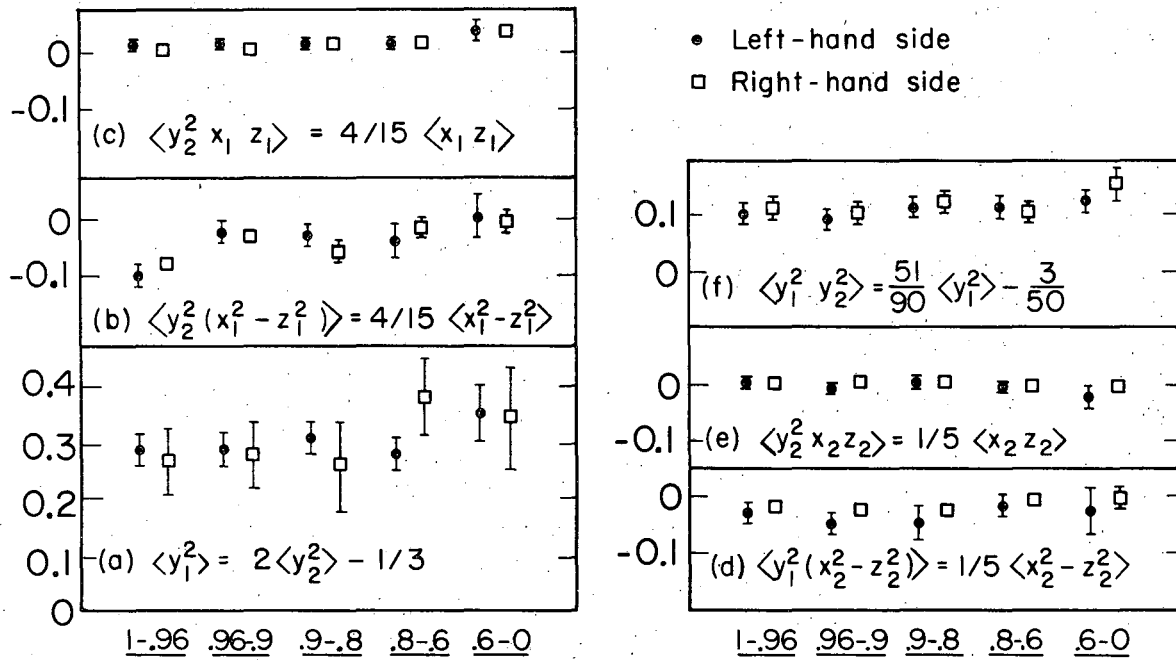


XBL 696-596

Fig. 8.



$\Omega_{\bar{K}^*} = (x_1 y_1 z_1), \quad \Omega_{\Delta} = (x_2 y_2 z_2)$



XBL6812-7358

Fig. 9.

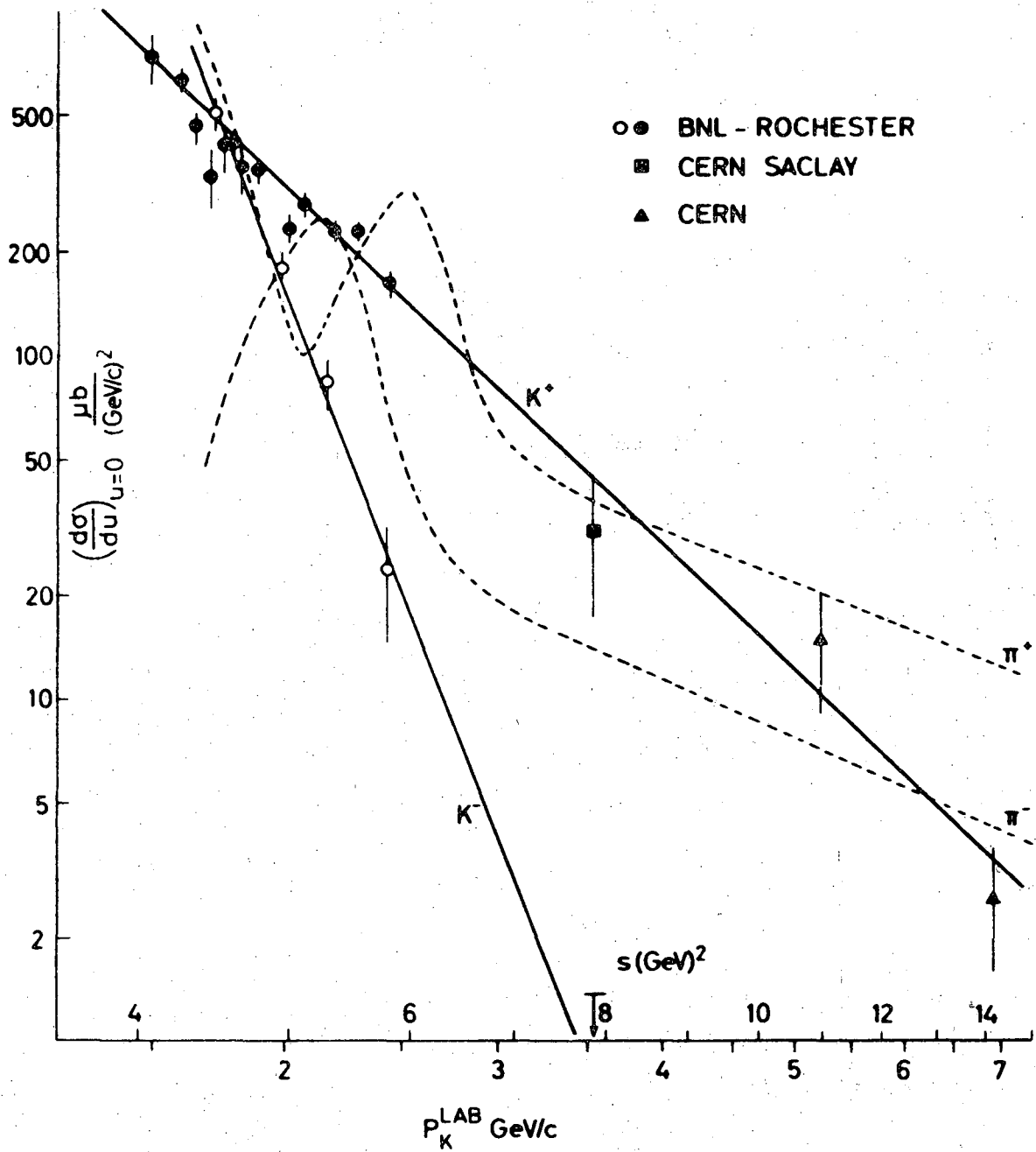
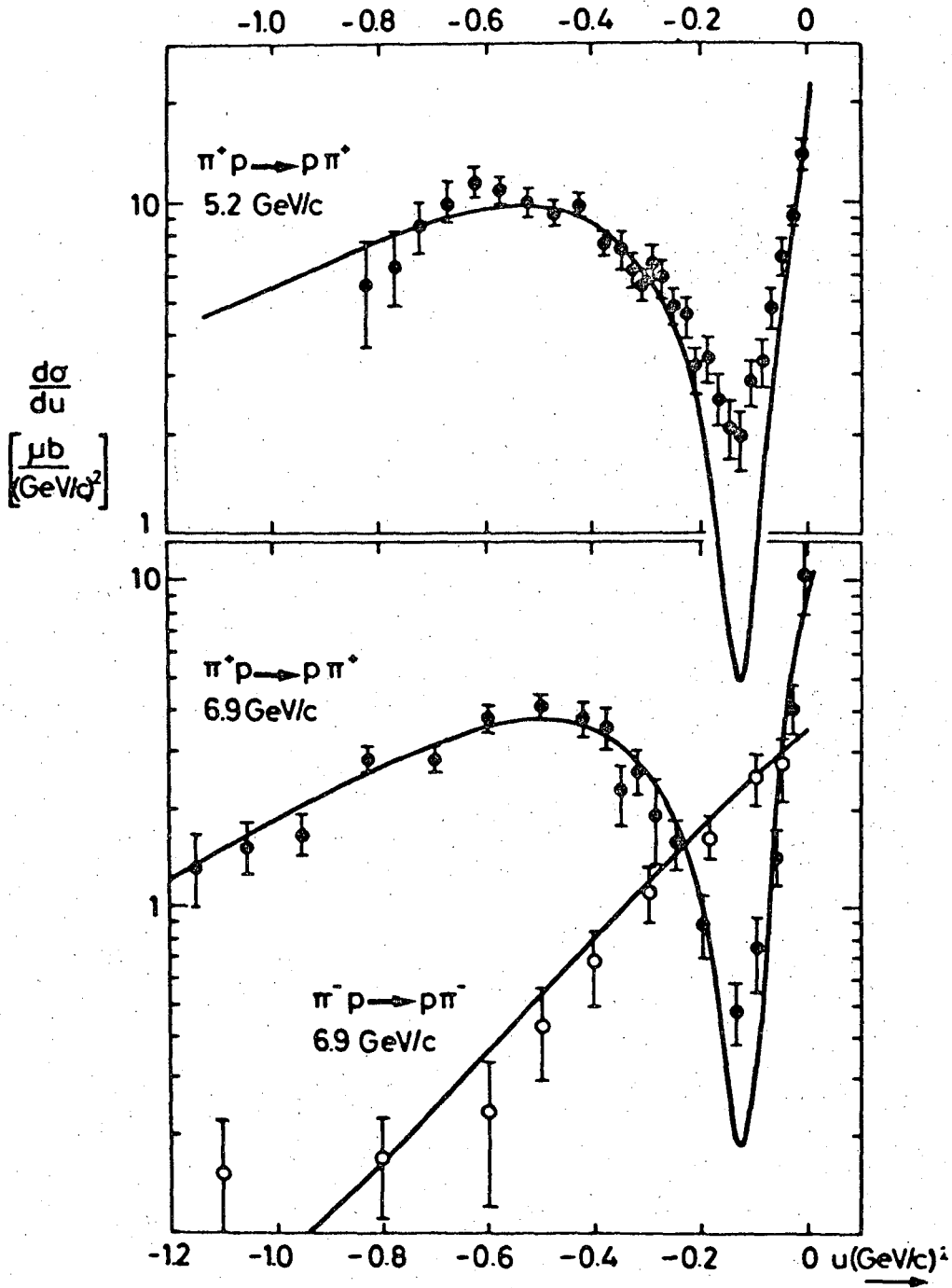


Fig. 10.



XBL 696-604

Fig. 11.

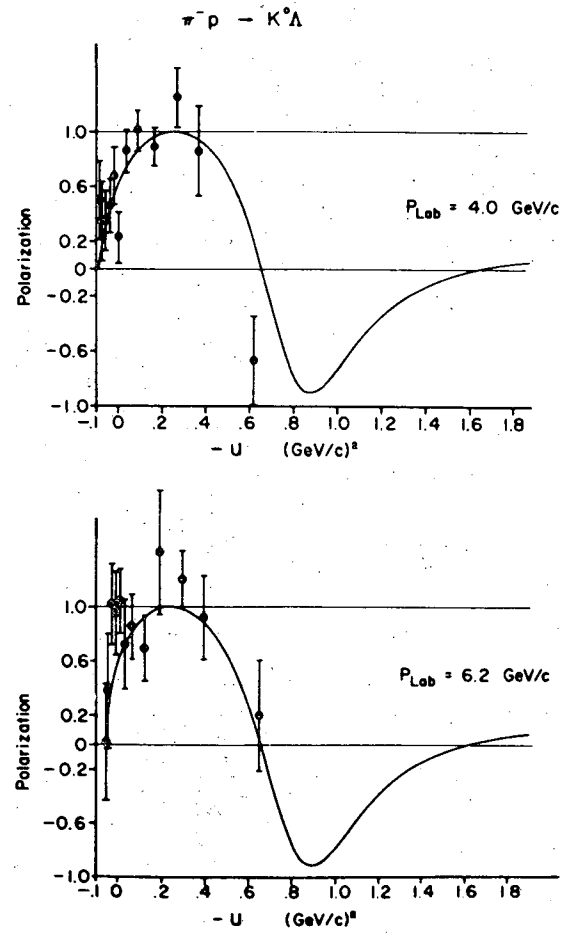
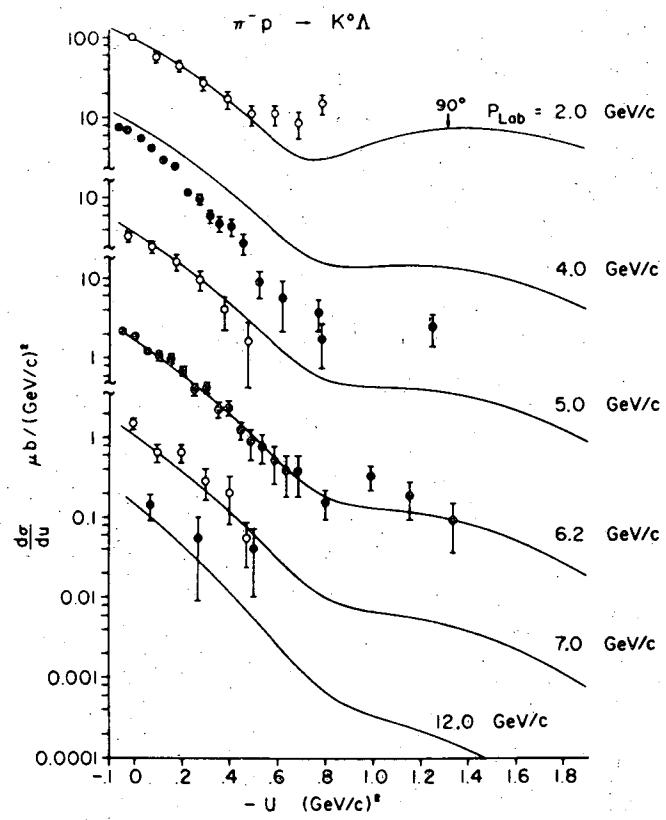
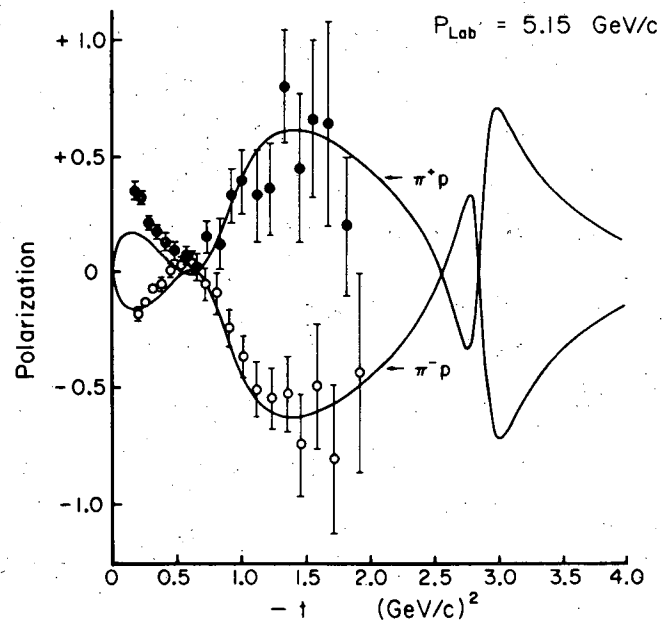
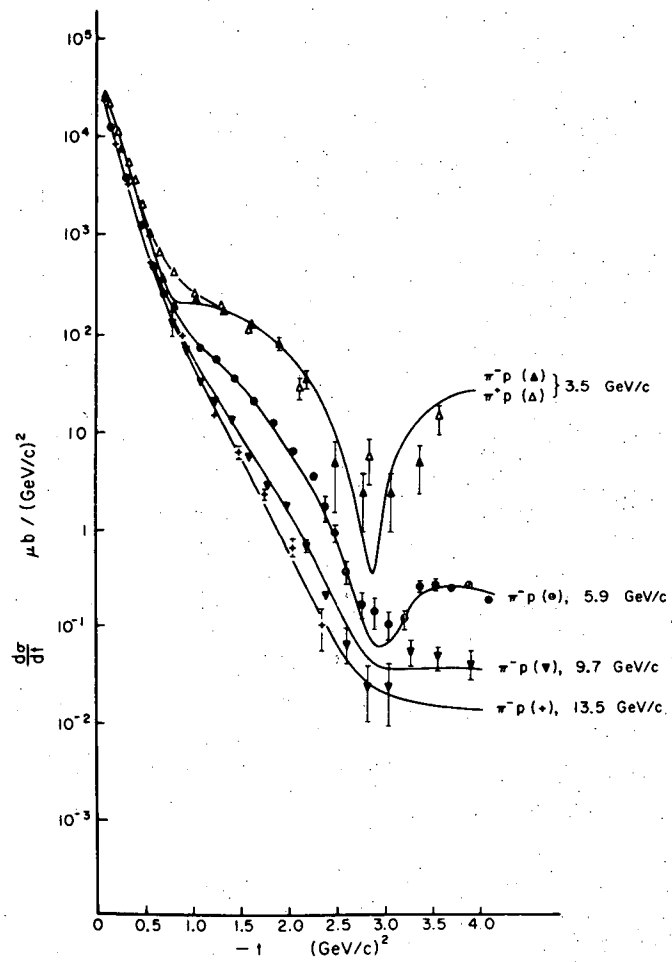


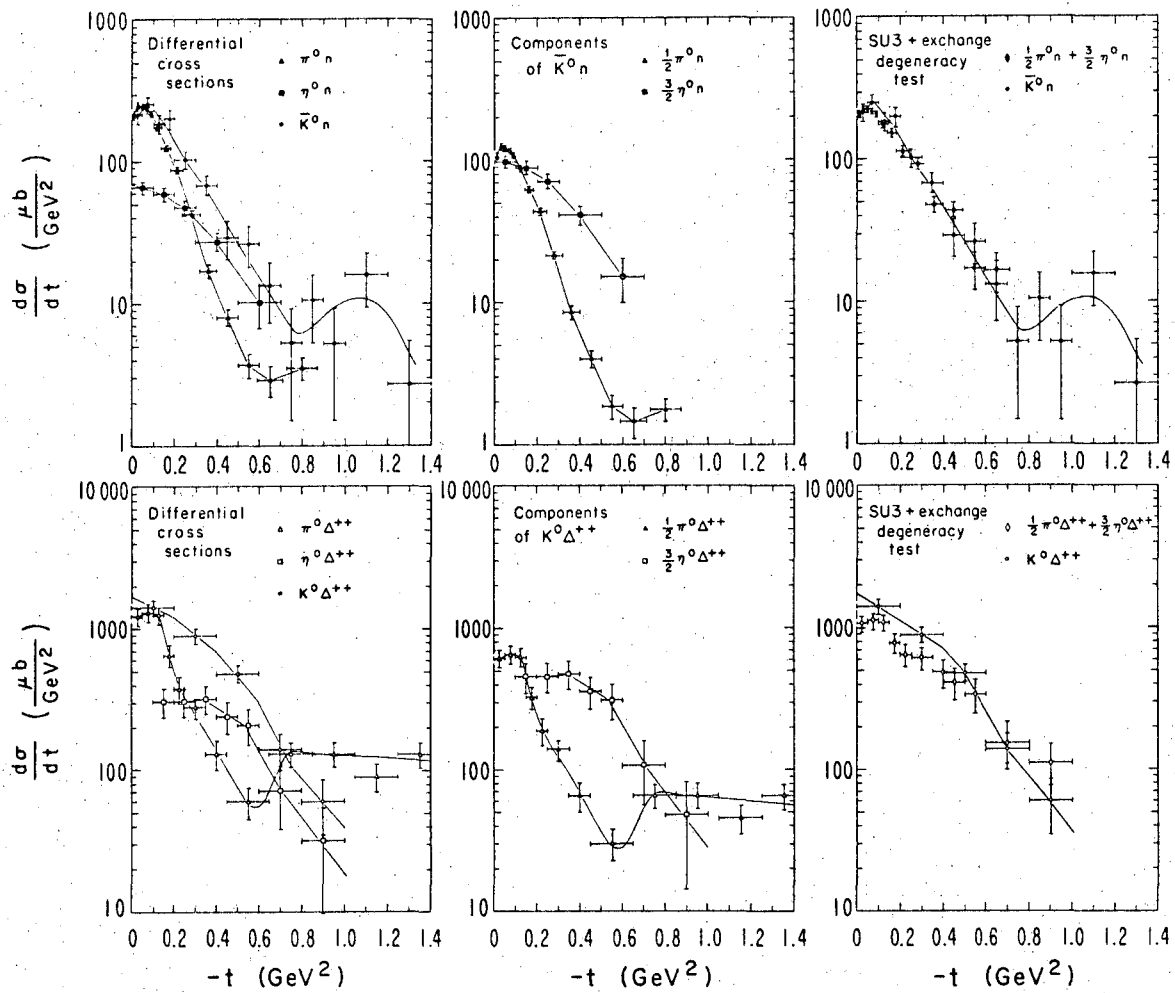
Fig. 12.

XBL 696-605



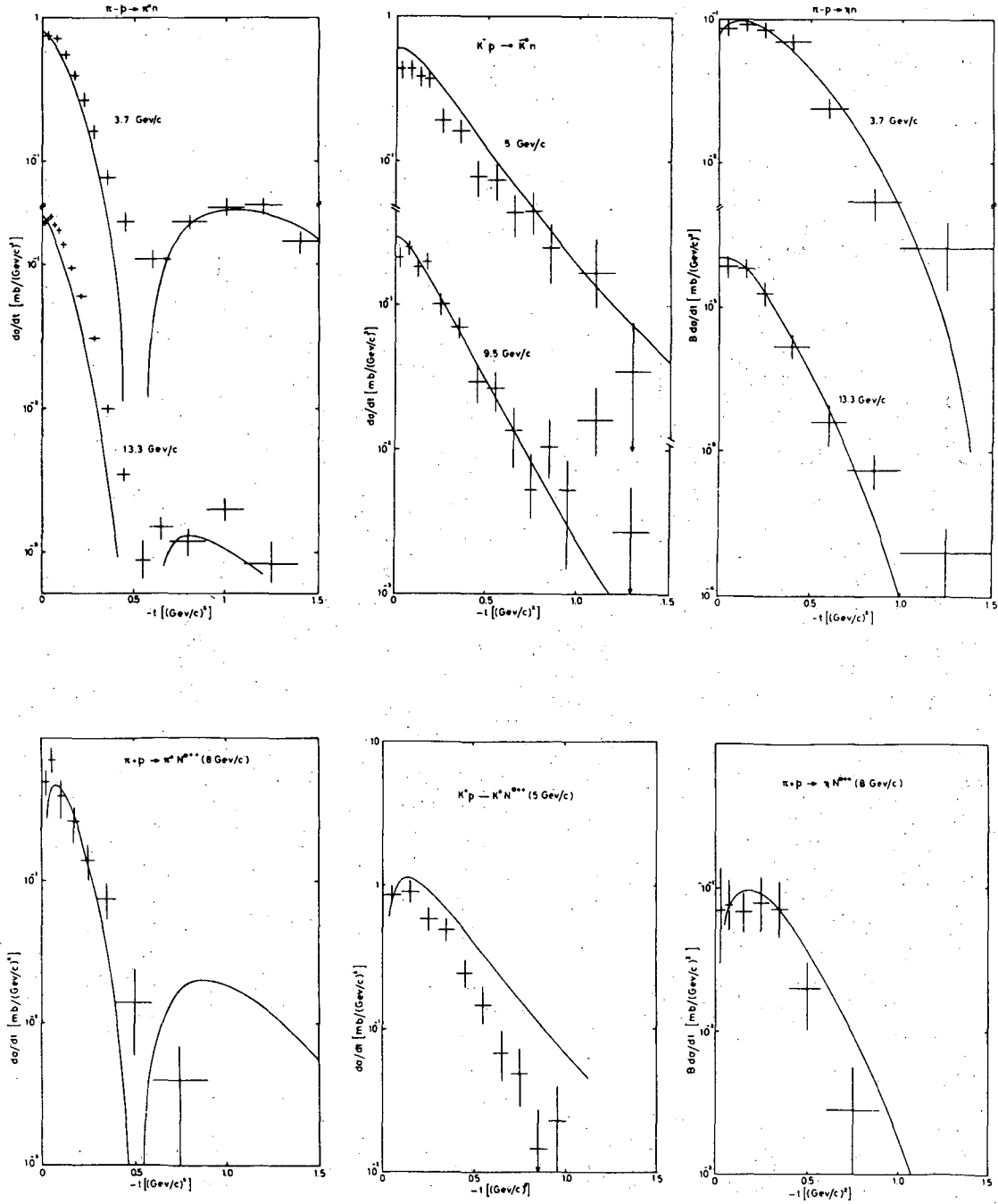
XBL 696-592

Fig. 13.



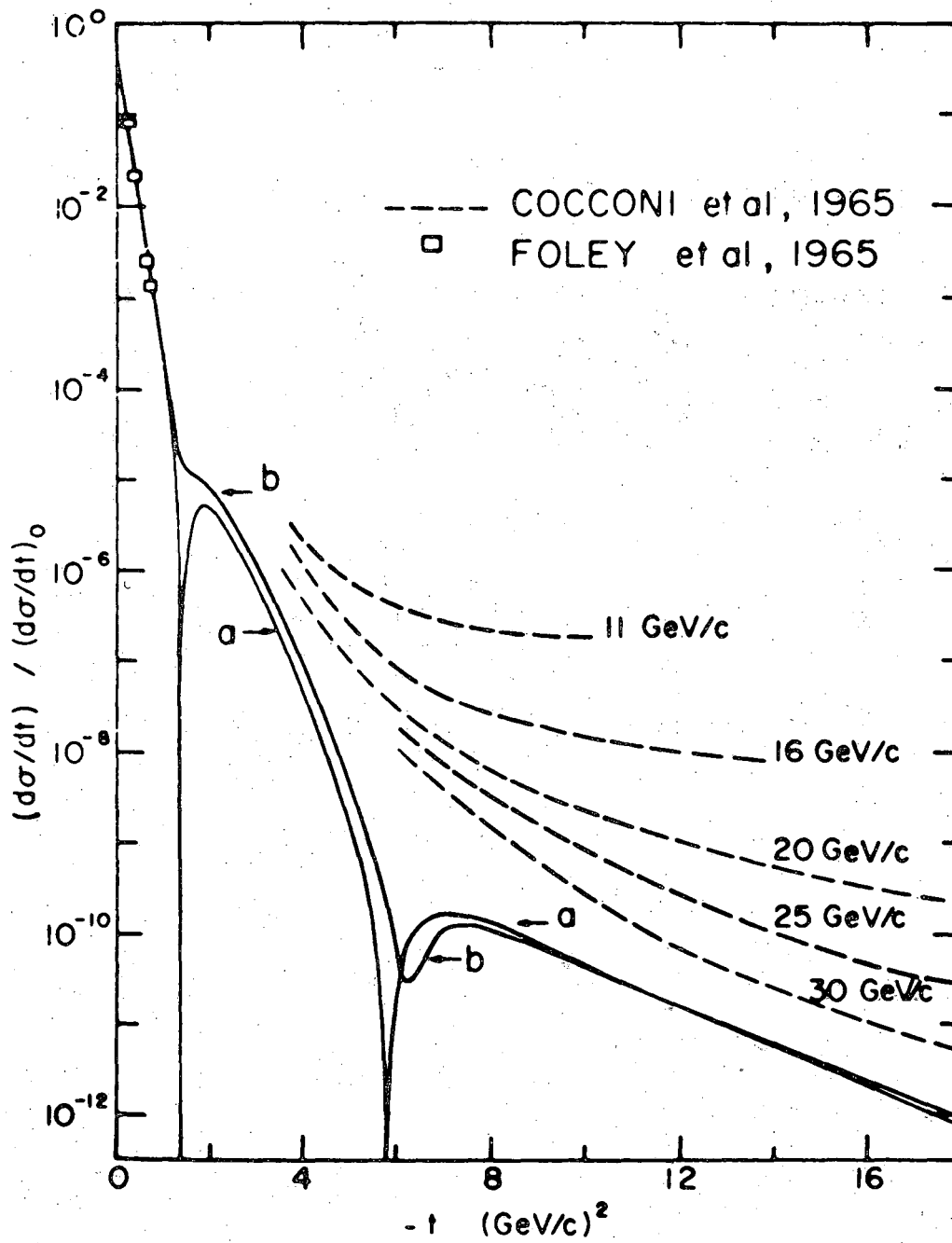
XBL691-1616

Fig. 14.



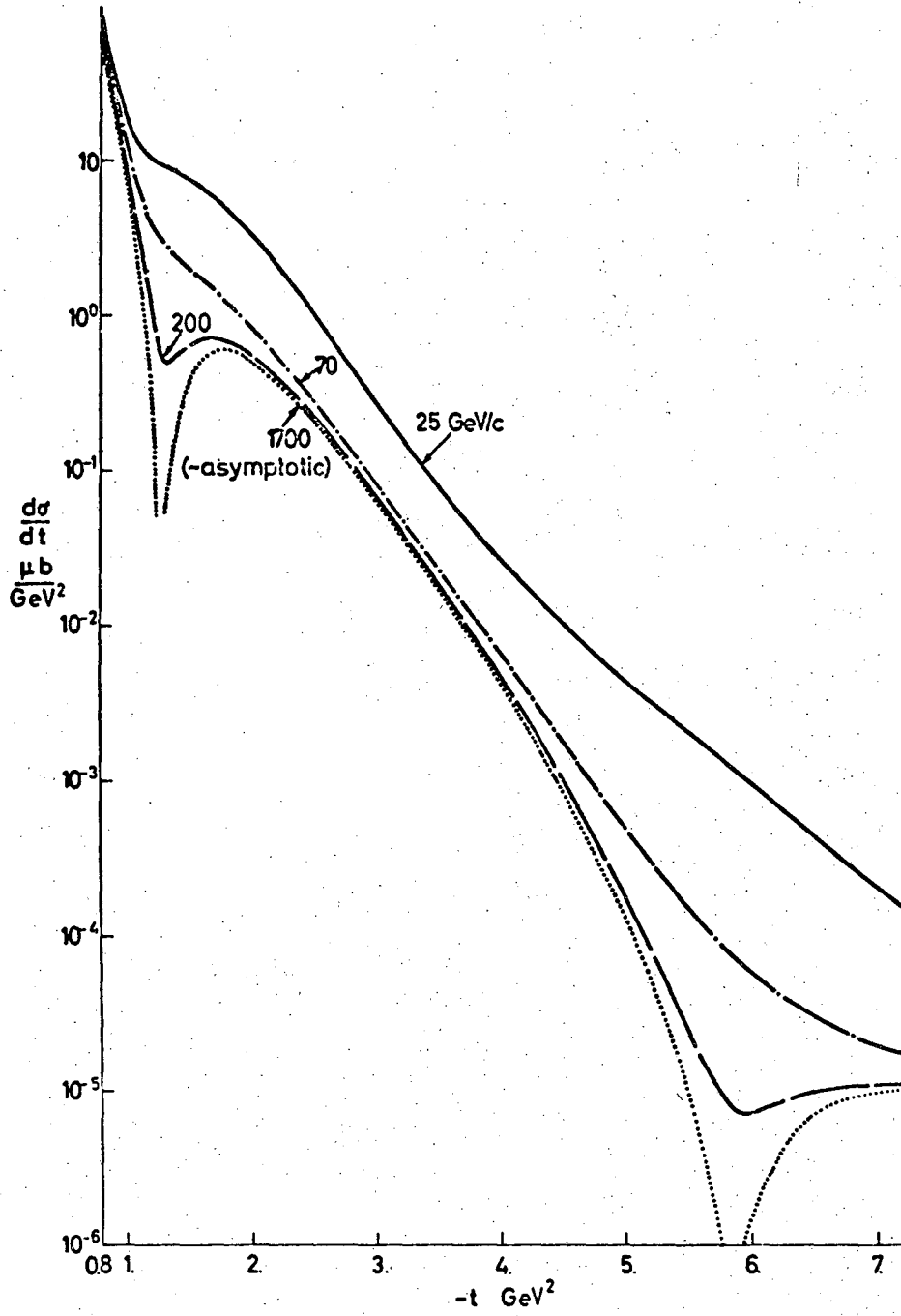
XBL 696-595

Fig. 15.



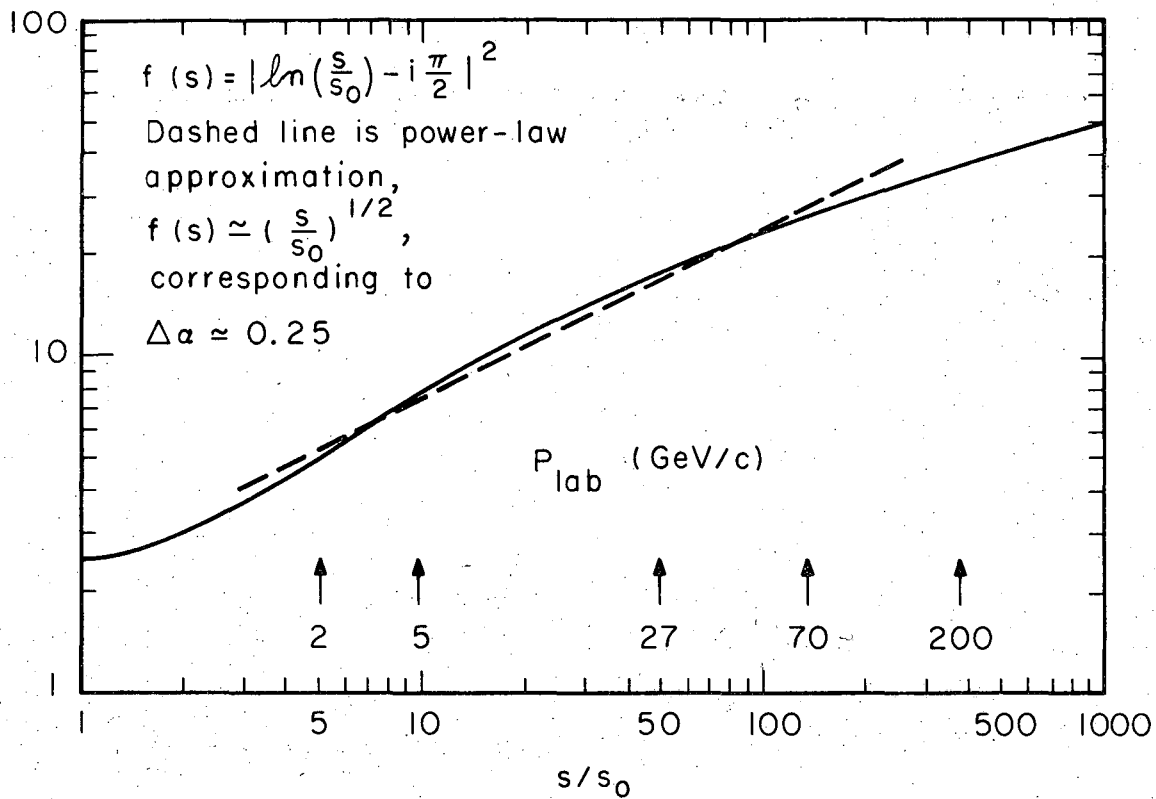
XBL 696-593

Fig. 16



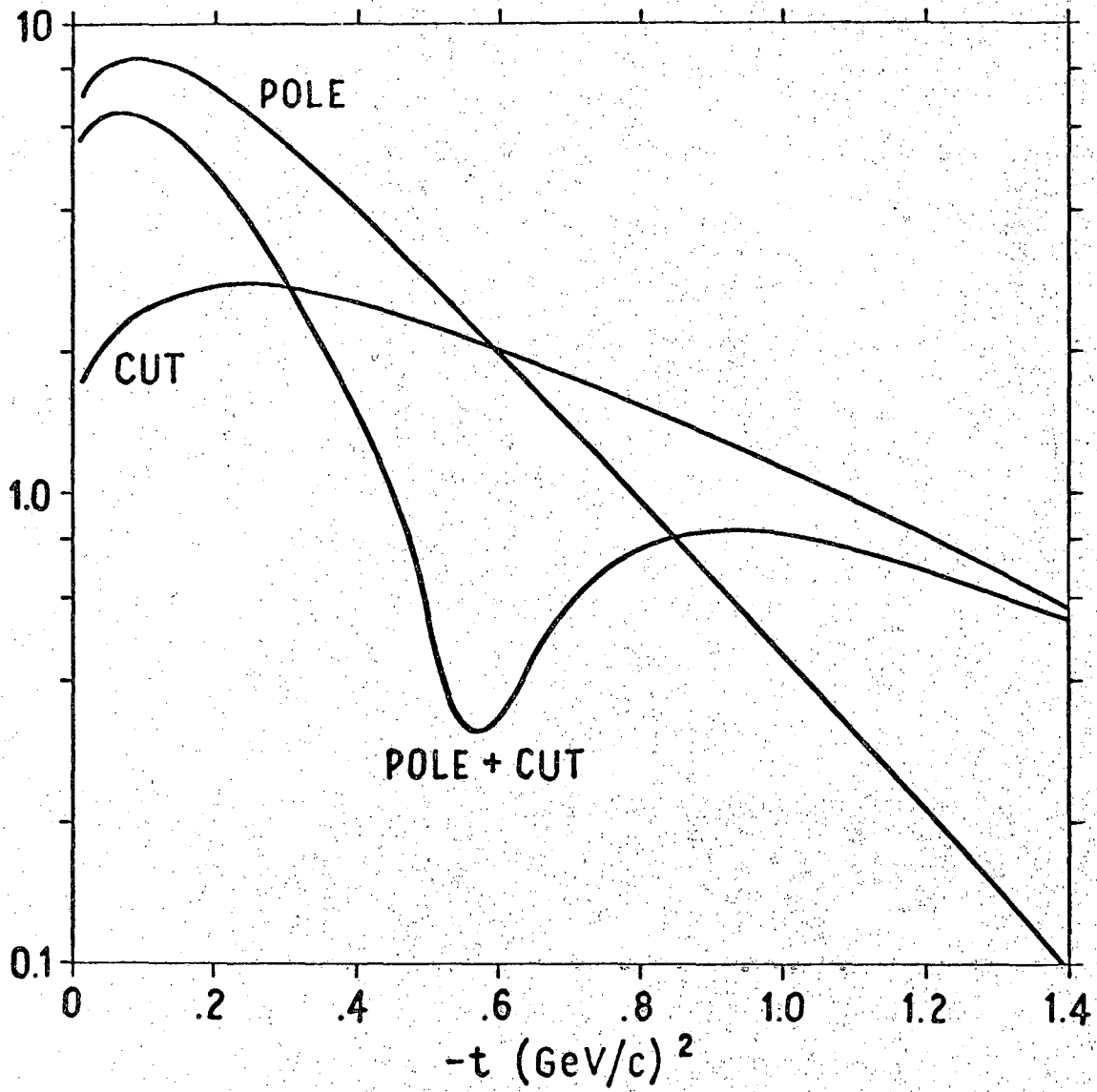
XBL 696-601

Fig. 17.



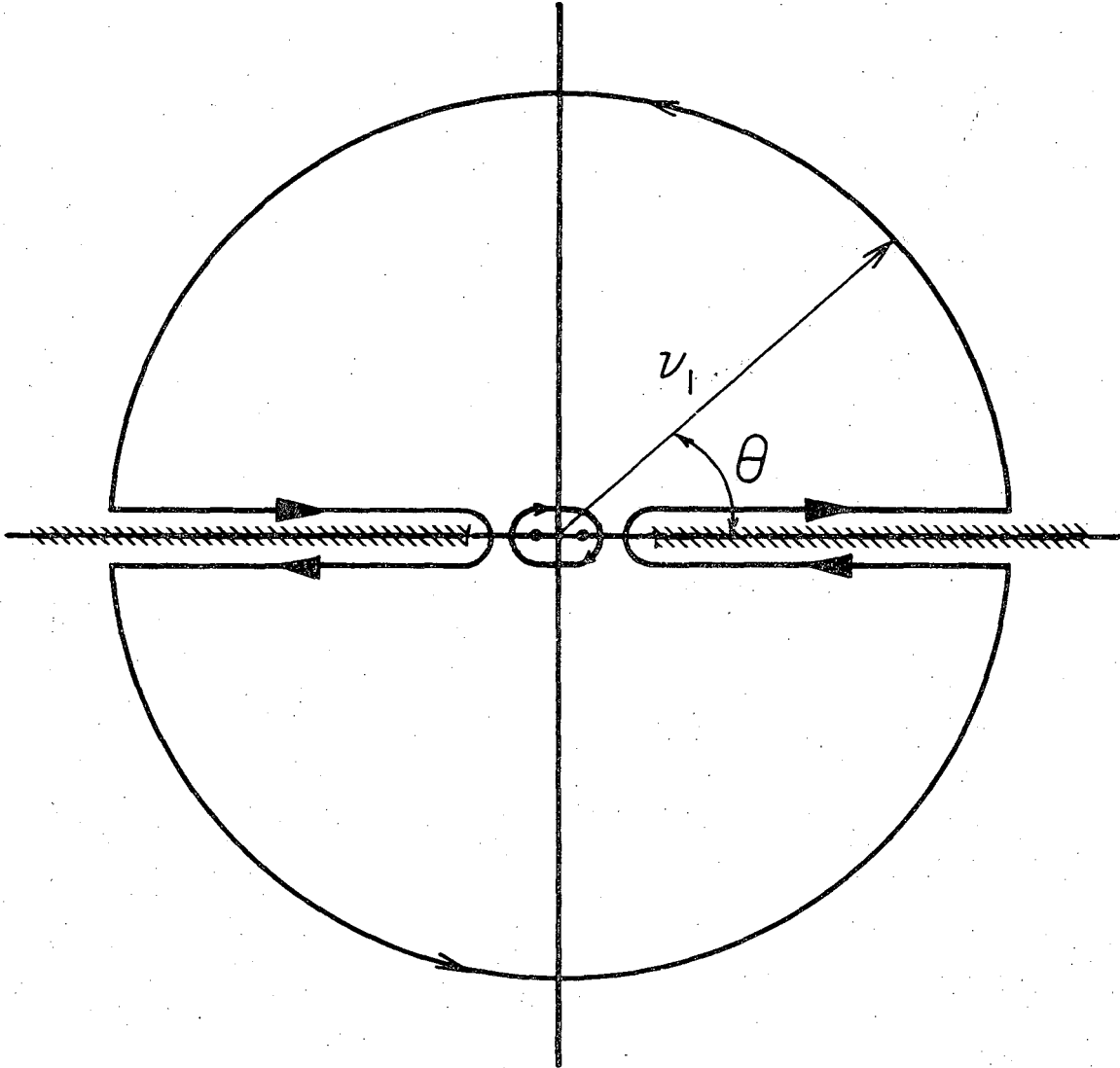
XBL696-2929

Fig. 18.



XBL 696-597

Fig. 19



XBL696-2932

Fig. 20.

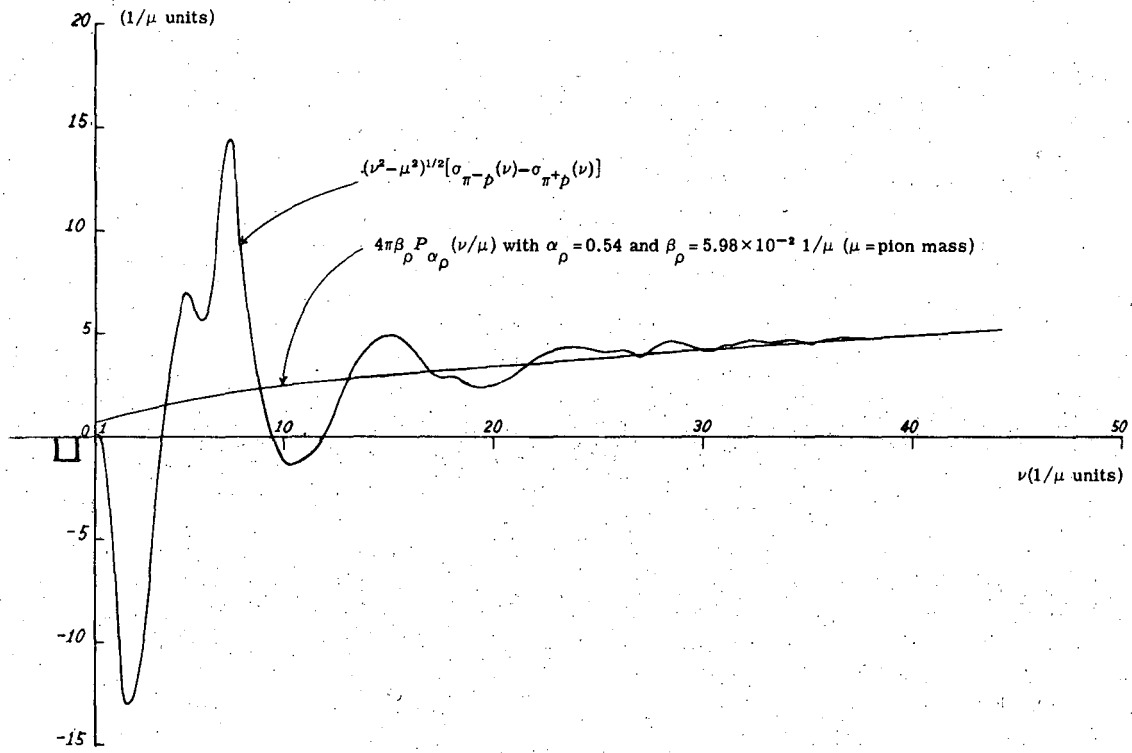


Fig. 21.

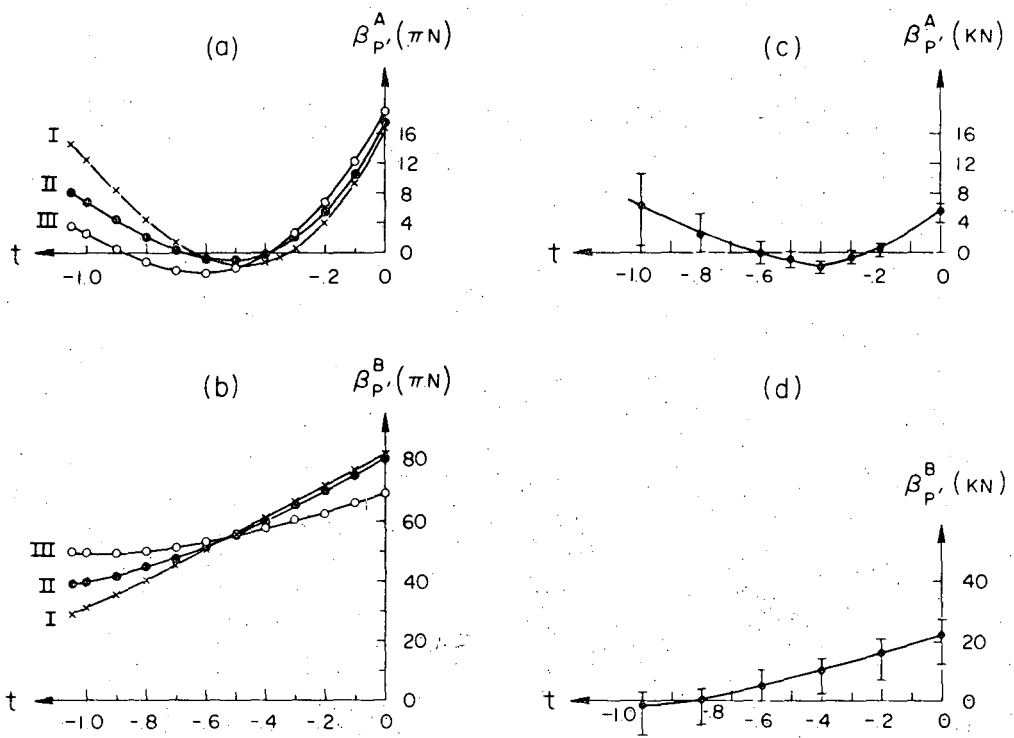
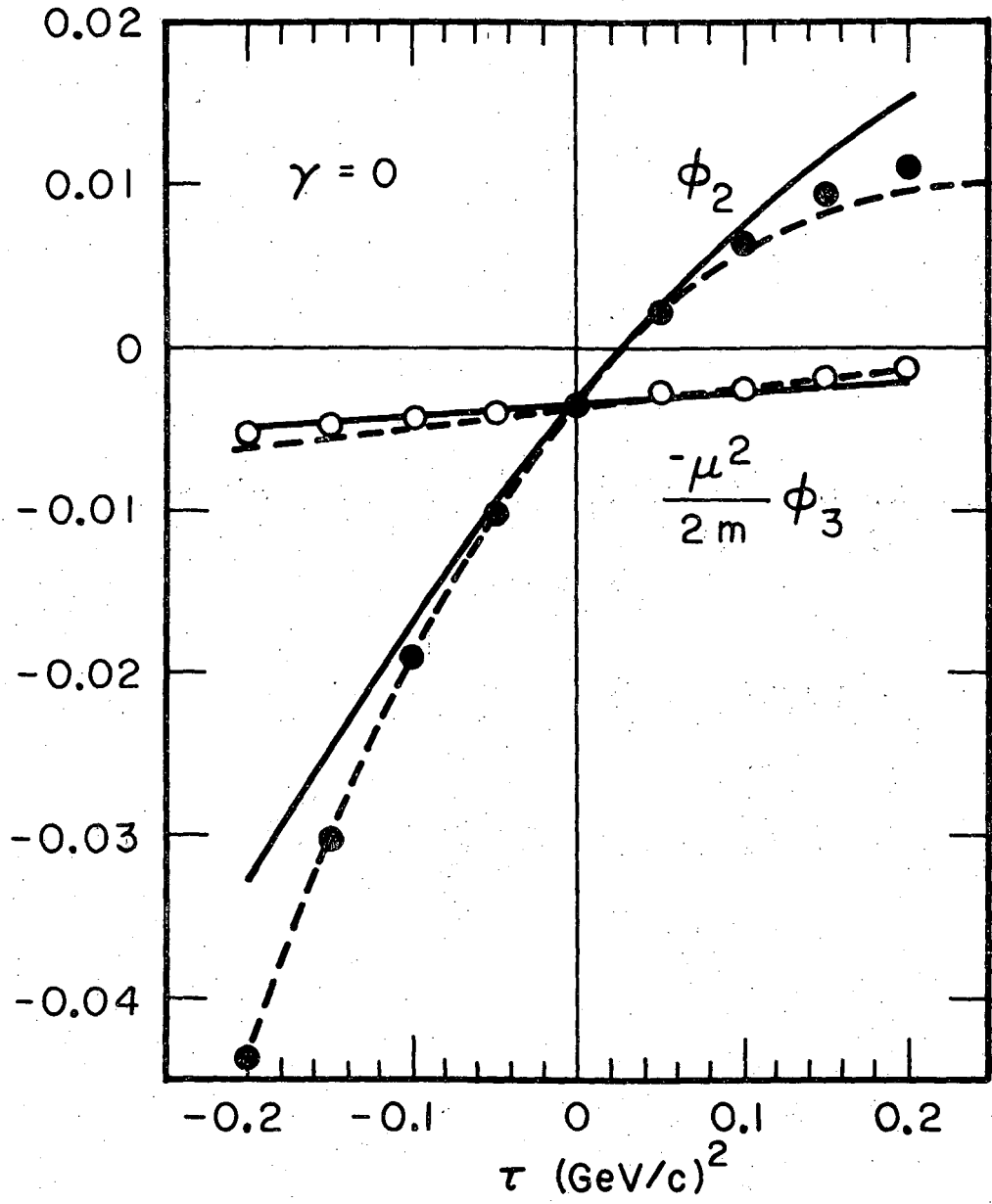
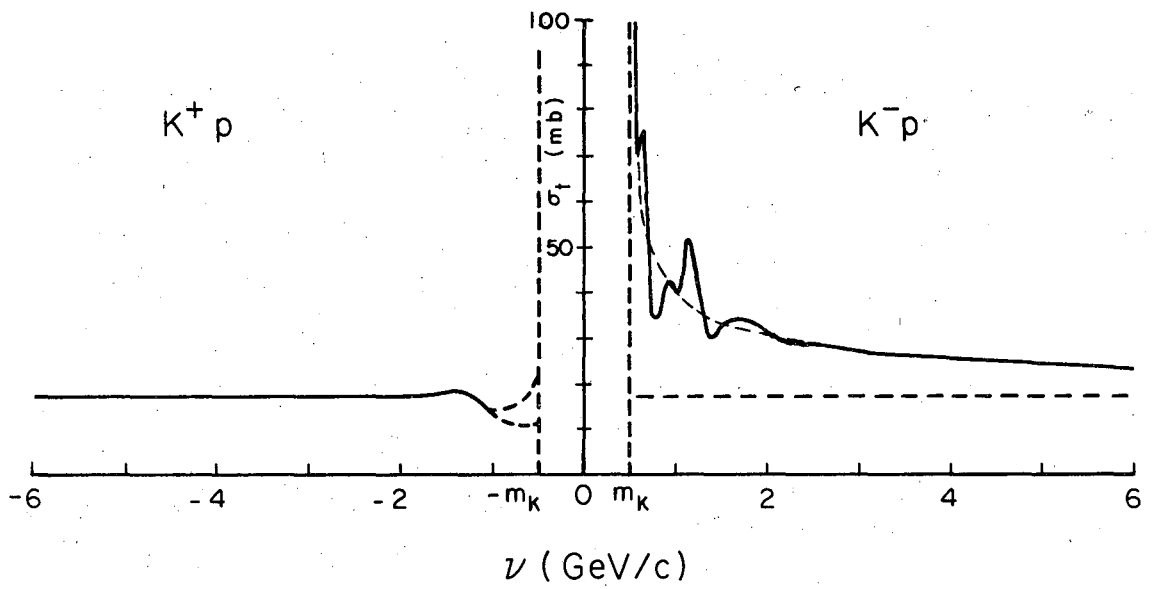


Fig. 22.



XBL 692-1947

Fig. 23.



XBL696-2980

Fig. 24

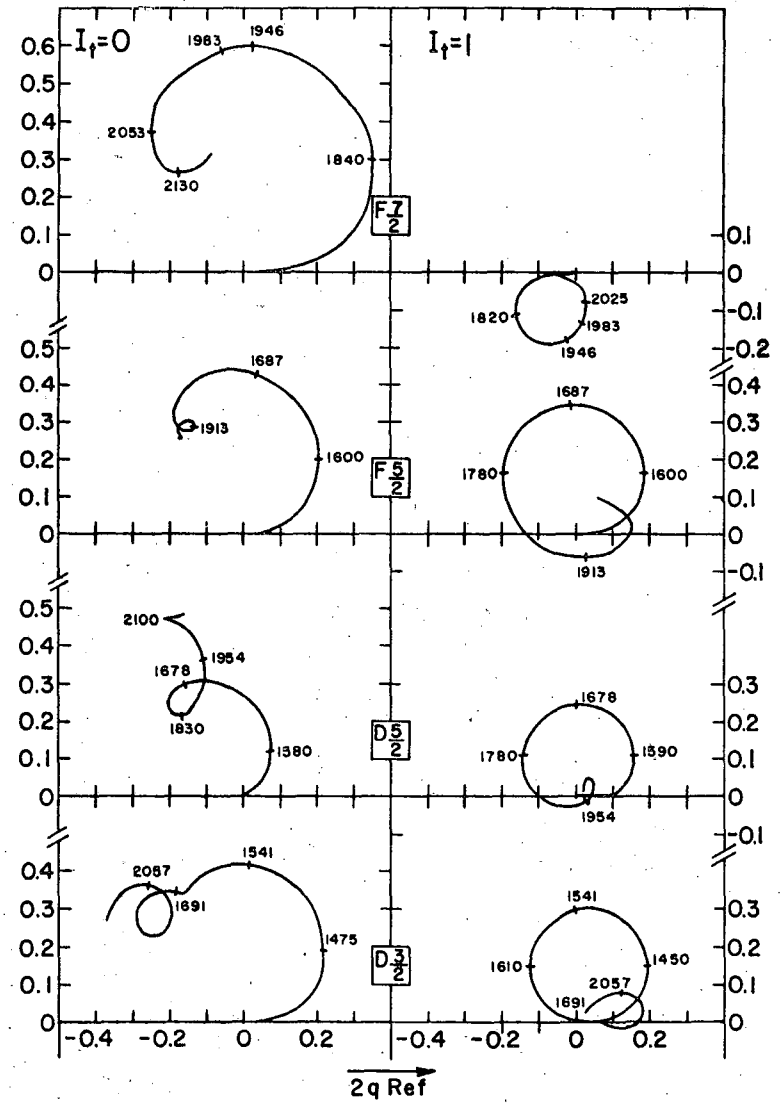
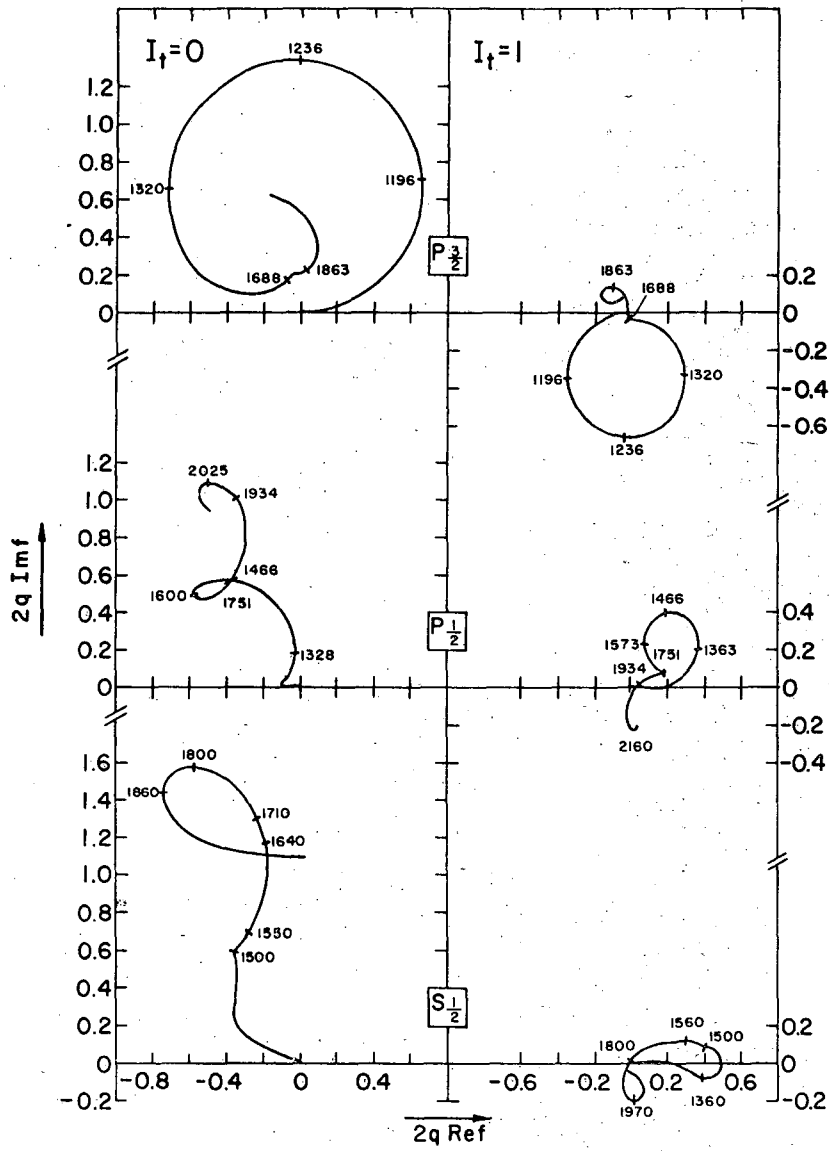
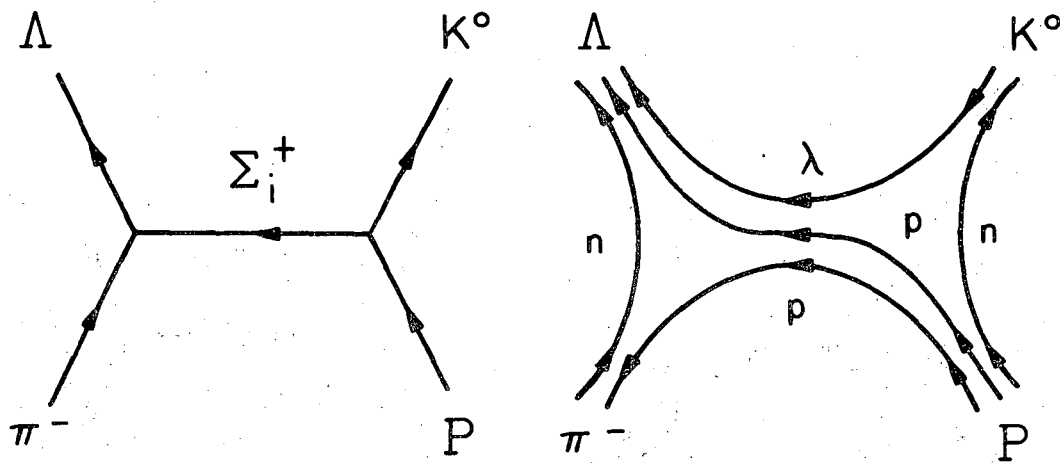
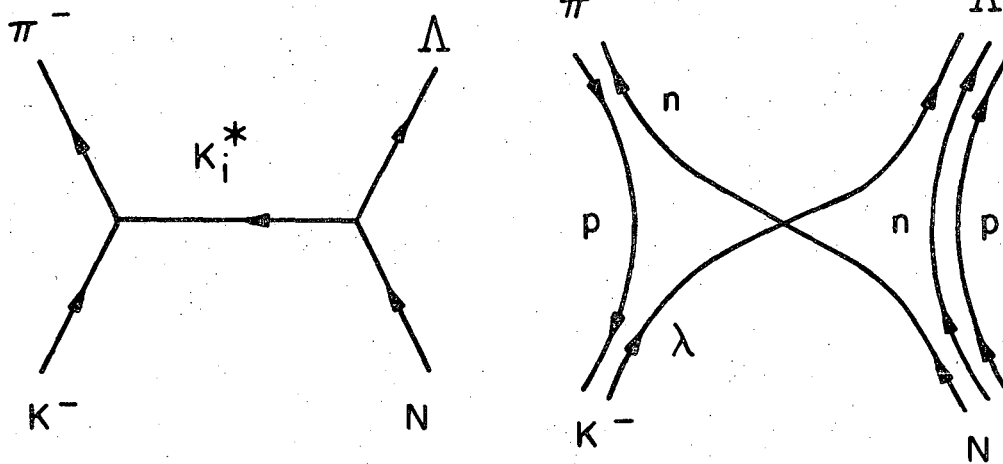


Fig. 25.



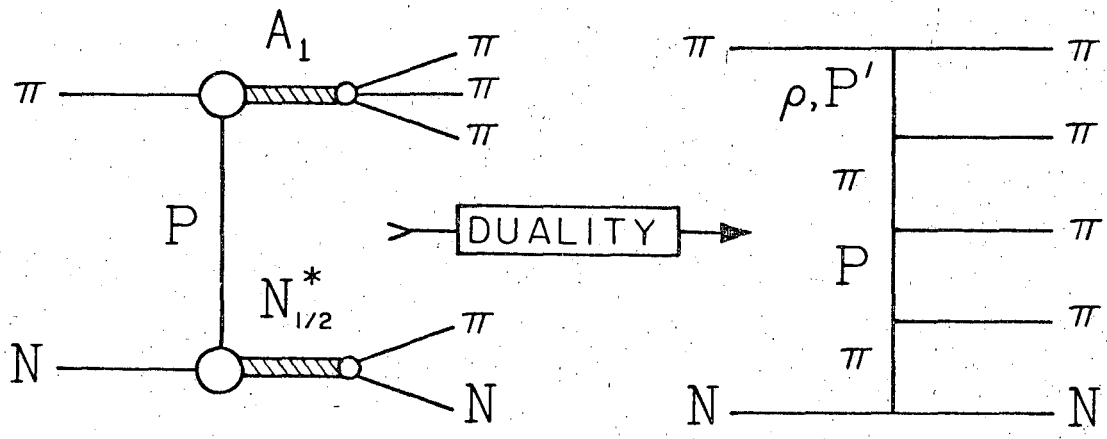
(a)



(b)

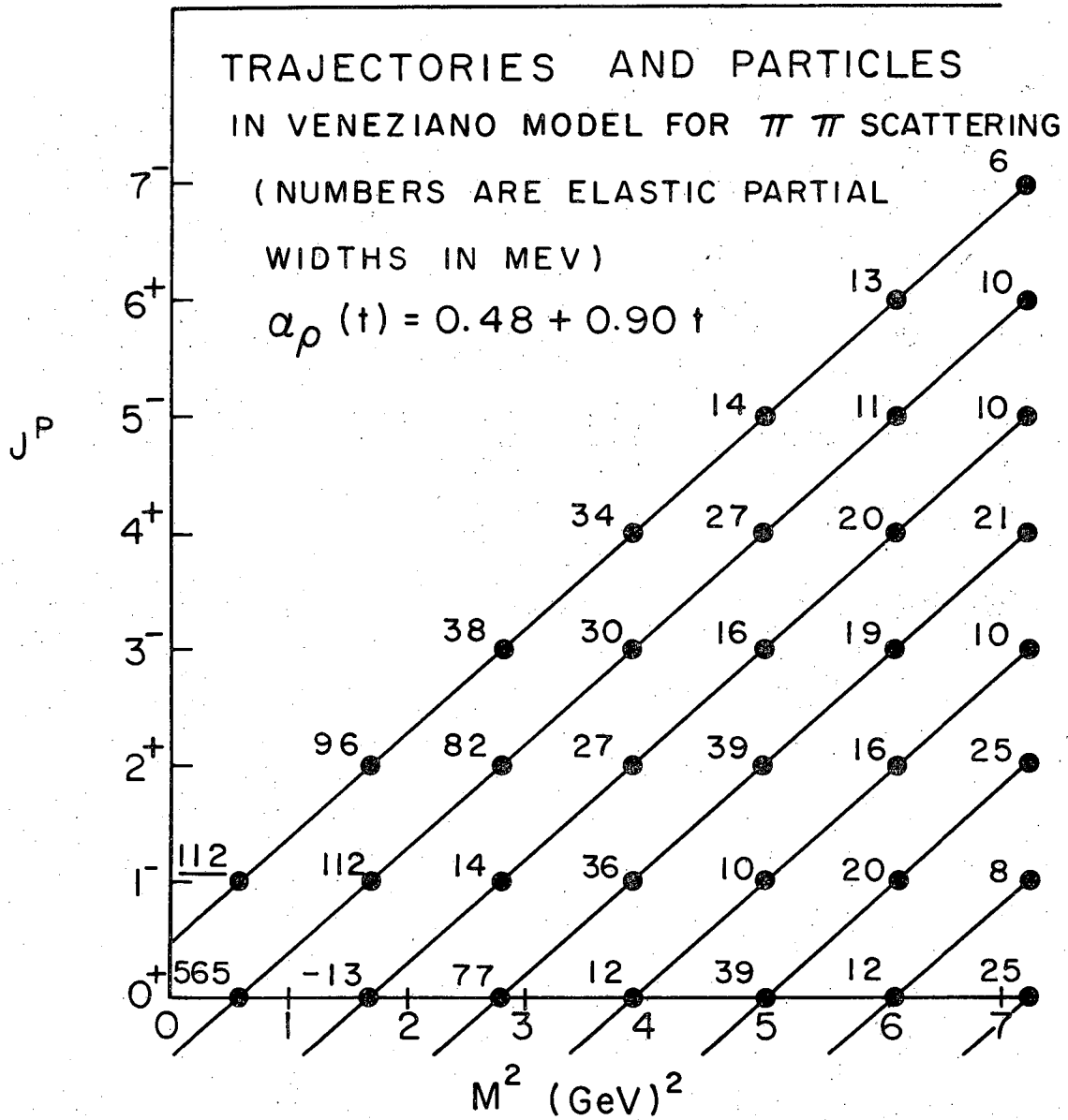
XBL696 - 2981

Fig. 26.



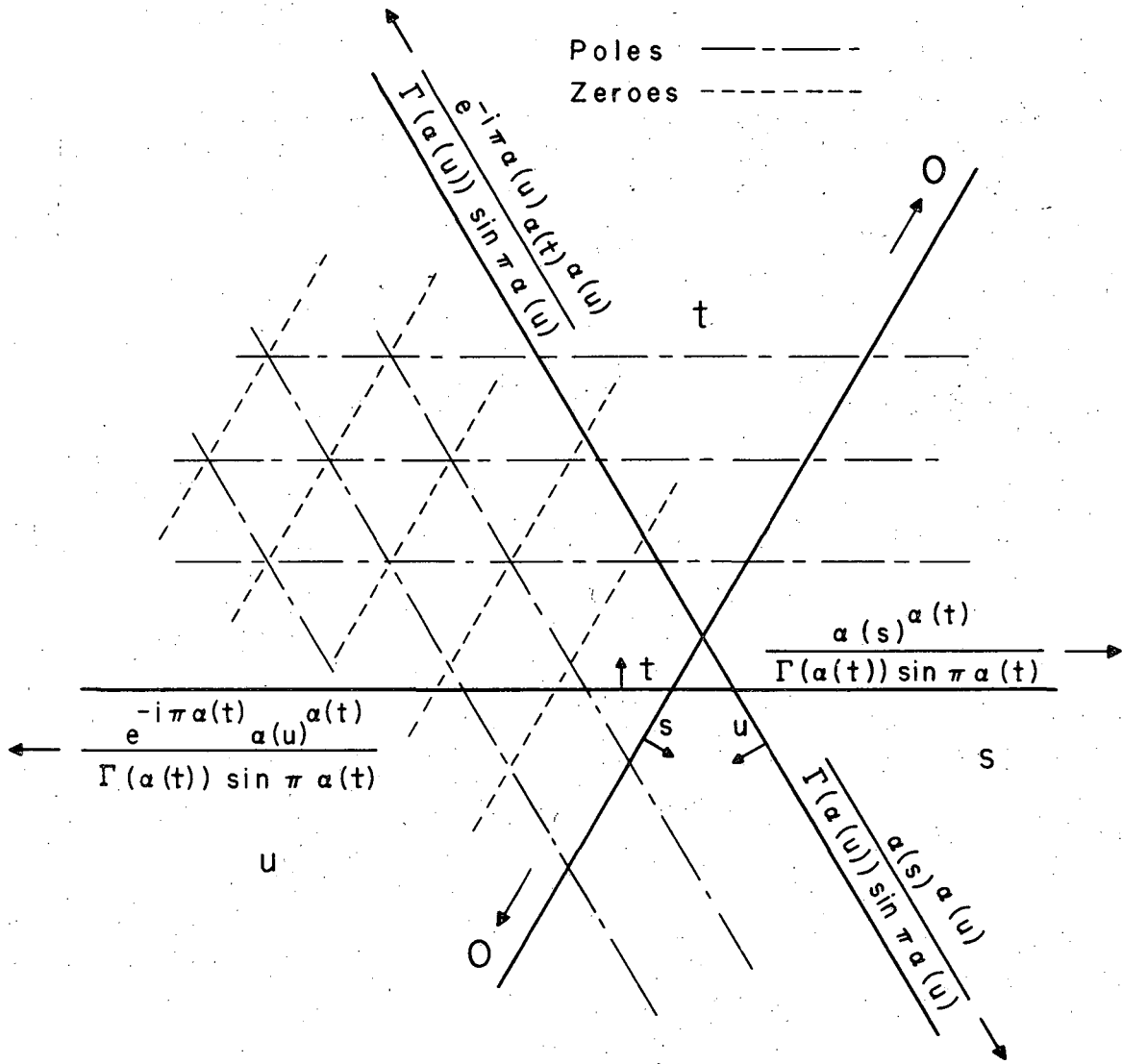
XBL696-2982

Fig. 27.



XBL 696-2983

Fig. 28.



XBL6811-7146

Fig. 29.

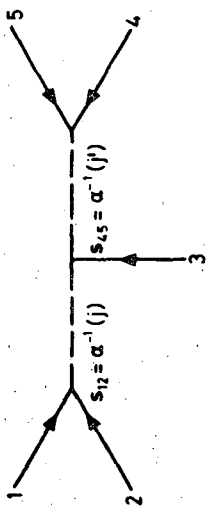
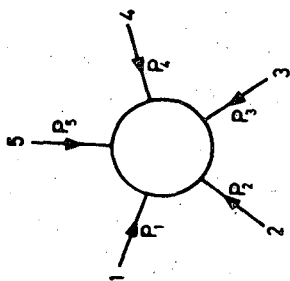
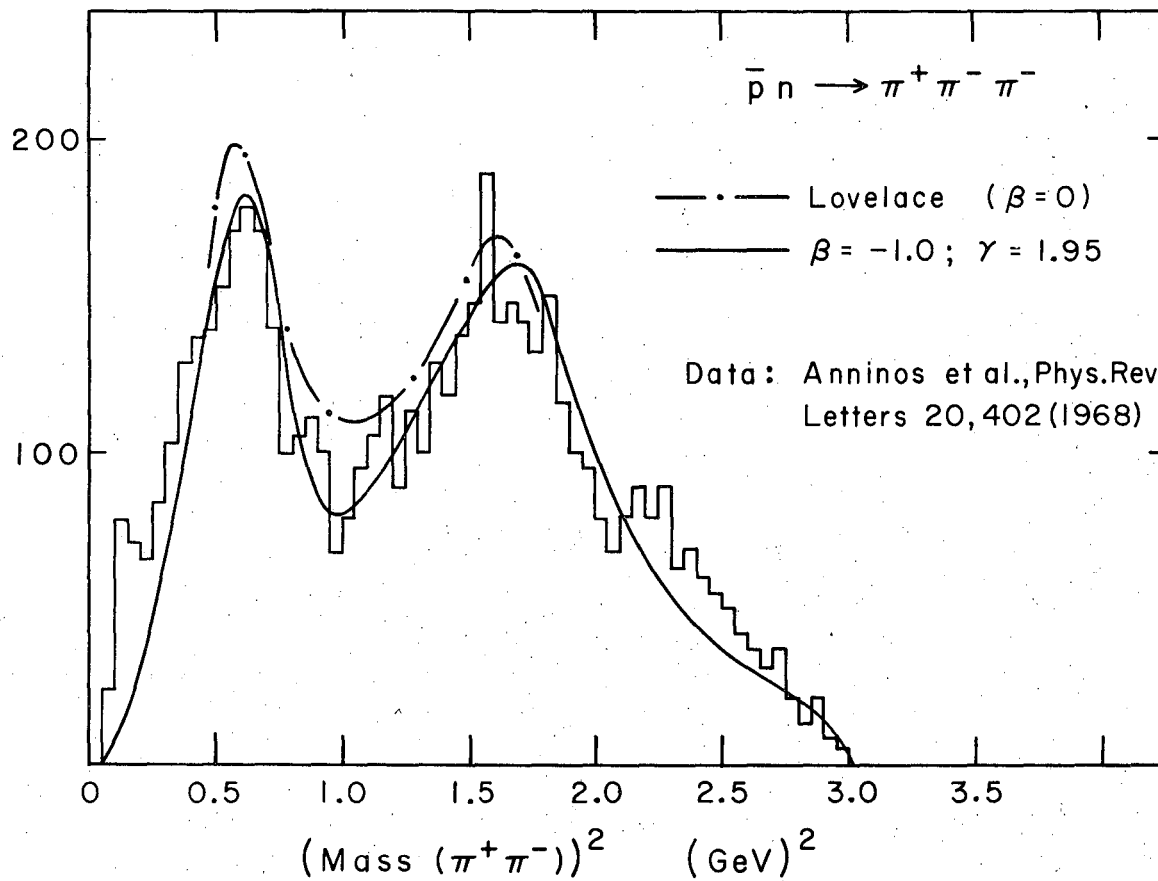
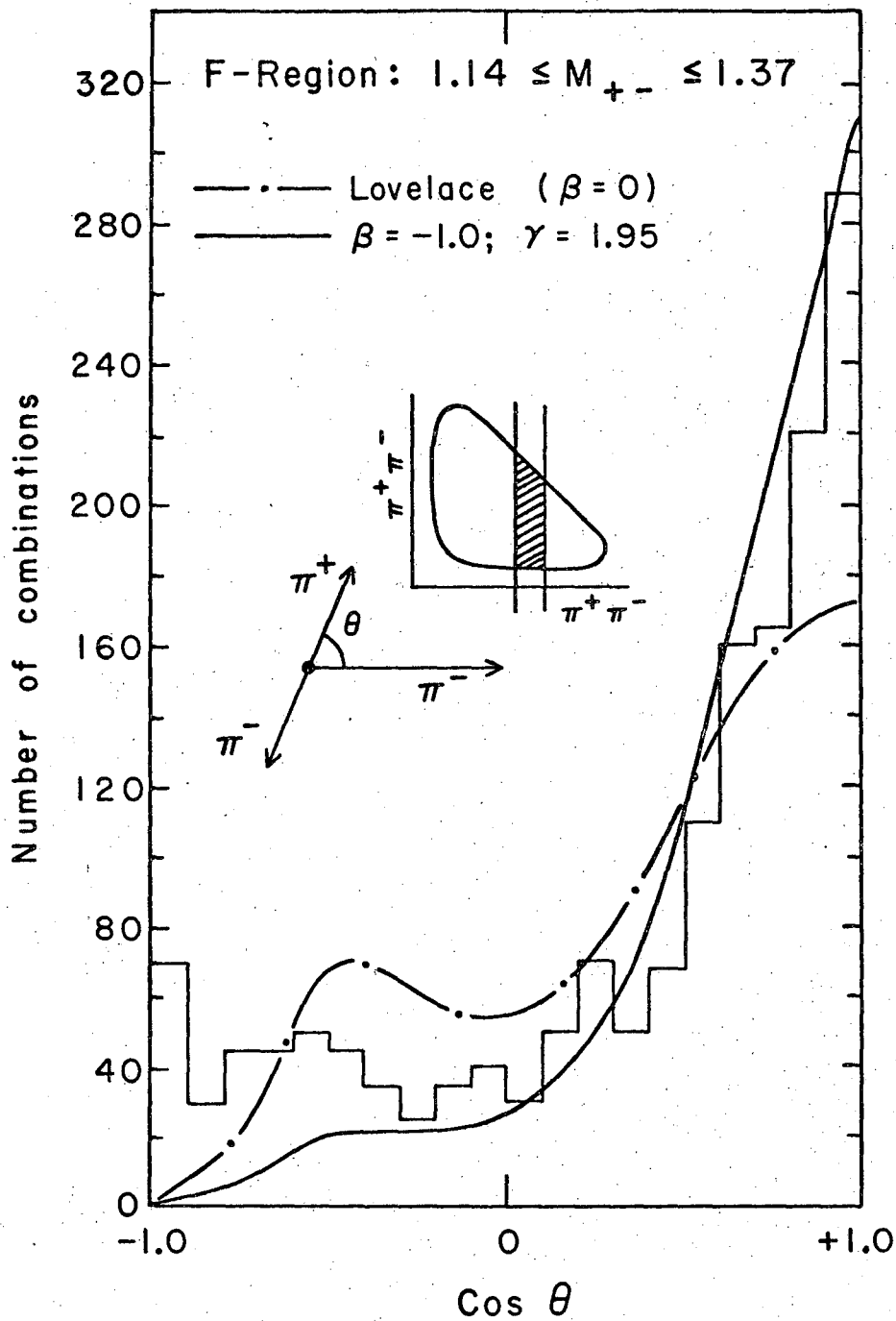


Fig. 30.



XBL 695-2669

Fig. 31.



XBL695-2667

Fig. 32.

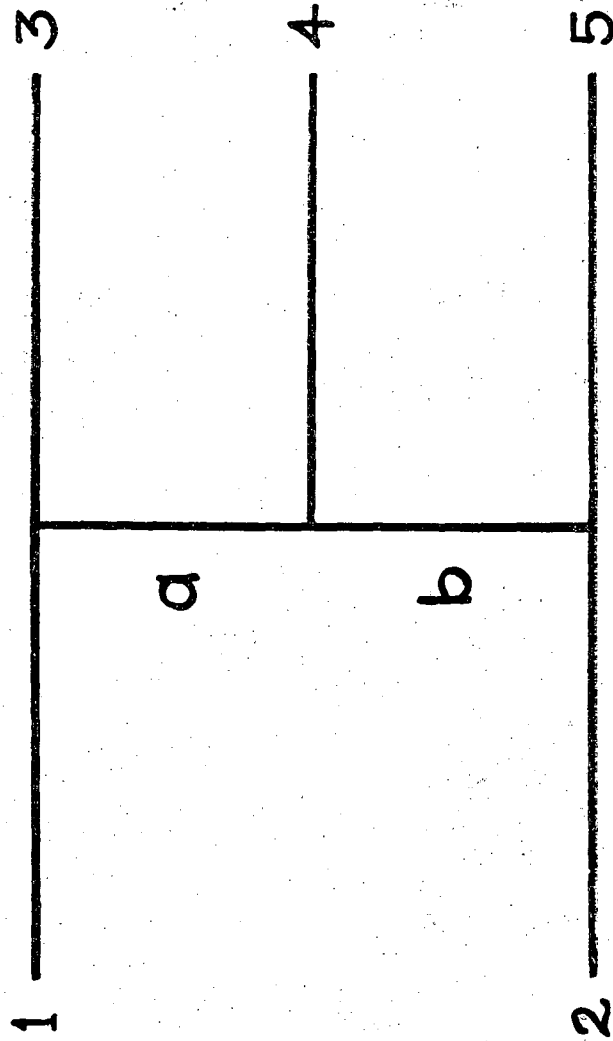


Fig. 33.

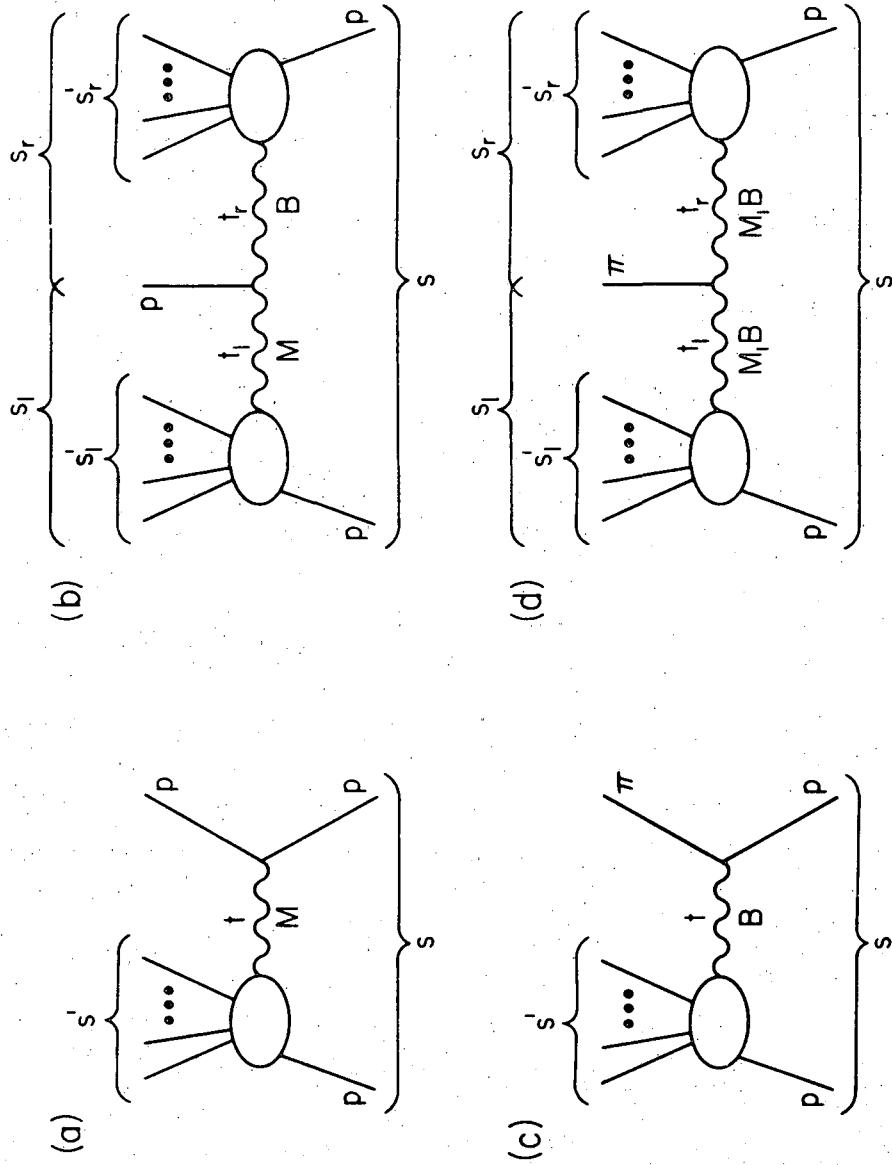


Fig. 34.

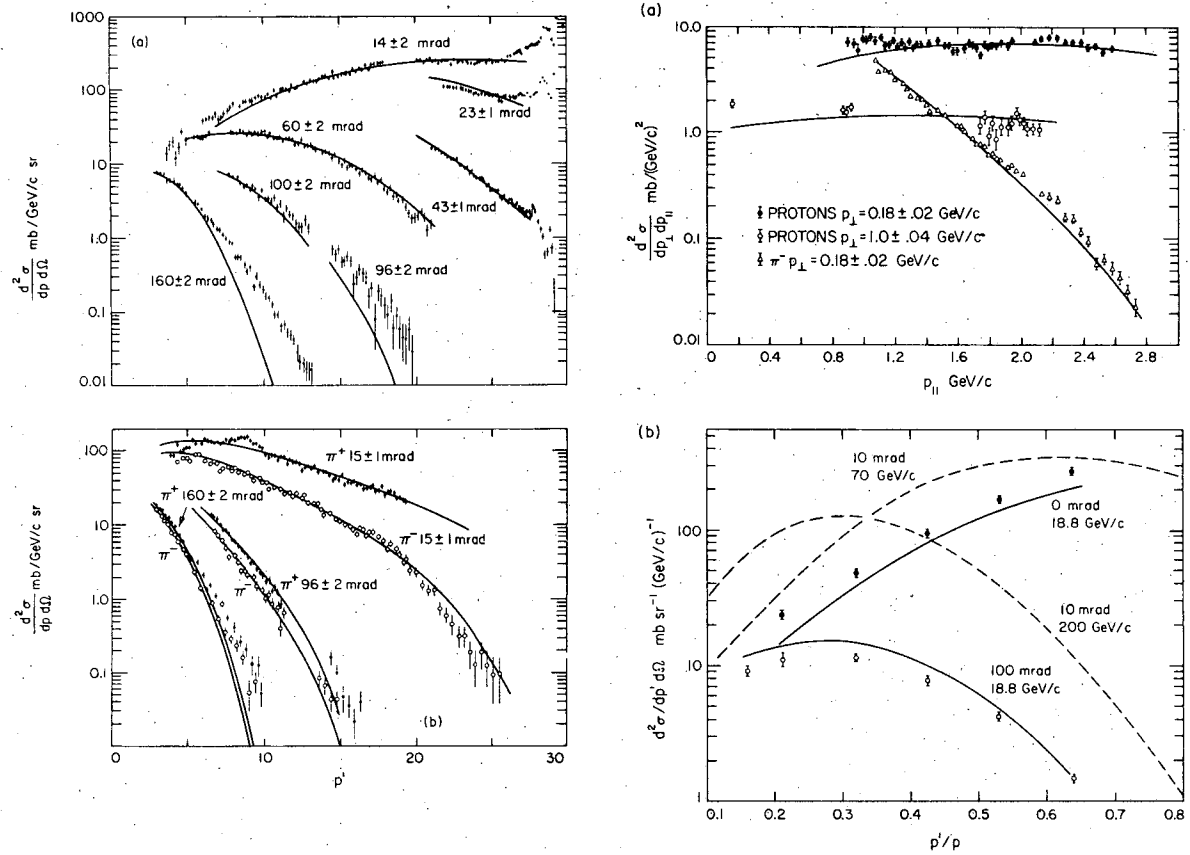


Fig. 35.

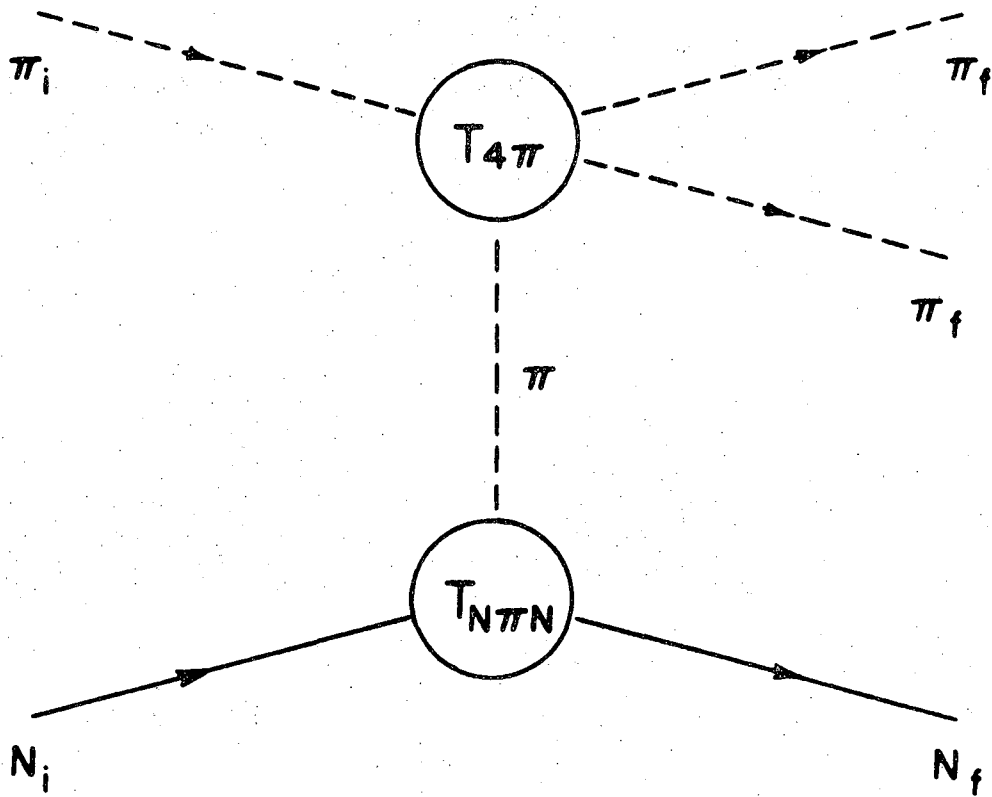


Fig. 36.

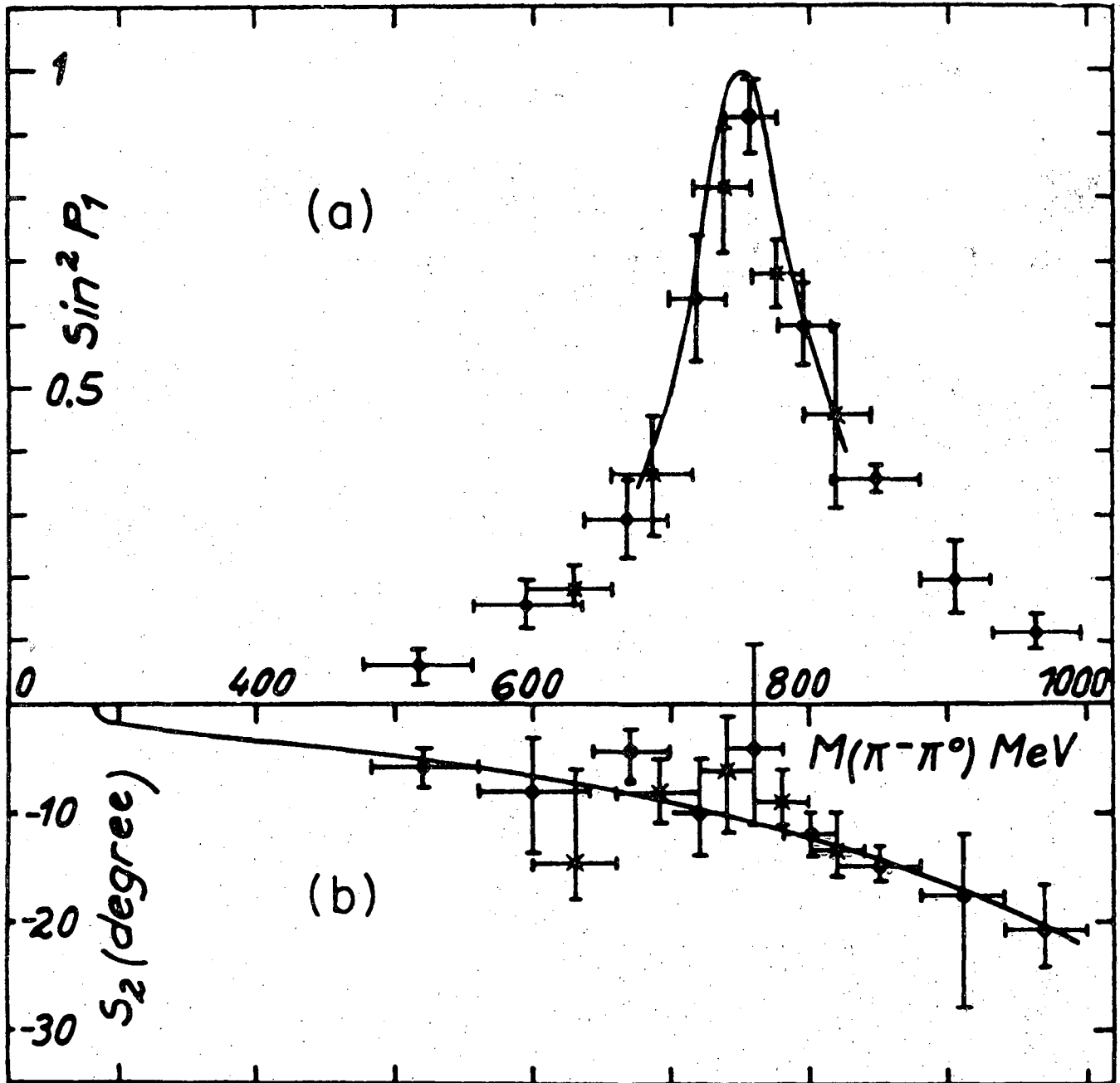


Fig. 37.

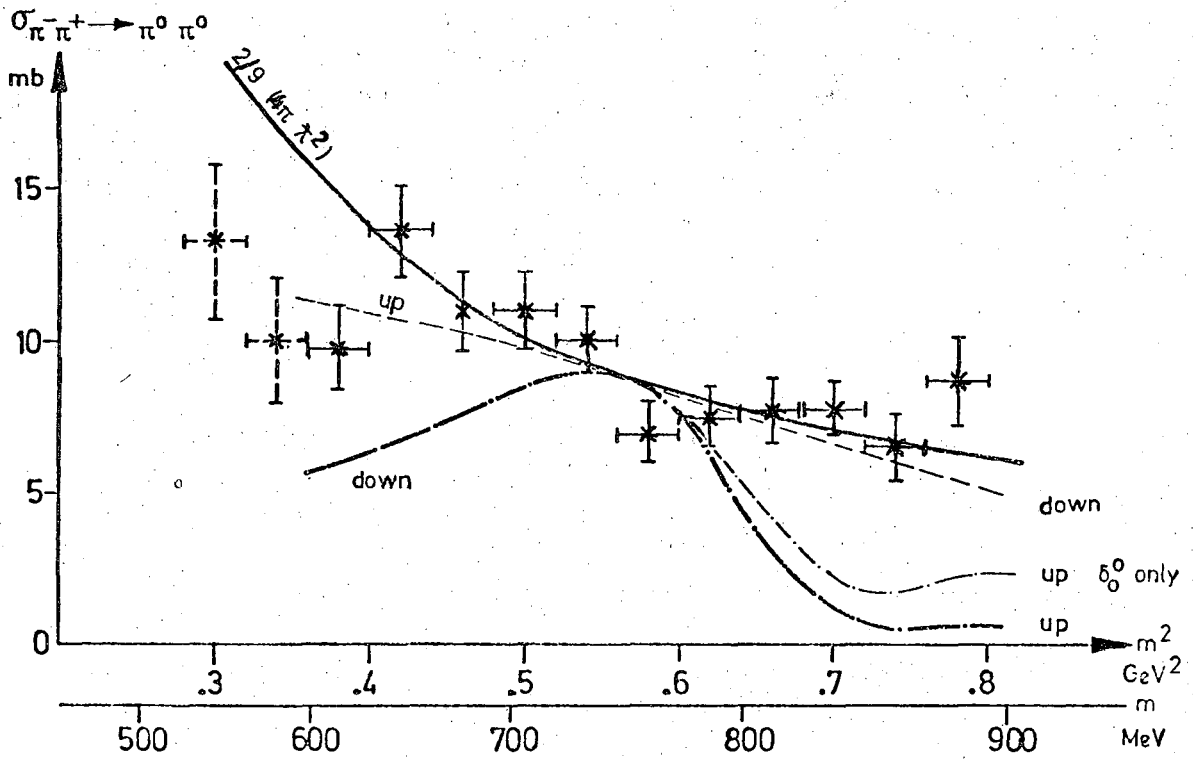
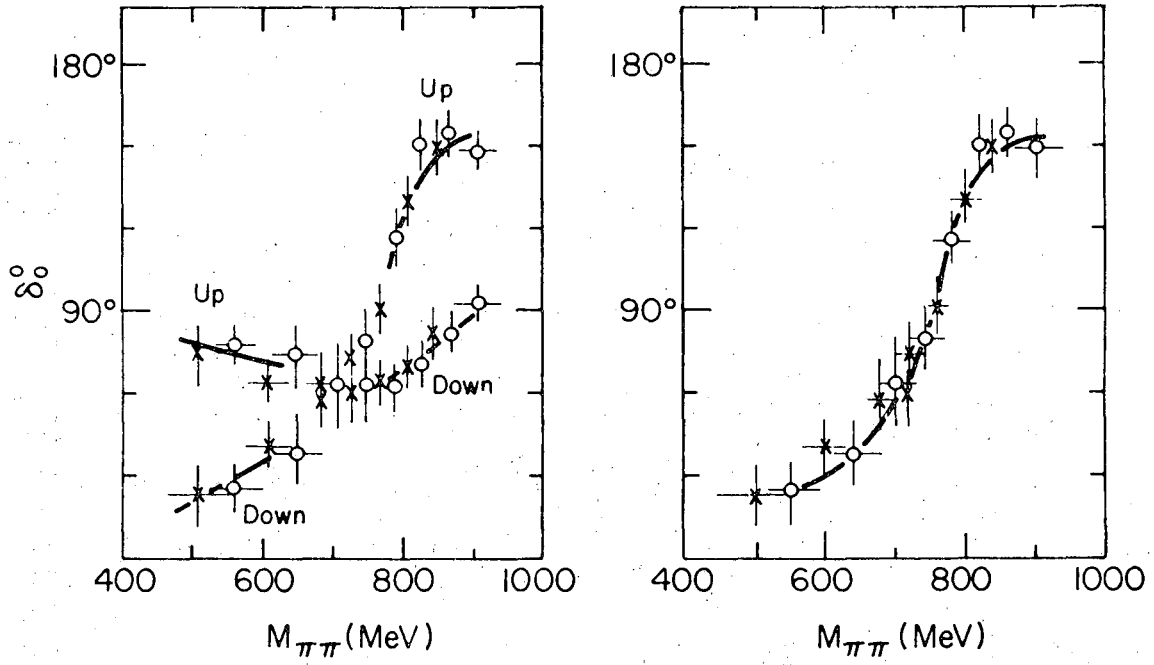


Fig. 38

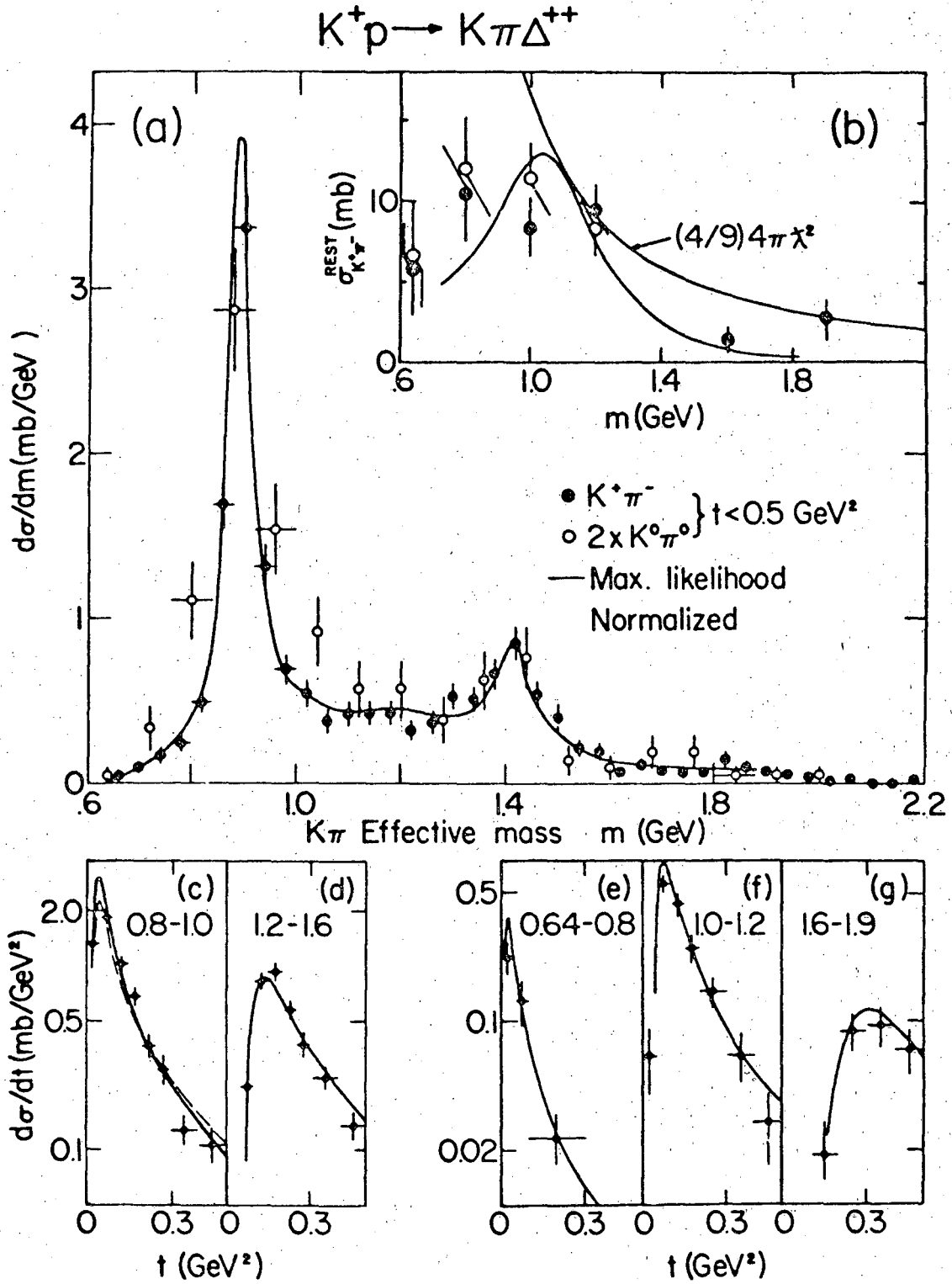


Fig. 39.

$$y = \frac{Qdm}{2\pi r^2 \sin \phi \cdot d\phi} = \frac{ntb^2 \cdot Q \cdot \operatorname{cosec}^4 \phi/2}{16r^2} \dots (5)$$

$$\begin{aligned} \frac{d\sigma}{dt} = & \frac{1}{4\pi(s-m^2)^2} \left[\frac{|\sin\theta_i|^2(1+\cos 2\varphi_\gamma) |t-(Y+m)^2| |t|^{-1} |\gamma_{\frac{1}{2}}^K|^2 (s/s_0)^{2(\alpha_K-1)} \alpha_K^2}{|\Gamma(\alpha+1) \sin \frac{1}{2}\pi\alpha_K|^2} + (1-\cos 2\varphi_\gamma) \right. \\ & \times |\sin\theta_i|^2 (t-m_K^2)^2 |t-(m-Y)^2| \left(\frac{\alpha_c^2 |t|^{-1} |\gamma_{\frac{1}{2}}^c|^2 (s/s_0)^{2(\alpha_c-1)}}{|\Gamma(\alpha_c+1) \sin \frac{1}{2}\pi\alpha_c|^2} + \frac{\alpha_V^2 |t|^{-1} |\gamma_{\frac{1}{2}}^V|^2 (s/s_0)^{2(\alpha_V-1)}}{|\Gamma(\alpha_V+1) \cos \frac{1}{2}\pi\alpha_V|^2} \right. \\ & + \frac{\alpha_T^2 |t|^{-1} |\gamma_{\frac{1}{2}}^T|^2 (s/s_0)^{2(\alpha_T-1)}}{|\Gamma(\alpha_T+1) \sin \frac{1}{2}\pi\alpha_T|^2} + \frac{2\alpha_c\alpha_V \sin \frac{1}{2}\pi(\alpha_V-\alpha_c) \gamma_{\frac{1}{2}}^c \gamma_{\frac{1}{2}}^V (s/s_0)^{\alpha_c+\alpha_V-2}}{|\Gamma(\alpha_c+1)\Gamma(\alpha_V+1) \sin \frac{1}{2}\pi\alpha_c \cos \frac{1}{2}\pi\alpha_V|} \\ & + \left. \frac{2\alpha_c\alpha_T \gamma_{\frac{1}{2}}^c \gamma_{\frac{1}{2}}^T \cos \frac{1}{2}\pi(\alpha_T-\alpha_c)(s/s_0)^{\alpha_c+\alpha_T-2}}{|\Gamma(\alpha_c+1)\Gamma(\alpha_T+1) \sin \frac{1}{2}\pi\alpha_c \sin \frac{1}{2}\pi\alpha_T|} \right) + (1+\cos^2\theta_i - \cos 2\varphi_\gamma \sin^2\theta_i) \\ & \times \frac{\alpha_K^4 |t-(m+Y)^2| |t-m_K^2| |\gamma_{\frac{1}{2}}^K|^2 (s/s_0)^{2(\alpha_K-2)}}{|\Gamma(\alpha_K+1) \sin \frac{1}{2}\pi\alpha_K|^2} + (1+\cos^2\theta_i + \cos 2\varphi_\gamma \sin^2\theta_i)(t-m_K^2)^2 \\ & \times |t-(m-Y)^2|^2 \left(\frac{|\gamma_{\frac{1}{2}}^c|^2 (s/s_0)^{2(\alpha_c-1)} \alpha_c^2 |t|^{-2}}{|\Gamma(\alpha_c+1) \sin \frac{1}{2}\pi\alpha_c|^2} + \frac{\alpha_V^4 |\gamma_{\frac{1}{2}}^V|^2 (s/s_0)^{2(\alpha_V-1)}}{|\Gamma(\alpha_V+1) \cos \frac{1}{2}\pi\alpha_V|^2} + \frac{\alpha_T^4 |\gamma_{\frac{1}{2}}^T|^2 (s/s_0)^{2(\alpha_T-1)}}{|\Gamma(\alpha_T+1) \sin \frac{1}{2}\pi\alpha_T|^2} + 2 \sin \frac{1}{2}\pi \right. \\ & \times (\alpha_V-\alpha_c) |t|^{-1} \frac{\gamma_{\frac{1}{2}}^c \gamma_{\frac{1}{2}}^V (s/s_0)^{\alpha_c+\alpha_V-2}}{|\Gamma(\alpha_c+1)\Gamma(\alpha_V+1) \sin \frac{1}{2}\pi\alpha_c \cos \frac{1}{2}\pi\alpha_V|} + \left. \frac{2 \cos \frac{1}{2}\pi(\alpha_T-\alpha_c) \gamma_{\frac{1}{2}}^c \gamma_{\frac{1}{2}}^T (s/s_0)^{\alpha_c+\alpha_T-2}}{|\Gamma(\alpha_c+1)\Gamma(\alpha_T+1) \sin \frac{1}{2}\pi\alpha_c \cos \frac{1}{2}\pi\alpha_V|} \right) + 4 \cos\theta_i (t-m_K^2) \\ & \times \left[(t-(m+Y)^2) [(t-(m-Y)^2)]^{1/2} |\gamma_{\frac{1}{2}}^K|^2 (s/s_0)^{\alpha_K-1} \alpha_K^2 \left(\frac{t^{-2} \gamma_{\frac{1}{2}}^c \alpha_c \cos \frac{1}{2}\pi(\alpha_K-\alpha_c)(s/s_0)^{\alpha_c-1}}{|\sin \frac{1}{2}\pi\alpha_c \Gamma(\alpha_c+1)\Gamma(\alpha_K+1) \sin \frac{1}{2}\pi\alpha_K|} \right. \right. \\ & \left. \left. + \frac{t^{-1} \sin \frac{1}{2}\pi(\alpha_V-\alpha_T) \alpha_V^2 \gamma_{\frac{1}{2}}^V (s/s_0)^{\alpha_V-1}}{|\Gamma(\alpha_K+1)\Gamma(\alpha_V+1) \sin \frac{1}{2}\pi\alpha_K \cos \frac{1}{2}\pi\alpha_V|} + \frac{t^{-1} \alpha_T \gamma_{\frac{1}{2}}^T \cos \frac{1}{2}\pi(\alpha_K-\alpha_T)(s/s_0)^{\alpha_T-1}}{|\Gamma(\alpha_T+1)\Gamma(\alpha_K+1) \sin \frac{1}{2}\pi\alpha_K \sin \frac{1}{2}\pi\alpha_V|} \right) \right]. \quad (75) \end{aligned}$$

XBL 696-602

Fig. 40.

"I desire to express my thanks to Mr. William Kay for his invaluable assistance in counting scintillations."

(Professor Sir Ernest Rutherford, April 1919)

"We would like to thank Professor J. Steinberger who participated in the design and in the earlier part of this experiment, and Professors W. Paul, P. Preiswerk and H. Faissner for support and encouragement. We acknowledge the assistance of Mr. J. Daub and Dr. P. Zanella, who made the measurement of the events on Luciole possible. Dr. L. Caneschi has helped in the running of the experiment. The detection apparatus was built with the help of Messrs. F. Blythe, K. Bussmann, J. M. Fillot, and G. Muratori. Finally, we would like to thank Dr. G. Petrucci, the CPS staff, and especially Dr. L. Hoffmann for the setting up and operation of the slow ejected proton beam."

(A. Bohm,^{*} P. Darriulat, C. Grosso,^{**} V. Kaftanov,^{***} K. Kleinknecht, H. L. Lynch,[†] C. Rubbia, H. Ticho,[‡] and K. Tittel,^{*} 30 May 1968)

Fig. 41.

LEGAL NOTICE

This report was prepared as an account of Government sponsored work. Neither the United States, nor the Commission, nor any person acting on behalf of the Commission:

- A. Makes any warranty or representation, expressed or implied, with respect to the accuracy, completeness, or usefulness of the information contained in this report, or that the use of any information, apparatus, method, or process disclosed in this report may not infringe privately owned rights; or*
- B. Assumes any liabilities with respect to the use of, or for damages resulting from the use of any information, apparatus, method, or process disclosed in this report.*

As used in the above, "person acting on behalf of the Commission" includes any employee or contractor of the Commission, or employee of such contractor, to the extent that such employee or contractor of the Commission, or employee of such contractor prepares, disseminates, or provides access to, any information pursuant to his employment or contract with the Commission, or his employment with such contractor.

TECHNICAL INFORMATION DIVISION
LAWRENCE RADIATION LABORATORY
UNIVERSITY OF CALIFORNIA
BERKELEY, CALIFORNIA 94720